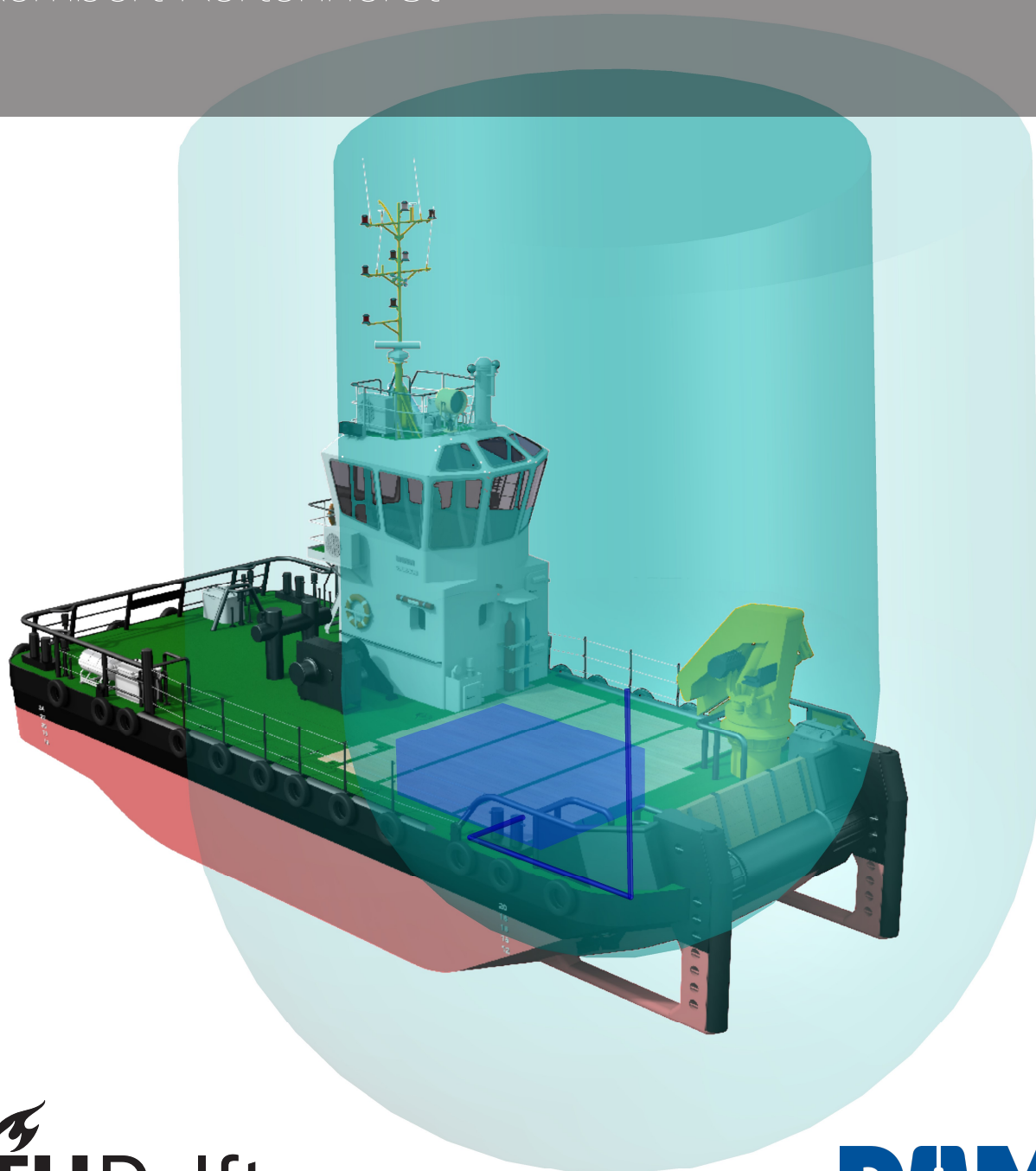


Enabling safe and practicable storage of methanol as a ship's fuel by describing and mitigating venting risks

An analytical modelling approach

Rembert Kortenhorst



Thesis for the degree of MSc in Marine Technology in the specialization of Marine Engineering

Enabling safe and practicable storage of methanol as a ship's fuel by describing and mitigating venting risks

An analytical modelling approach

by

Rembert Kortenhorst

Performed at

DAMEN Shipyards

This thesis (MT.21/22.053.M) is classified as confidential in accordance with the general conditions for projects performed by the TUDelft.

October 11, 2022

Company supervisors

Responsible supervisor Ir. K. Jansen DAMEN Shipyards

Thesis exam committee

Chair Ir. K. Visser TU Delft
Committee Dr. Ir. P. de Vos TU Delft
Committee Ir. A.W. Vredevelde TNO

Author details

Student number 4390679

Abstract

To reduce the climate change impact of shipping and retain compliance with increasingly strict emission regulations, alternative fuels are required. Methanol is expected to be one of the renewable alternatives. However, it evaporates easily compared to for example Diesel and its vapours are toxic and flammable. Regulations prescribe the use of 10m radius hazardous areas around the vent mast connected to the ship's tank. These areas pose stringent limitations on the use of a ship. In this context, knowledge is lacking on the actual risks induced by possible outflows, let alone on outflow mitigation measures. In this research an analytical thermodynamical model of a ship's methanol fuel tank is developed, it is analysed what appropriate safety measures are and what their effectiveness is.

The thermodynamical phenomena inside a ship's tank are inventoried from literature and on a selection of these a model is derived. With the model, outflow values of methanol mass with and without outflow mitigation measures are simulated for various scenarios and tank sizes. The scenarios are (1) heating during the transition from night to day or (2) due to a fire and (3) the most critical post bunker situation. The latter occurs after the ship's tank is filled for the first time prior to which no methanol vapours are present.

It is found that outflow values correspond to a hazardous area size much smaller than the prescribed 10m except for the fire scenario. However, mitigating the outflow with a PRV and with locating the tank floor in contact with the seawater is found to be very effective. With application of mitigation measures, only the most critical post bunker situation results in a hazardous area of larger than 1m, being 1.17m. Assessment of the model accuracy is limited to the presented scenarios, limiting the model applicability to the ranges in which the parameters are varied within this research.

Keywords: Methanol; Ship; Fuel; Tank; Storage; Risks; Safety; Venting; Outflow; Hazardous area

Preface

Whilst our planet is experiencing a human and largely wealth induced climate change, subsequent droughts and floods strike many parts of the world, I ask myself the following question: What is wealth? What is wealth when it comes at the price of the lives of those who do not profit nor have a choice in undergoing their fate? I believe the wealthy parts of the world owe a tremendous debt to people in other parts of the world and nature everywhere. By choosing a thesis topic that might contribute to more sustainable shipping, I hope to contribute for a tiny bit to protecting those who and that which cannot protect themselves from the harm we inflict and with this relieving a tiny bit of our debt.

In my efforts of achieving this, I would like to thank my supervisors. These were Klaas Visser from the university and Koen Jansen from DAMEN Shipyards. Together, I hope we have accomplished a work that is relevant for both the industry and for academic purposes and can contribute to sustainable shipping.

I would like to thank my fellow graduating students for providing motivation throughout the graduation period, including a summer in which the faculty was a lot more quiet but not a bit less enjoyable, motivating and a place of good ideas. Furthermore, I would like to thank all other friends and my family for being there. At last but definitely not least, I want to thank Judith for her support and inspiration throughout the period of my thesis.

How do you try to relieve our debt?

*Rembert Kortenhorst
Delft, October 2022*

Contents

Abstract	i
Preface	ii
List of Figures	v
List of Tables	vi
Nomenclature	vii
1 Introduction	1
1.1 Problem statement	2
1.2 Knowledge gap	2
1.3 Research objectives	3
1.4 Research questions	3
1.5 Scope of the research	4
1.6 Methodology and chapter outline	4
2 Thermodynamic phenomena in a ship's tank	5
2.1 Description of case	5
2.2 Inventory of phenomena	5
2.3 Illustration of phenomena	6
2.3.1 Energy and mass flows	6
2.3.2 Effects near boundaries	6
2.4 Conclusions	8
3 Model derivation	9
3.1 Processing of phenomena	9
3.2 Model description	10
3.2.1 Overview of the thermodynamical model and definition of areas	10
3.2.2 Detailed view of the interactions occurring near the boundaries	12
3.3 Governing equations	13
3.3.1 Energy balances for an aerated tank	14
3.3.2 Energy flow equations for an aerated tank	15
3.3.3 Volume flow equations for an aerated tank	16
3.3.4 Mass flow equations for an aerated tank	19
3.3.5 Empty tank situation	20
3.3.6 Boiling behaviour	20
3.3.7 Adaptations towards a tank with PRV	21
3.4 Model synthesis	22
3.4.1 Definition of state equations	22
3.4.2 Evaporation rate with saturated conditions	23
3.4.3 Adaptations towards a tank with PRV: Energy balance in the vapour phase	24
3.4.4 Model overview	24
3.5 Solving the model	26
3.6 Modelling parameters	26
3.7 Conclusions	30

4	Case study	31
4.1	Choice of executed simulations	31
4.1.1	Definition of scenarios	31
4.1.2	Selection of tank dimensions	32
4.1.3	Mitigation measures for methanol outflow	33
4.1.4	Initial filling grade	33
4.1.5	Duration of simulation	33
4.1.6	Resulting set of simulations	33
4.2	Interpreting outflow values with IEC norm	34
4.3	Scenario 1: Night to day	35
4.3.1	No mitigation measures	36
4.3.2	Influence of PRV	37
4.3.3	Influence of tank floor against seawater	38
4.3.4	Combined influence	40
4.4	Scenario 2: Fire	40
4.4.1	No mitigation measures	40
4.4.2	Influence of PRV	43
4.4.3	Influence of tank floor against seawater	43
4.4.4	Combined influence	45
4.5	Scenario 3: Most critical post bunker situation	45
4.5.1	No mitigation measures	45
4.5.2	Influence of PRV	47
4.5.3	Influence of tank floor against seawater	47
4.5.4	Combined influence	47
4.6	Cross comparison	47
4.6.1	Observations on tank size	47
4.6.2	Influence of mitigation measures	48
5	Discussion	49
5.1	Uncertainties in model outcomes	49
5.1.1	Impact of uncertainty in Schmidt number	49
5.1.2	Impact of uncertainty in liquid heat transfer coefficient	51
5.1.3	Impact of neglecting heat flow between wall sections	52
5.1.4	Impact of assuming constant enthalpy of evaporation with varying temperature	54
5.1.5	Unquantified aspects of uncertainty	55
5.1.6	Conservative assessment of total impact	56
5.2	Applicability	57
5.2.1	Limitations on input parameters	57
5.2.2	Suggested applications	58
6	Conclusions and recommendations	59
6.1	Conclusions	59
6.2	Recommendations	60
6.2.1	Applicability	60
6.2.2	Accuracy	60
	Bibliography	63

List of Figures

1.1	Impact of hazardous areas on a DAMEN Multicat 1908	2
2.1	Energy and mass flows throughout a ship's tank	6
2.2	Illustration of temperature distribution as derived from the analysis of [11] (left) and of methanol concentrations (right) at the wall and phase boundaries	7
3.1	Overview of the thermodynamic model in this research	11
3.2	Overview of the dimensioning used in the model	12
3.3	Detail of the boundaries near wall 1 and 2 of the thermodynamic model in this research	13
3.4	Detail of the boundaries of wall 3 in the thermodynamic model in this research	13
3.5	Vapour pressure curve for methanol using the Antoine equation	17
3.6	Error between the vapour pressure curve of methanol described by Refprop [22] and by the Antoine parameters presented in [21]	28
4.1	Hazardous area sizing based on the volumetric release characteristic [7]	35
4.2	Temperatures for scenario 1, $\epsilon_0=10\%$ and Tank 2 with all walls surrounding ambient air	36
4.3	Volume and mass flows and pressure build up for scenario 1, $\epsilon_0=10\%$ and Tank 2 with all walls surrounding ambient air	37
4.4	Relative and absolute vapour fractions for scenario 1, $\epsilon_0=10\%$ and Tank 2 with all walls surrounding ambient air	37
4.5	Volume and mass flows and pressure build up for scenario 1, $\epsilon_0=10\%$ and Tank 1 with all walls surrounding ambient air	38
4.6	Volume and mass flows and pressure build up for scenario 1, $\epsilon_0=10\%$ and Tank 2 with one wall adjacent to seawater	39
4.7	Temperatures for scenario 1, $\epsilon_0=10\%$ and Tank 2 with one wall adjacent to seawater	40
4.8	Temperatures for scenario 2, $\epsilon_0=10\%$ and Tank 2 with all walls surrounding ambient air	41
4.9	Volume and mass flows and pressure build up for scenario 2, $\epsilon_0=10\%$ and Tank 2 with all walls surrounding ambient air	42
4.10	Volume and mass flows and pressure build up for scenario 2, $\epsilon_0=90\%$ and Tank 2 with all walls surrounding ambient air	43
4.11	Temperatures for scenario 2, $\epsilon_0=10\%$ and Tank 2 with one wall adjacent to seawater	44
4.12	Volume and mass flows and pressure build up for scenario 2, $\epsilon_0=10\%$ and Tank 2 with one wall adjacent to seawater	45
4.13	Temperatures for scenario 3, $\epsilon_0=90\%$ and Tank 2 with all walls surrounding ambient air	46
4.14	Volume and mass flows and pressure build up for scenario 3, $\epsilon_0=90\%$ and Tank 2 with all walls surrounding ambient air	47
5.1	Volume and mass flows and pressure build up for scenario 2, $\epsilon_0=10\%$ and Tank 2 with one wall adjacent to seawater for $0.1k_{liq}$	52
5.2	Selected value for the enthalpy of evaporation versus the values presented in [22]	55

List of Tables

1.1	Overview of knowledge gap. This research focuses on the blue marked part of the gap.	3
3.1	Overview of phenomena involved and how they are led into further research	10
3.2	Modelling parameters used	27
4.1	Definition of scenarios	31
4.2	Outflow values, outflow timing, tank pressures and hazardous area radii ¹ for all executed simulations. Gray cells represent outcomes without mitigation measures, yellow cells with PRV, blue cells with the tank floor adjacent to seawater and green cells with both.	34
5.1	Error percentages induced by variations in Schmidt number Sc , values for tank 2	50
5.2	Error percentages induced by variations in heat transfer coefficient for liquids k_{liq} , values for tank 2	52
5.3	Ratios of wall heat flows to heat flows in wall 1	54
5.4	Possible underestimations caused by uncertainties discussed and total impact on scenarios	57

¹Due to limited applicability of the hazardous area description in [7], its values that are smaller than 1m should only be used to provide interpretation to outflow values and be treated as effectively resulting in a radius of 1m.

Nomenclature

Physics symbols

β	Mass transfer coefficient	[m/s]
Δh_{evap}	Specific enthalpy of evaporation	[J/kg]
\dot{H}	Enthalpy flow	[J/s]
\dot{V}	Volume flow	[m ³ /s]
ϵ	Filling level	[-]
λ	Thermal conductivity	[W/(m K)]
ϕ	Ratio of vapour fraction over saturation vapour fraction (relative concentration level)	[-]
ρ	Density	[kg/m ³]
A	Area, Antoine equation parameter	[m ²], [-]
B	Breadth, Antoine equation parameter	[m], [-]
C	Air changes per unit time, Antoine equation parameter	[1/s], [-]
c_p	Specific heat at constant pressure	[J/(kg K)]
c_v	Specific heat at constant volume	[J/(kg K)]
H	Height	[m]
k	Heat transfer coefficient	[W/(m ² K)]
L	Length	[m]
Le	Lewis number	[-]
LEL_V	Lower Explosivity Limit (LEL) on volume basis	[kg/m ³]
M	Molecular mass	[kg/mole]
m	Mass	[kg]
p	Pressure	[kPa], [bar]
Pr	Prandtl number	[-]
Q	Heat flow	[J/s]
R	Universal gas constant	[J/(K mole)]
r	Radius	[m]
Sc	Schmidt number	[-]
T	Temperature	[K]
t	Time	[s]
U	Internal energy	[J]

V	Volume	[m ³]
v	Speed	[m/s]
y	Volumetric vapour fraction	[-]

Subscripts

0	Initial value
1	Denoting parameter related to bulk or wall 1
12	Denotes heat flow between the bulk 1 and 2
2	Denoting parameter related to bulk or wall 2
3	Denoting parameter related to wall 3
<i>air</i>	Denoting gas inside the tank when this is air
<i>amb</i>	Ambient
<i>circ</i>	Circumference
<i>evap</i>	Evaporation
<i>expans</i>	Expansion
<i>gas</i>	Denoting gas inside the tank
<i>HA</i>	Hazardous area
<i>in</i>	Denotes heat flow between the ambient and the wall
<i>int</i>	Denotes heat flow between the wall and corresponding bulk phase
<i>liq</i>	Liquid
<i>max</i>	Maximum
<i>min</i>	Minimum
<i>mt</i>	Mass transfer
<i>N2</i>	Denoting gas inside the tank when this is nitrogen
<i>par</i>	Denoting condition at which parameters are evaluated
<i>PRV</i>	Pressure Relief Valve (PRV)
<i>sat</i>	At saturation level
<i>surf</i>	The free surface of the liquid phase
<i>tank</i>	Denoting outside area of the tank
<i>vap</i>	Vapour

Introduction

In the current use of Diesel and Heavy Fuel Oil (HFO) [1] as the main energy source of vessels, there is a wide range of negative fuel borne impacts on the environment [2] [1]. These include carbon dioxide emissions, emissions of air pollutants (carbon dioxide is a greenhouse gas, not an air pollutant) and oil spills [2]. Use of methanol as a shipping fuel can eliminate the harmful impact of fuel spills as it is not toxic to the marine environment [3]. Also, as methanol does not contain sulphur, no fuel borne sulphoxide is emitted. It are regulations on air pollutants that largely motivate the shipping industry to alternatives [4].

Within a world experiencing climate change [5], in 2018 shipping had a 2.89% share in the total anthropogenic greenhouse gas emissions [1]. When the energy to make methanol is obtained carbon neutrally and the required carbon atom is sequestered from the atmosphere, its total cycle from source to combustion is carbon neutral. Methanol can be produced carbon neutrally from biomass or with electric synthesis [4]. However, to scale up to industrial needs, quantities are required in which biomass cannot fulfil [4]. In view of electrically synthesized fuels, methanol is the cheapest in terms of energy that can be stored as a liquid under ambient conditions [4].

However, despite a set of promising characteristics of the fuel, the large scale implementation of methanol has its challenges. Methanol is produced on a large scale for various chemical processes, however it is generally made from fossil sources and renewable production is only starting [4]. Furthermore, methanol has a much higher vapour pressure of 0.129 bar compared to Diesel or HFO, being less than 0.001 bar [3]. Compared to Diesel its vapours are much less toxic [3], however due to its high vapour pressure, the toxicity levels are expected to be reached much earlier. Furthermore, its vapours are already ignitable at a flashpoint of 10°C, for HFO and Diesel this is only beyond 55°C [3]. The combination of the tendency to evaporate and its low flashpoint results in the risk of flammable vapours escaping from a vent mast and as such care has to be taken in handling and storing the fuel. The risks are reflected in regulations as the International Maritime Organization (IMO) has developed interim guidelines specifically for the storage of methanol and ethanol [6]. These guidelines present hazardous areas around a vent mast of 10m in radius in which restrictions apply on the installation of electronics and the presence of unauthorized crew is prohibited [6]. It states however that if this definition of the hazardous areas is deemed inappropriate, the IEC-60079-10-1:2015 norm [7] should be used. Throughout the remainder of this report, this is referred to as the IEC norm. This norm provides a description for scaling hazardous area when outflow values are known [7].

The hazardous areas can be interpreted as the nominal risk mitigation measure related to the possible venting of methanol from a ship's fuel tank. Next to that, the IMO guidelines on methanol also prescribe the use of a Pressure Relief Valve (PRV) combined with inerting the tank atmosphere by replacing air with nitrogen as risk mitigation measures related to the tank [6]. As opposed to Diesel and HFO [8], it is allowed to store methanol directly adjacent to ship's outer hull whenever this is always below the sea level [6]. Doing so can function as a mitigation measure that dampens the effects of heat ingress.

1.1. Problem statement

With a hazardous area radius of 10m required around a vent mast, much usable deck area of a ship is lost. As illustrated for a vessel of 19m in [Figure 1.1](#) and on the cover page of this report, this is especially stringent for smaller ships. Many ships in the DAMEN portfolio are smaller than 35 meters, for which such hazardous areas prove to be unworkable. Furthermore, despite regulations prescribing risk mitigation measures, knowledge of the actual risks of flammability and toxicity induced by possible outflows from a ship's vent mast is lacking, let alone on the effectiveness of outflow mitigation measures.

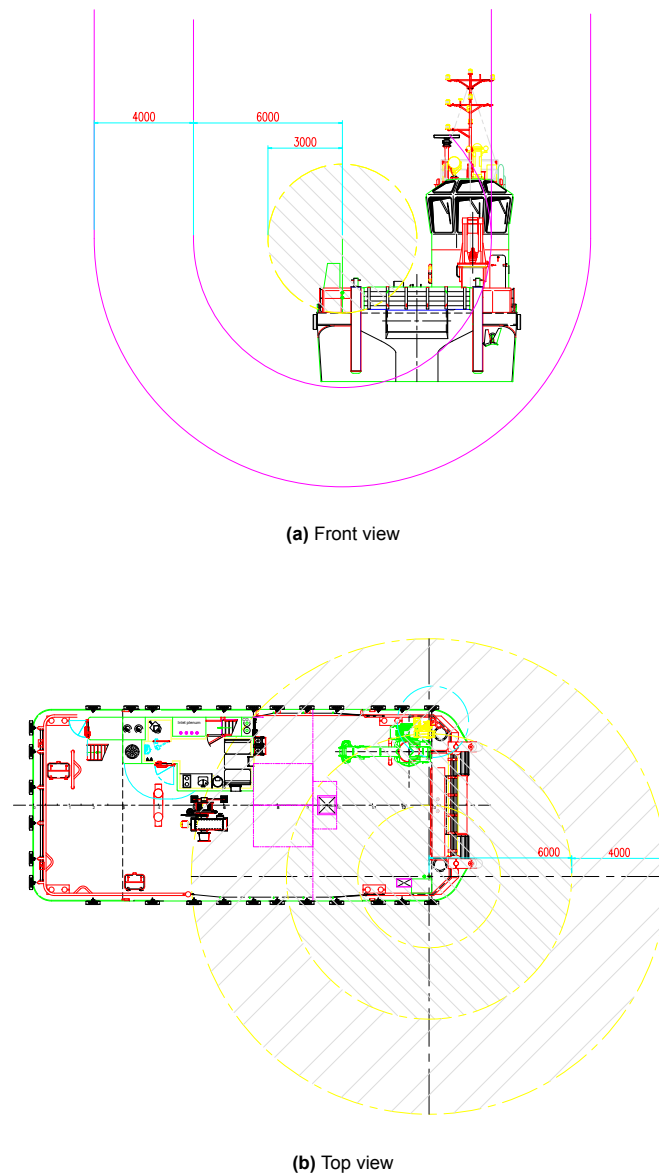


Figure 1.1: Impact of hazardous areas on a DAMEN Multicat 1908

1.2. Knowledge gap

Because of the care that should be taken to avoid the toxicity and explosivity risks of methanol and because the 10m hazardous area radius is stringent to a ship design, for safe and effective implementation of methanol as a ship fuel, knowledge of the onboard storage of methanol as a fuel is required. The required knowledge can be split up into knowledge on ship's methanol fuel tanks and on a possible

plume that occurs when vapours are vented from a ship's vent mast. In scientific literature, knowledge on this topic is lacking. Knowledge is however available on closely related topics as displayed in [Table 1.1](#) and discussed below.

Regarding the modelling of tanks, first of all, there is scientific knowledge on airbreathing methanol tanks that cool down during a rain shower. A basic model is provided [9], that is extended [10], validated and put in context [11]. This provides insights into how a thermodynamic model for a tank can be built. Secondly, as Liquefied Natural Gas (LNG) is a thermodynamically challenging fluid, knowledge is available on the application of its tanks on ships [12], [13] and [14]. These studies provide the ship context that is required. On plume models, there is knowledge available on the Computational Fluid Dynamics (CFD) modelling of LNG plumes in the context of ships [15], [16]. Outside of the ship context, a plume model is presented that assumes Gaussian distribution [17] that is extended by [18].

From the analysis above and the overview provided in [Table 1.1](#), it is found that a knowledge gap lies in understanding the thermodynamic behaviour of methanol in a ship's fuel tank and the behaviour of a plume in the case methanol is vented. Knowledge of the thermodynamic behaviour of a ship's methanol fuel tank is required to provide input to a plume model and in the end assess the risks incurred. Therefore, the part of the knowledge gap that describes the thermodynamic behaviour of the tank is the chosen starting point in filling this larger gap and is the focus of this research. As assessing the effectiveness of outflow risk mitigation measures, falls fully within the gap described above, no scientific knowledge is available on this. The size of a hazardous area is however quantified in regulations [7].

Table 1.1: Overview of knowledge gap. This research focuses on the blue marked part of the gap.

	Methanol		Other fluids	
	Tank	Plume	Tank	Plume
Ship	Gap	Gap ^a	[12] [13] [14]	[15] [16]
General	[9] [10] [11] ^b	Gap ^c	Many	[17] [18]

^aDespite not being specified for methanol specifically, the Gaussian distribution models ([17] and [18]) presented for the plume of other fluids than methanol can be applied to it, also in the context of ships.

^bThese researches only describe the cooling and subsequent inbreathing of tanks, where outbreathing behaviour is sought after.

^cThe remark above on the Gaussian distribution models also applies to other contexts than ships.

1.3. Research objectives

The main objective of this research is to gain an understanding in what are appropriate safety measures for mitigating the explosivity and toxicity risks related to the possible venting of methanol when stored on board a ship as its fuel. This understanding is to reflect on the appropriateness of the stringent mitigation measure that are hazardous areas. Also, insight is to be gained in how this stringency can be reduced through other mitigation measures.

To attain this main objective, two subobjectives are formulated. First of all, understanding must be gained of the thermodynamic behaviour of a ship's methanol fuel tank. Secondly, the effectiveness of outflow mitigation measures must be assessed.

1.4. Research questions

The research questions are derived from the research objectives and are presented below. Answering the sub-questions will result in an answer to the main research question.

Main research question:

How can the safe and practicable storage of methanol as a ship's fuel be enabled regarding explosivity and toxicity risks related to venting?

Sub questions:

1. How can the thermodynamic behaviour of a ship's methanol fuel tank be described?
2. How can the outflow risks of methanol from a ship's fuel tank effectively be mitigated?

1.5. Scope of the research

Within the described research objectives and questions, there is only one main limitation of the scope. These are the outflow mitigation measures that are included in the research. The measures included are mentioned here:

1. Describing a hazardous area in which the use of electronics and presence of occupants is limited as prescribed in regulations [7].
2. Closing off the ship's tank with a PRV as prescribed in regulations [7].
3. Locating the floor of the tank directly against seawater to dampen temperature fluctuations.

These are selected as measure 1 and 2 are already prescribed by regulations [7] and measure 3 is expected to be effective and does not require any additional systems that might require approval by regulatory instances.

1.6. Methodology and chapter outline

A literature based inventory of the thermodynamic phenomena in a ship's fuel tank is executed in [Chapter 2](#). This inventory aims to provide a complete overview of the phenomena involved. Only for a selection of these phenomena a thermodynamic model is developed in [Chapter 3](#). Here, the selected phenomena are further simplified to arrive at a model. For interpretability of the results, an analytical model is derived as this describes each modelled element individually. With this model, a case study on several scenarios is executed in [Chapter 4](#). The scenarios modelled are (1) night to day, (2) fire and (3) the most critical post bunker situation, which is the bunkering into a tank that does not initially contain vapours. For each scenario, for various tank sizes and for different combinations of mitigation measures the outflow of methanol mass is modelled. The outflow values are used to scale the hazardous areas according to the IEC norm. Both of the model and the case study a discussion is provided in [Chapter 5](#) to draw conclusions and provide recommendations in [Chapter 6](#).

2

Thermodynamic phenomena in a ship's tank

In this chapter, the thermodynamic phenomena that are relevant for the case concerned are discussed. Here, the phenomena are discussed qualitatively on a high level and not yet analysed quantitatively.

2.1. Description of case

In this research, a ship's fuel tank filled with methanol is modelled. A description of this case is provided here. Note that this description is still broader than what is modelled.

Due to the diversity of ships, fuel tanks can significantly differ. Not only for different ships, but also within a ship, fuel tanks can have different shapes, safety systems and surroundings. The simplest shape is rectangular, but many tanks are placed around other systems or follow the smooth patterns of a ship's hull. Without safety systems, a methanol fuel tank can be aerated. However, to avoid explosion risks, designers can (be forced to) choose to omit air into a tank. This can be achieved by replacing the air with nitrogen (a nitrogen blanket) and closing off the tank with a Pressure Relief Valve (PRV) as required in [6]. To further reduce explosion risks, cofferdams filled with nitrogen can be required for a significant part of the walls [6]. Due to the ship's motion, sloshing can occur inside the tank. During its use, the ship uses fuel from the tank, which is later refilled. Furthermore, the tank can experience heating from many sources such as the ambient air and seawater surrounding the ship, a fire next to the tank and heat losses from nearby equipment.

2.2. Inventory of phenomena

To attain a complete overview of the thermodynamic phenomena that are to be expected in a tank, as described in [Section 2.1](#), a literature based inventory is executed. In this inventory, it is found that Schmidt et al. [11] provide an overview of the available knowledge on land-based methanol tanks that experience cooling due to a rain shower. Furthermore, the context of a tank inside a ship is adapted from knowledge of Liquefied Natural Gas (LNG), which is ample as it is a challenging fuel or cargo concerning thermodynamics. Relevant knowledge is found in Al-Breiki et al. [12], Iannaccone et al. [13] and Zakaria et al. [14]. The findings are further processed and additional insights are obtained. All of which are discussed below. An overview of these phenomena along with how they are led into the further parts of this research (see also [Section 3.1](#)), is provided in [Table 3.1](#).

The basis provided in [11] entails condensation, heat and mass transfer throughout and between the liquid and vapour phase, varying ambient temperature and pressure, varying temperature throughout the wall, liquid phase and vapour phase and inflow of air. Directly derived from these phenomena are the evaporation in case of heating, the saturation of the vapour phase and the outflow of vapours.

In providing the shipping context, in [12], [13] and [14], additional phenomena are described. These are sloshing due to motion of the ship and heat ingress through an adjacent space or cofferdam, such as due to fire.

Additional phenomena are added by the author that are relevant in the case. Those are described

in Section 2.1. These are the behaviour of a PRV, heat ingress into the wall from air and seawater, the compression and expansion of the tank contents, a varying waterline, the scenario of refuelling and the behaviour of non-ideal, non-perfect gases.

2.3. Illustration of phenomena

To explain the interaction of the phenomena, illustrations are provided on a selection of parameters. These illustrations are for a ship's fuel tank containing methanol, which is heating up under influence of outside conditions.

2.3.1. Energy and mass flows

In Figure 2.1, an overview is provided of the energy and mass flows of the tank concerned in this section. Note that this overview is purely illustrative of the phenomena involved and the direction of arrows can be incorrect. It can be observed that the tank is heated up resulting from heat ingress by a Q_{in} . This Q_{in} varies per location, depending on its location with relation to the water level, fuel level and cofferdams. In case there is a temperature difference between the liquid and vapour phases, heat transfer will occur between those. As the heat inflow causes temperature gradients, large scale convection occurs, both inside the vapour and liquid phase. Due to the increasing temperature, evaporation of the liquid phase occurs, retracting heat and volume from the liquid phase and introducing a significantly larger volume to the vapour phase. For the open tank, the increasing temperature also causes the liquid and vapour phases to expand. For the PRV tank, both the expansion and the evaporation increase the pressure inside the tank until the point at which vapours are expelled in accordance with the behaviour of a PRV.

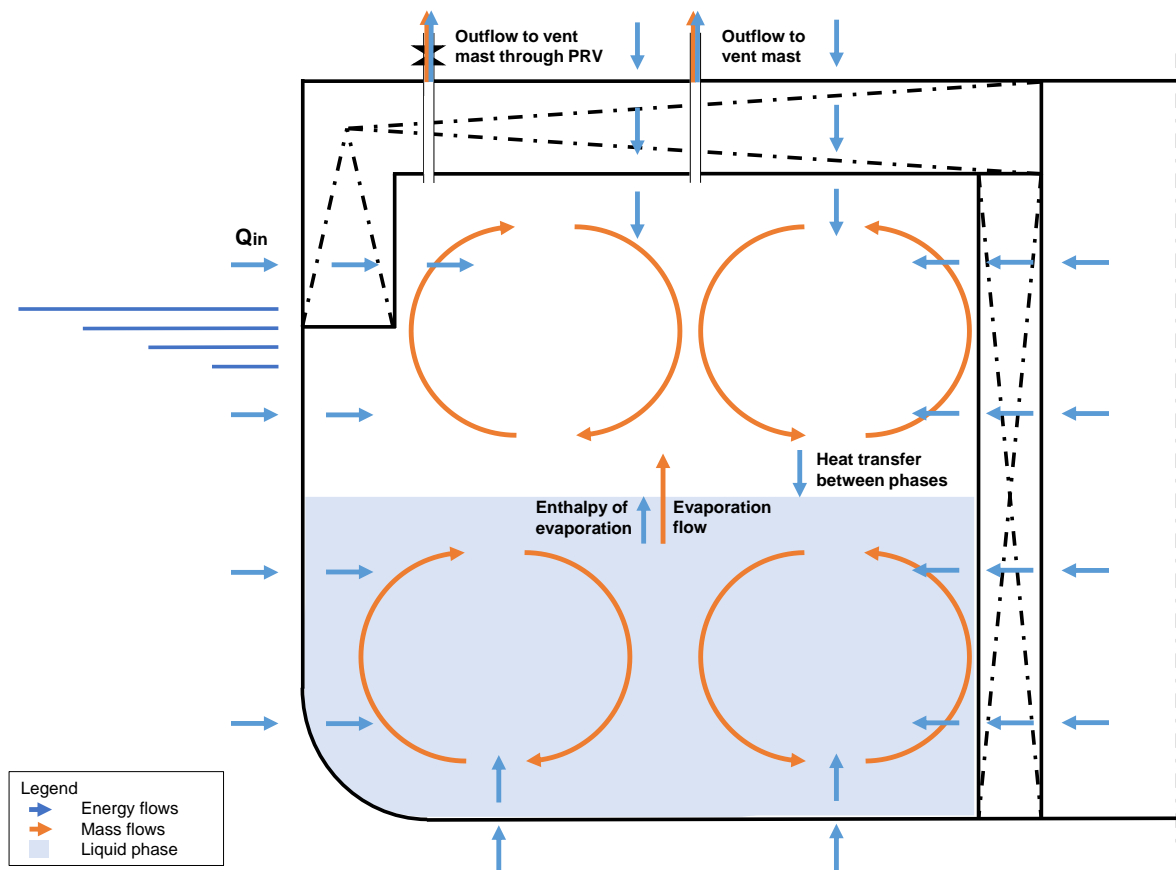


Figure 2.1: Energy and mass flows throughout a ship's tank

2.3.2. Effects near boundaries

To comprehend the heat transfer through a wall, in Figure 2.2 a qualitative sketch of the temperature distribution at the intersection of the wall and phase boundaries is provided. For simplicity reasons, this

illustration only includes conduction effects and no convection. Here, the air is separated from the tank contents by a steel wall. The wall is represented by a black line and therefore the heat profile throughout the wall is not depicted. The heat profile of the tank wall is however part of the heat balances discussed here. The temperature sketch is derived from the analysis of the heat transfer through a tank wall by [11], however the liquid phase is added by the author and so is the concentration distribution.

Temperature distribution

In Figure 2.2, multiple effects are described. The liquid phase is heated up slower than the vapour phase due to its high thermal mass [3]. However, as also the heat conductance of the liquid phase is higher than that of the vapour phase [11], it absorbs more heat and therefore cools the ambient air to a larger extent. Next to heat transfer from the outside, internally also heat transfer is occurring, resulting in vertical gradients throughout both phases.

Concentration distribution

In Figure 2.2, also the concentration distribution of methanol is sketched. It is straightforward that the ambient air contains no significant amount of methanol and the liquid phase experiences the highest methanol concentrations. More interesting is the vapour phase, where higher concentrations are found near the liquid surface and away from the wall. This concentration distribution is a result of three effects: the vapour phase is saturated near the free surface; the saturation concentration level is higher for higher temperatures; mass transfer of vapour in gas is governed by absolute concentration differences [19]. Linking this to the temperature profile, a translation from temperature profile to concentration profile can be made: at the free surface, the concentration is highest close to the wall; due to the high concentration at the free surface, the concentration difference towards the vapours further away is larger; thus mass transfer is larger and finally, the concentrations are higher near the wall.

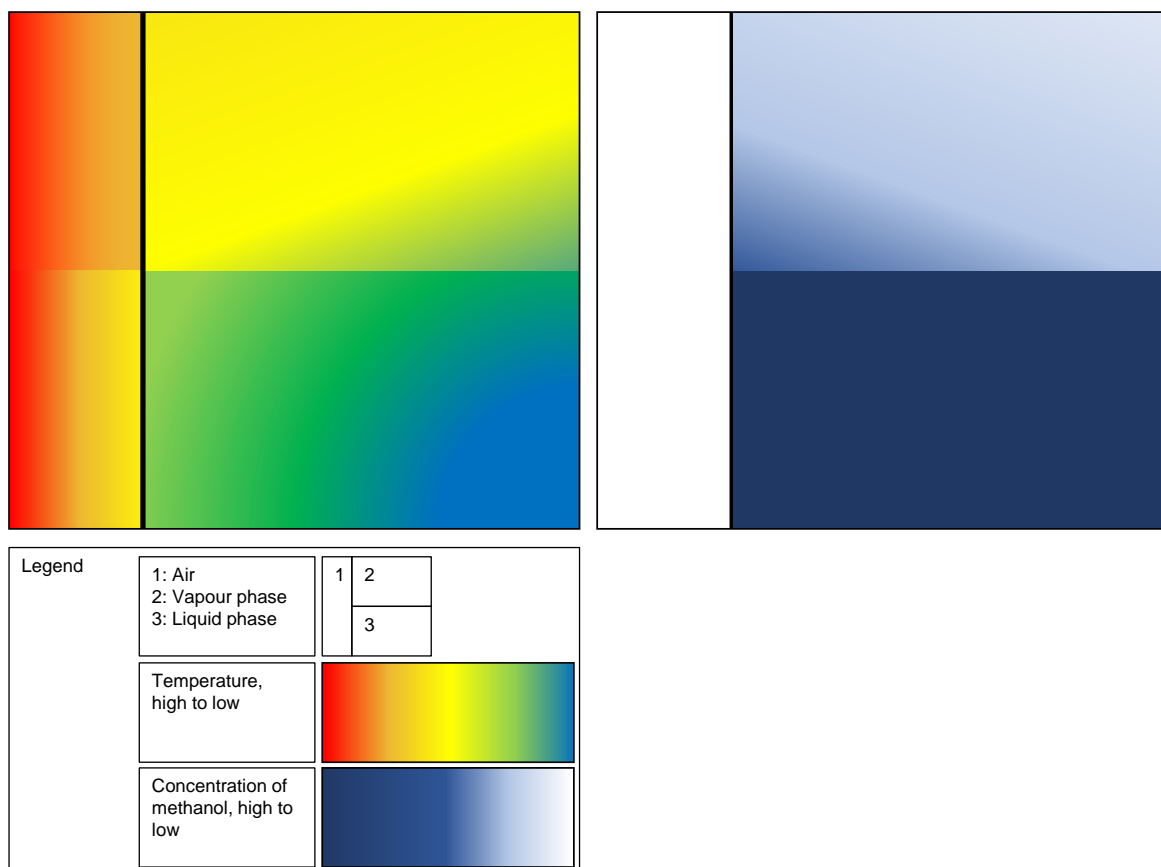


Figure 2.2: Illustration of temperature distribution as derived from the analysis of [11] (left) and of methanol concentrations (right) at the wall and phase boundaries

2.4. Conclusions

In this chapter, the thermodynamic phenomena of a ship's methanol tank are described. The phenomena general to methanol storage originate from [11]. The elements that describe the context inside a ship are partially found in [12], [13] and [14] and are partially derived by the author. An overview of the inventory is presented below.

Described in [11]:

- Heat transfer throughout vapour phase
- Mass transfer throughout vapour phase
- Varying ambient temperature
- Heat transfer throughout liquid phase and between liquid and vapour phase
- Varying temperatures throughout:
 - Liquid phase
 - Vapour phase
 - Tank walls
- Varying ambient pressure
- Condensation
- Inflow of air

Derived from [11]:

- Evaporation
- Saturation of vapour phase
- Outflow of vapours

Described in the field of LNG [12], [13] and [14]:

- Scenario of fire in cofferdam or space adjacent to cofferdam
- Sloshing
- Heat ingress into the wall from adjacent cofferdam

Added by the author:

- Behaviour of a PRV
- Heat ingress into the wall from ambient air
- Compression and expansion of tank contents
- Heat ingress into the wall from seawater
- In- and outflow of liquid fuel

3

Model derivation

In this chapter, the model derived in this research is described. As a venture point, the inventory of phenomena is processed until a set of phenomena remains that can be modelled. The model derived is yet again a simplification of these phenomena.

3.1. Processing of phenomena

To arrive at a model, here it is discussed how the observed phenomena are led into the further parts of the research. The basis of the solution is presented in Moncalvo et al. [10]. Here a model is presented of an aerated land-based tank which is cooling down under influence of a rain shower. This model includes the phenomena of condensation, heat and mass transfer throughout the vapour phase, a varying ambient temperature and an inflow of air. The remainder of the observed phenomena are derived in this analysis, neglected or placed out of scope. The phenomena that are placed out of scope are listed here: condensation; inflow of air; sloshing; heat ingress through a cofferdam and the in- and outflow of liquid fuel. All the phenomena that remain, are derived in this analysis. An overview is presented in [Table 3.1](#).

Per phenomenon that is placed out of scope, a brief motivation is provided on the exclusion. As mainly the outflow of methanol is of interest, the focus is put on evaporation and an outflow of vapours and condensation and an inflow of air are excluded from the scope. As an analytical model is sought after, it is expected that, with the resources at hand, it is impossible to model sloshing. The same holds for modelling cofferdams, as it would dramatically increase the complexity of the shapes modelled compared to one rectangular shape. Also for reasons of simplicity, the modelling of the in- and outflow of liquid fuel are excluded.

Table 3.1: Overview of phenomena involved and how they are led into further research

Source of phenomenon/How tackled	Solution presented in [10]	Solution presented in this research	Out of scope
Described in [11]	<ul style="list-style-type: none"> • Heat transfer throughout vapour phase • Mass transfer throughout vapour phase • Varying ambient temperature 	<ul style="list-style-type: none"> • Heat transfer throughout liquid phase and between liquid and vapour phase • Varying temperatures throughout: <ul style="list-style-type: none"> ○ Liquid phase ○ Vapour phase ○ Tank walls • Varying ambient pressure 	<ul style="list-style-type: none"> • Condensation • Inflow of air
Derived from [11]		<ul style="list-style-type: none"> • Evaporation • Saturation of vapour phase • Outflow of vapours 	
Described in the field of Liquefied Natural Gas (LNG) [12], [13] and [14]		<ul style="list-style-type: none"> • Scenario of fire in cofferdam or any ambient adjacent to tank 	<ul style="list-style-type: none"> • Sloshing • Heat ingress into the wall through cofferdam
Added by the author		<ul style="list-style-type: none"> • Behaviour of a PRV • Heat ingress into the wall from ambient air • Heat ingress into the wall from seawater • Compression and expansion of tank contents 	<ul style="list-style-type: none"> • In- and outflow of liquid fuel

3.2. Model description

To assist the reader, a description of the model is already provided here and illustrated in [Figure 3.1](#), [Figure 3.3](#) and [Figure 3.4](#). This description is however a result of the analysis executed in later parts of this chapter. There, the translation from phenomena to a model is made and the underlying motivations, assumptions and implementation steps are provided.

3.2.1. Overview of the thermodynamical model and definition of areas

The overview of the thermodynamic model in this research is provided in [Figure 3.1](#). The model is set up for a rectangular tank, it can model the influence of heat ingress and can be closed off with a Pressure Relief Valve (PRV) or can be aerated. The tank can be modelled as to be fully surrounded by the ambient air or have the tank wall touching the sea. Heat ingress Q_{in} occurs as a result of an ambient temperature T_{amb} that is higher than the initial temperature of the tank wall T_{wall-0} and tank contents T_{bulk-0} .

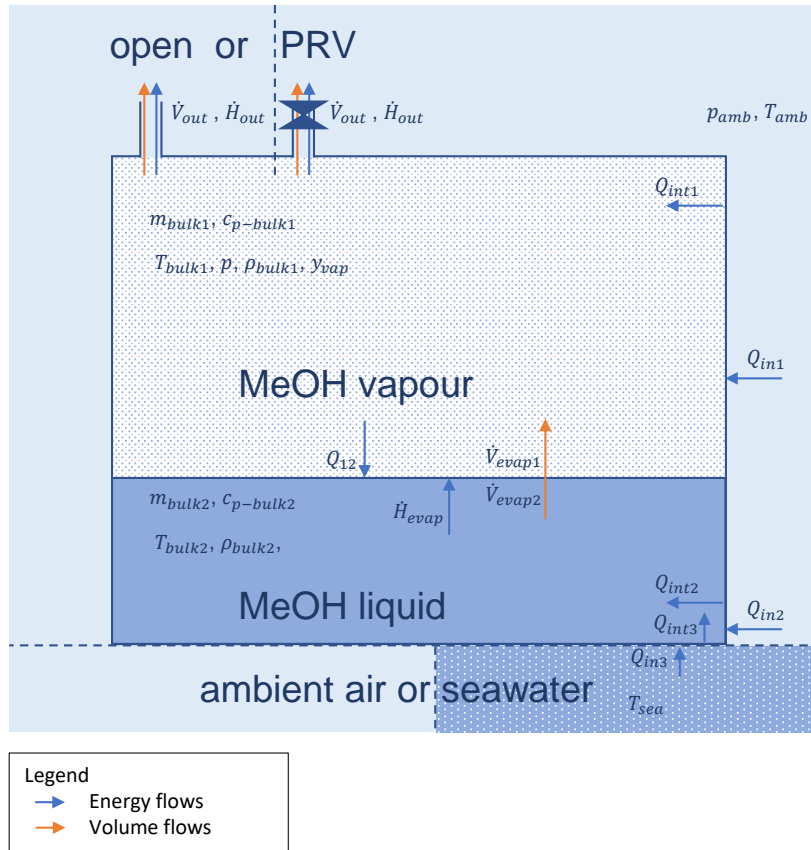


Figure 3.1: Overview of the thermodynamic model in this research

The bulk phase is split up into a vapour phase and a liquid-phase of pure methanol. The vapour phase is a mixture of methanol vapours with a gas being either air or nitrogen. In total, this yields four to five regions to be modelled (depending on the presence of seawater):

1. the vapour phase, bulk 1;
2. the liquid phase, bulk 2;
3. the wall touching the vapour phase, wall 1;
4. the wall touching the liquid phase, wall 2;
5. and if the presence of seawater is modelled, the tank floor is referred to as wall 3, and wall 2 is reduced to being the sides of the tank adjacent to the liquid phase.

Using the dimensions as displayed in Figure 3.2, $A_{floor} = LB$ and $L_{circ} = 2(L + B)$, the areas are defined as follows:

- Whether the presence of seawater is modelled or not:
 1. $A_{tank1} = A_{floor} + (H_{tank} - H_{liq})L_{circ}$ being the area adjacent to the vapour phase.
- If the tank is modelled with air as only ambient condition:
 2. $A_{tank2} = A_{floor} + H_{liq}L_{circ}$ being the area adjacent to the liquid phase.
- If the tank is modelled with air and seawater against the tank floor as ambient conditions:
 2. $A_{tank2} = H_{liq}L_{circ}$ being the area between the liquid phase and ambient air.
 3. $A_{tank3} = A_{floor}$ being the area between the liquid phase and the seawater, which is the tank floor.

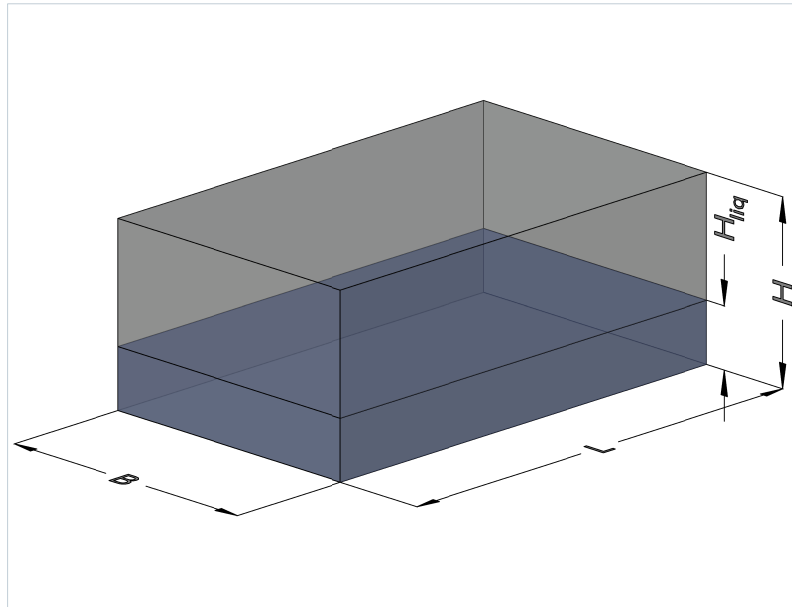


Figure 3.2: Overview of the dimensioning used in the model

The interactions between the various regions in the model are explained here when influenced by heat ingress. Note however that evaporation can also be caused by a low vapour concentration level in the vapour phase of the tank. Both bulk 1 and 2 experience heat ingress and also between them occurs heat and mass transfer. The mass transfer is a result of liquid methanol evaporating into the vapour phase. For an aerated tank, the heat ingress directly results in expansion of the vapour phase \dot{V}_{expans} or for a closed tank into pressure build-up. It indirectly results in evaporation of the liquid phase \dot{V}_{evap-1} due to which a relatively small liquid volume then occupies a large volume as a vapour. The latter is an endothermic process, which consumes energy from the liquid phase \dot{H}_{evap} . When a tank is closed off with a PRV, the combination of the evaporation and heating up of the vapour phase will cause a pressure build up until the PRV reaches its setting pressure and opens. At that point, the vapour phase will expand and some vapours will be expelled \dot{V}_{out} . For an aerated tank, this process is an immediate consequence of heat ingress.

3.2.2. Detailed view of the interactions occurring near the boundaries

A detailed view of the interactions occurring near the boundaries of wall 1 and wall 2 in the thermodynamic model is displayed in Figure 3.3. Here, five different regions can be observed: the vapour phase, the liquid phase, the tank wall next to the vapour phase, the tank wall next to the liquid phase and the ambient air. Each region has its own separate temperature, which is assumed to be constant throughout that region. How the complex boundary phenomena observed in Section 2.3.2 are modelled is discussed in Section 3.3.2. Here, it suffices to understand that the heat flows between these regions depend on fluid or material characteristics and temperature differences – the larger the temperature difference, the larger the heat flow.

As a result of the different heat capacities and heat transfer characteristics in the liquid phase and vapour phase, these can have different temperatures. Combining this with the temperature dependency for internal heat flows Q_{int1} and Q_{int2} , it follows that the temperature of the wall next to the vapour phase T_{wall1} can differ from that next to the liquid phase T_{wall2} . With the same reasoning, a heat ingress from the ambient air into the wall can also differ and is split up into Q_{in1} and Q_{in2} . For the description of the heat and mass transfer between the liquid and vapour phases and the expansion and evaporation effects, the reader is referred to ??.

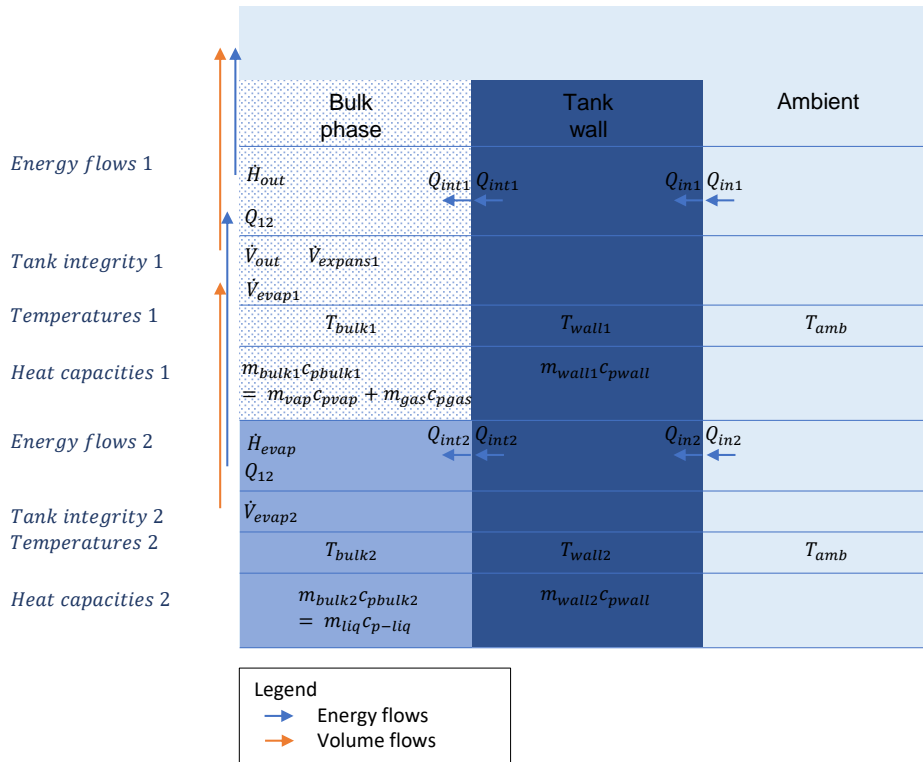


Figure 3.3: Detail of the boundaries near wall 1 and 2 of the thermodynamic model in this research

If the presence of seawater against the tank floor is modelled, the temperature equilibrium of the tank floor is modelled separately as wall 3. The detail on its boundaries is displayed in Figure 3.4. Note that this wall interacts with bulk 2 and there is no bulk 3. However, the values for the heat flows can be different than for wall 2 and therefore Q_{int3} and Q_{in3} are described.

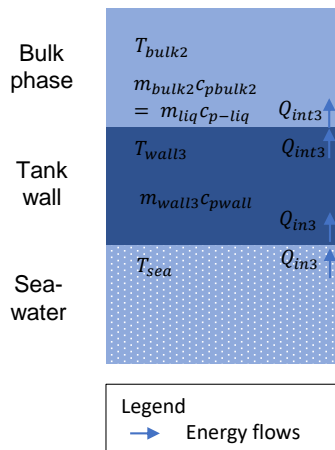


Figure 3.4: Detail of the boundaries of wall 3 in the thermodynamic model in this research

3.3. Governing equations

In this section, the thermodynamic basis for the model is provided. This is a translation of the thermodynamic phenomena, presented in Chapter 2, towards a model. Descriptions of heat and mass transfer are provided and ultimately bundled together by the 1st law of thermodynamics that states that in a closed system energy cannot be created nor destroyed [20]. The 1st law makes its appearance here as keeping track of where energy comes from and goes to. As the translation of phenomena towards a

model is a process involving assumptions, for each phenomenon each step of this process is presented separately and if necessary additional elaboration is provided:

1. Why is this phenomenon modelled?
2. How is this phenomenon modelled?
3. What are the assumptions made?

Firstly, the basis is provided for an airbreathing tank and secondly, the adaptations towards a tank with PRV are provided. When the thermodynamic basis is formed, the integration towards a model is executed in [Section 3.4](#).

3.3.1. Energy balances for an aerated tank

Temperature differences

1. The temperature differences occurring throughout a ship's tank are expected to be significant. Also, it are driving forces in the transients when a tank is heated.
2. Temperature differences throughout the tank are modelled by splitting the tank and its contents up into the four or five aforementioned regions. These four to five regions all have their own energy balance in which the interactions with the other regions and the ambient air are described. This is similar to what is described in [10], except for the fact that in that analysis there is only a combined (liquid and vapour) bulk phase and therefore also only one wall energy balance.
3. Here it is assumed that throughout each region, the temperature is constant.

Heat capacity

1. The fluid and material characteristics of the tank and its contents vary greatly per region and therefore require individual representation.
2. The heat capacity of each region is modelled by its mass multiplied by its specific heat capacity for constant pressure c_p . For the vapour phase, this is split up into an addition of the methanol vapour heat capacity $m_{vap}c_{p-vap}$ with the heat capacity of the gas inside the tank $m_{gas}c_{p-gas}$. This is either air $m_{air}c_{p-air}$ or nitrogen $m_{N_2}c_{p-N_2}$. This approach is in close resemblance to the approach in [10].
3. In this, multiple assumptions are made:
 - The specific heat values c_p are constant with varying temperatures.
 - All the regions experience perfect mixing.

Interactions between the regions

1. The interactions between the different regions and the ambient air describe how the driving forces interact and will eventually find a balance.
2. As presented in [10], the interactions between the regions are modelled by various heat flows, here presented per region. A sign convention is used that defines inward heat flow as positive, therefore the interactions are presented when under influence of heat ingress:
 - The vapour phase experiences heat ingress from the adjacent wall Q_{int1} and loses heat to the liquid phase Q_{12} . Together with the aforementioned phenomena, this results in [Equation \(3.1\)](#).
 - The liquid phase experiences heat ingress from the adjacent wall (either only Q_{int2} or Q_{int2} and Q_{int3}) and the vapour phase Q_{12} . Next to that, heat is extracted due to the process of evaporation being endothermic \dot{H}_{evap} . Together with the aforementioned phenomena, this results in [Equation \(3.2\)](#).
 - The wall adjacent to the vapour phase experiences heat ingress from the ambient air Q_{in1} and loses heat towards the vapour phase Q_{int1} . Together with the aforementioned phenomena, this results in [Equation \(3.3\)](#).

- The wall adjacent to the liquid phase experiences heat ingress from the ambient air Q_{in2} and loses heat towards the liquid phase Q_{int2} . Together with the aforementioned phenomena, this results in [Equation \(3.4\)](#).
- When seawater is modelled, the energy flow from wall 2 is split up into wall 2 and wall 3 and the energy balance for the liquid bulk becomes [Equation \(3.5\)](#).
- When seawater is modelled, the tank floor (wall 3) experiences heat ingress from the ambient air Q_{in3} and loses heat towards the liquid phase Q_{int3} . Together with the aforementioned phenomena, this results in [Equation \(3.6\)](#).

3. In this, multiple assumptions are made:

- Heat transfer between wall 1 and wall 2 and between wall 2 and wall 3 is neglected.
- The resistance in transferring heat provided by the wall is assumed to be of negligible extent compared to the resistance of the adjoining fluids. This neglects a temperature gradient over the thickness of the wall and any insulation provided by coating layers.
- The heating of newly evaporated mass from T_{bulk2} to T_{bulk1} is assumed to be negligible towards the energy consumed by evaporating this amount of mass.
- When during a simulation the liquid level is changing, the heat involved in changing the wall temperature from T_{wall1} to T_{wall2} or vice versa is neglected.
- The heat transfer resistance of the wall is assumed negligible towards the heat transfer resistance of the vapour phase, the ambient air and the liquid phase.

Resulting equations

$$\frac{dU_{bulk1}}{dt} = (m_{vap}c_{p-vap} + m_{gas}c_{p-gas}) \frac{dT_{bulk1}}{dt} = Q_{int1} - Q_{12} \quad (3.1)$$

$$\frac{dU_{bulk2}}{dt} = m_{liq}c_{p-liq} \frac{dT_{bulk2}}{dt} = Q_{int2} + Q_{12} - \dot{H}_{evap} \quad (3.2)$$

$$\frac{dU_{wall1}}{dt} = m_{wall1}c_{p-wall} \frac{dT_{wall1}}{dt} = -Q_{int1} + Q_{in1} \quad (3.3)$$

$$\frac{dU_{wall2}}{dt} = m_{wall2}c_{p-wall} \frac{dT_{wall2}}{dt} = -Q_{int2} + Q_{in2} \quad (3.4)$$

$$\frac{dU_{bulk2}}{dt} = m_{liq}c_{p-liq} \frac{dT_{bulk2}}{dt} = Q_{int2} + Q_{int3} + Q_{12} - \dot{H}_{evap} \quad (3.5)$$

$$\frac{dU_{wall3}}{dt} = m_{wall3}c_{p-wall} \frac{dT_{wall3}}{dt} = -Q_{int3} + Q_{in3} \quad (3.6)$$

3.3.2. Energy flow equations for an aerated tank

Heat transfer

1. The heat transfer characteristics between the different regions and the ambient air are very different for the different interactions between the regions. Here, it is intended to capture the behaviour near the boundaries as discussed in [Section 2.3.2](#).
2. Identical to what is presented in [10], these heat transfer characteristics are modelled by the heat transfer coefficient k multiplied by the area A_{tank} and the temperature difference involved. For the individual heat flows, this is described in [Equation \(3.7\)](#) through to [Equation \(3.13\)](#). This captures the interactions presented in [Section 3.3.1](#) and describes the heat flows as illustrated in [Figure 3.1](#), [Figure 3.3](#) and [Figure 3.4](#). A note to the reader is that the heat flows will explain themselves when taking a look at these figures whilst studying the equations.
3. In this, multiple assumptions are made:
 - The heat transfer rates are constant throughout a boundary.

- The heat transfer rate is linearly dependent on only the temperature difference over a boundary.
- The heat transfer rate between the liquid and vapour phases is governed by the heat transfer characteristics of the vapour phase.

Energy consumption of evaporation

1. The evaporation of the liquid methanol requires energy, which can be of a significant influence on the total heat balance.
2. In parallel to what is presented in [10], the flow of the enthalpy of evaporation \dot{H}_{evap} is determined by its density ρ_{vap} multiplied by its volume flow \dot{V}_{evap-1} and the specific enthalpy of evaporation Δh_{evap} . This is described in Equation (3.14).
3. Here it is assumed that the enthalpy of evaporation is constant with varying temperature and pressure. The impact of the assumption is discussed in Section 5.1.4.

Resulting equations

$$Q_{in1} = k_{in} A_{tank1} (T_{amb} - T_{wall1}) \quad (3.7)$$

$$Q_{in2} = k_{in} A_{tank2} (T_{amb} - T_{wall2}) \quad (3.8)$$

$$Q_{in3} = k_{liq} A_{tank3} (T_{sea} - T_{wall3}) \quad (3.9)$$

$$Q_{int1} = k_{vap} A_{tank1} (T_{wall1} - T_{bulk1}) \quad (3.10)$$

$$Q_{int2} = k_{liq} A_{tank2} (T_{wall2} - T_{bulk2}) \quad (3.11)$$

$$Q_{int3} = k_{liq} A_{tank3} (T_{wall3} - T_{bulk2}) \quad (3.12)$$

$$Q_{12} = k_{vap} A_{surf} (T_{bulk1} - T_{bulk2}) \quad (3.13)$$

$$\dot{H}_{evap} = \rho_{vap} \dot{V}_{evap-1} \Delta h_{evap} \quad (3.14)$$

3.3.3. Volume flow equations for an aerated tank

As from now on the description of concentration levels is of importance, its descriptions are elaborated on here. Mainly the volumetric vapour fraction y_{vap} is used which describes the volume fraction that the vapour occupies. It is therefore identical to the absolute concentration level on volumetric basis. When the ideal gas law is assumed, each molecule in a gas mixture occupies the same amount of volume irrespective of which substance it is. Then, the volumetric vapour fraction is equal to the molar vapour fraction. However, as molar masses can differ, it is not equal to the vapour fraction on a mass basis, even when the ideal gas law is assumed. The values of the volumetric vapour fraction can vary between 0 and 1 and is generally simply referred to as *the vapour fraction* without specifying that it is on volumetric basis.

As opposed to the absolute concentration level, occasionally the relative concentration level ϕ is used. This is the ratio of the (absolute) vapour fraction to the saturation vapour fraction. It finds its parallel in the term *relative humidity* and can also not exceed 1 [20].

Methanol vapour pressure

1. At the free surface of a liquid, molecules tend to escape. This is the driving force of evaporation.
2. This tendency to evaporate can be represented by the vapour pressure p_{vap} , which varies for varying temperature and is unique per substance. In turn, the semi-empirical Antoine equation describes the vapour pressure, as also used in [9] and displayed in Equation (3.15). The values for A, B and C are presented in Table 3.2. The accuracy of the fit with experimental data is deemed satisfactory [21] and is discussed more in depth in Section 3.6. For methanol, the vapour pressure against temperature curve is displayed in Figure 3.5 showing a continuous increase for increasing temperature.

3. Here it is assumed that:

- The tendency of molecules to evaporate can be accurately represented by a single value for the vapour pressure at a certain temperature.
- The Antoine equation can accurately represent the vapour pressure curve.

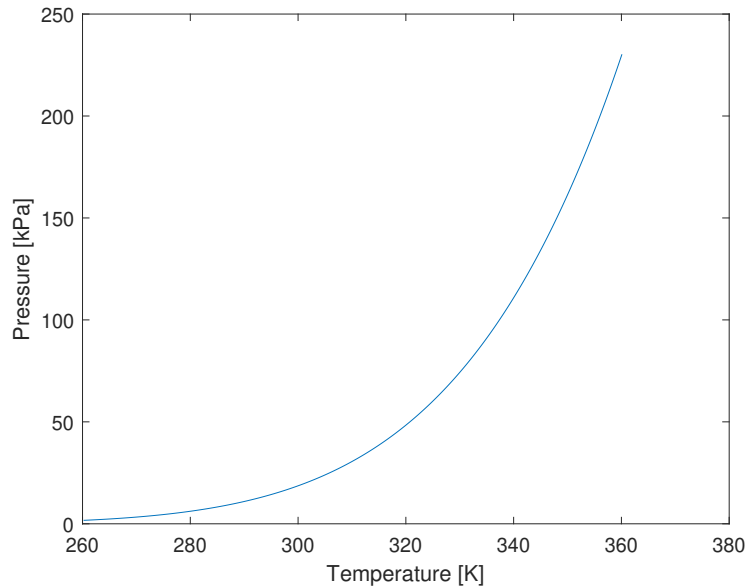


Figure 3.5: Vapour pressure curve for methanol using the Antoine equation

Free surface concentration levels

1. For describing mass transfer rates, it is required to have a description of the concentration levels at the free surface of the liquid.
2. At the surface of a liquid, vapour is always saturated and the concentration is determined only by the temperature T_{bulk2} at the free surface and pressure p . The saturation concentration $y_{vap-surf}$ is determined by the partial pressure of the vapour, also the vapour pressure, divided by the total pressure. The combined result is depicted in Equation (3.16). This for example means that if the liquid temperature is 320K this results in a vapour pressure of 48.4 kPa (see Figure 3.5). Which for an ambient pressure of 100 kPa results in a vapour fraction at the free surface of $y_{vap-surf} = 0.484$.

3. Here it is assumed that:

- The temperature at the free surface is equal to the temperature of the bulk phase T_{bulk2} .
- The gas is an ideal gas, neglecting interparticle forces [19]. Together with the assumption that the c_p and c_v values are constant (Section 3.3.1), this results in the perfect gas assumption.
- The Dalton Law (based on the assumption of an ideal gas) holds. This means that the concentration level of a constituent in a gas mixture is determined by its partial pressure over the total pressure [19].

Saturation limit and vapour phase concentration

1. When the vapour phase reaches its saturation limit, it can no longer take in additional vapours. If nonetheless the free surface concentration is higher, evaporation will still take place and an equivalent amount condenses in the vapour phase to eventually precipitate out [19].

2. In the vapour phase, the methanol concentration $y_{vap-bulk1}$ can be determined by the ideal gas law, with the limitation that it is below the saturation level $y_{vap-bulk1-sat}$ for that temperature and pressure and is described in Equation (3.17). In [10], this limitation is absent, resulting in situations where the saturation limit is exceeded and large vapour volumes are present.
3. Here it is assumed that:
 - The methanol concentration is constant throughout the vapour phase except for the volume close to the free surface, which is assumed to be of negligible size.
 - The saturation limit can be treated as a stop in evaporation. This neglects an enthalpy flow of enthalpy of evaporation consumed by the liquid phase that is released in the vapour phase when condensation occurs.

Evaporation rate

1. As the evaporation of methanol can be a significant contributor to outflow, a description of its rate is required.
2. The evaporation rate has to take the inequality in Equation (3.17) into account and therefore results in two different evaporation rates:
 - As long as the vapour concentration is below the saturation limit, the evaporation rate will be determined by the mass transfer relation. Similar to the approach in [10], a mass transfer coefficient β_{bulk} is multiplied by the concentration difference ($y_{vap-surf} - y_{vap-bulk1}$) and the area over which this difference occurs $A_{surf} = A_{floor}$ and is described in Equation (3.19). The description of the mass transfer coefficient (as displayed in Equation (3.18)) is used in the context of stationary tanks [9] and in more general applications [20] and here is a function of the chemical characteristics of methanol and air or nitrogen. The concentration levels that determine the concentration difference are different between what is described in [10] and here due to a different situation being modelled. Note that despite that both descriptions presented here for the evaporation rate describe a *mass transfer*, this first description is labelled $\dot{V}_{evap-mt}$ as throughout literature this equation is named the *mass transfer relation* [9] [10] [11].
 - However, at the saturation limit, the evaporation rate is modelled by the temperature derivative of the saturation concentration curve $\frac{d(y_{vap-bulk1-sat})}{dT_{bulk1}}$ and the derivative of the temperature itself $\frac{dT_{bulk1}}{dt}$ as presented in Equation (3.20). Note that the temperature derivative of the saturation concentration curve is different for different temperatures.
3. Here it is assumed that:
 - The mass transfer rate is constant across the free surface.
 - For non-saturated conditions, the mass transfer rate is linearly dependent on only the concentration difference between the free surface and the vapour phase.
 - For saturated conditions, the time derivatives of V_{bulk1} and p are neglected.

Outbreathing rate

1. As the outbreathing rate of methanol and air or nitrogen is sought after, it should be modelled. Next to that, it is required for conservation of mass in combination with modelling the tank integrity.
2. In line with [10], the outbreathing rate is the sum of the expansion of the vapour phase as a consequence of a temperature increase $\frac{V_{bulk1}}{T_{bulk1}} \frac{dT_{bulk1}}{dt}$ with the evaporation flow \dot{V}_{evap-1} and is displayed in Equation (3.21).
3. Here it is assumed that:
 - The exchange of gasses and vapours between the tank and the environment is only a consequence of a surplus or deficit in the total volume of the contents of the tank. This assumption neglects any exchange of gasses and vapours that might take place without having net volume flows. In practice, for an open tank, this is a result of concentration differences being present over the length of the piping towards the vent mast. It is this behaviour that is neglected. For a tank with PRV, this does not apply.

- The expansion of the liquid phase is negligible.
- In determining the value for the contribution of evaporation to the total outflow \dot{V}_{out} , the volume that is no longer occupied by the liquid methanol is assumed to be negligible towards the volume newly occupied by the evaporated methanol. At 15°C and a pressure of 101.3 kPA, the specific density of vaporized methanol is $5.87 * 10^5$ as large as its density when liquid [22]. As a result $\dot{V}_{evap-1} \gg \dot{V}_{evap-2}$, which forms the basis of this assumption.
- The tank is a stiff structure.

Resulting equations

$$p_{vap} = 10^{A - \frac{B}{C+T}} \quad (3.15)$$

$$y_{vap-surf} = \frac{10^{A - \frac{B}{C+T_{bulk2}}}}{p} \quad (3.16)$$

$$y_{vap-bulk1} = \frac{m_{vap}RT_{bulk1}}{V_{bulk1}pM_{cargo}} \leq y_{vap-bulk1-sat} = \frac{10^{A - \frac{B}{C+T_{bulk1}}}}{p} \quad (3.17)$$

$$\beta_{bulk} = \frac{k_{vap}}{\rho_{bulk1}c_{p-vap}Le^{2/3}} \quad (3.18)$$

$$\dot{V}_{evap-mt} = \beta_{bulk1}A_{surf}(y_{vap-surf} - y_{vap-bulk1}) \quad (3.19)$$

$$\dot{V}_{evap-sat} = \frac{d(y_{vap-bulk1-sat})}{dT_{bulk1}} \frac{dT_{bulk1}}{dt} V_{bulk1} \quad (3.20)$$

$$\dot{V}_{out} = \frac{V_{bulk1}}{T_{bulk1}} \frac{dT_{bulk1}}{dt} + \dot{V}_{evap-1} \quad (3.21)$$

3.3.4. Mass flow equations for an aerated tank

Densities in the vapour phase

1. To keep track of mass flows and link them with volume flows, the densities of the individual elements in the vapour phase require a description. Therefore, the use of partial densities is introduced.
2. The ideal gas law is used to determine the partial densities which are presented in Equation (3.22) and Equation (3.23) for ρ_{vap} and ρ_{gas} , respectively.
3. Here it is assumed that:
 - The partial density of the vapour is constant throughout the vapour phase.
 - The average molecular mass of air can be represented universally by one M_{air} .

Evaporation

1. The same motivation for modelling the evaporation of methanol mass described in Section 3.3.3 applies here.
2. The evaporation rate in terms of mass flow is modelled as a multiplication of the volumetric evaporation rate \dot{V}_{evap-1} with the partial density of the vapour ρ_{vap} and is presented in Equation (3.24).
3. This does not involve additional assumptions.

Outbreathing

1. The same motivation for modelling the outbreathing rate of methanol and air or nitrogen described in Section 3.3.3 applies here.
2. Outbreathing of one substance is modelled as its concentration fraction multiplied by the total outflow \dot{V}_{out} and results in Equation (3.25) and Equation (3.26).
3. This does not involve additional assumptions as perfect mixing is already assumed.

Resulting equations

$$\rho_{vap} = \frac{pM_{vap}}{RT_{bulk1}} \quad (3.22)$$

$$\rho_{gas} = \frac{pM_{gas}}{RT_{bulk1}} \quad (3.23)$$

$$\dot{m}_{liq} = -\dot{V}_{evap-1}\rho_{vap} \quad (3.24)$$

$$\dot{m}_{vap} = \rho_{vap}(\dot{V}_{evap-1} - y_{vapbulk1}\dot{V}_{out}) \quad (3.25)$$

$$\dot{m}_{gas} = -\rho_{gas}(1 - y_{vapbulk1})\dot{V}_{out} \quad (3.26)$$

3.3.5. Empty tank situation

When the tank runs empty, there are a few changes in the equations which can be easily understood by taking a look at [Figure 3.1](#) and are presented in [Equation \(3.27\)](#) through to [Equation \(3.29\)](#) for when no seawater is modelled. With the exception of the energy balance of the liquid phase, all energy balances ([Equation \(3.1\)](#), [Equation \(3.3\)](#) and [Equation \(3.4\)](#)) are evaluated. However, now the inflow from wall 2 into the bulk phase, goes directly into the vapour phase and is therefore related to T_{bulk1} instead of T_{bulk2} and is determined by k_{vap} instead of k_{liq} . To link it to the vapour phase, it is linked to Q_{12} , but in opposite direction as it is defined to flow in opposite direction (see [Figure 3.1](#)). Furthermore, as there is no liquid phase anymore, there is no evaporation, so the evaporation rate is zero. This does not involve additional assumptions.

$$Q_{int2} = k_{vap}A_{tank2}(T_{wall2} - T_{bulk1}) \quad (3.27)$$

$$Q_{12} = -Q_{int2} \quad (3.28)$$

$$\dot{V}_{evap-1} = 0 \quad (3.29)$$

When modelling seawater, the area definition is slightly different (see [Section 3.2.1](#)). Then, wall 2 is the wall area touching the sides of the liquid, which becomes zero ($A_{tank2} = 0$). In this case, [Equation \(3.27\)](#) and [Equation \(3.28\)](#) do not apply and are replaced by [Equation \(3.30\)](#) and [Equation \(3.31\)](#).

$$Q_{int3} = k_{vap}A_{tank3}(T_{wall3} - T_{bulk1}) \quad (3.30)$$

$$Q_{12} = -Q_{int3} \quad (3.31)$$

3.3.6. Boiling behaviour

Initiation of boiling

1. The temperature at which boiling is initiated varies with pressure and therefore requires modelling.
2. Boiling occurs when $p_{vap} = p$ which is identical to $y_{vap} = 1$. Therefore, when the vapour pressure reaches the pressure inside the tank, boiling is initiated. Whenever this is not the case anymore, boiling stops.
3. This is a highly simplified representation of boiling, which in practice requires a wall temperature higher than the boiling temperature [20], making this representation conservative.

Evaporation rate during boiling

1. The evaporation rate is no longer limited by its diffusion rate, but is determined by the inflow of heat. Therefore, it requires a different description.
2. The evaporation is modelled to take in all heat as shown in [Equation \(3.32\)](#) and [Equation \(3.33\)](#), for without or with modelling seawater respectively. This results in the evaporation rate in [Equation \(3.34\)](#).
3. Here it is assumed that:

- The description of heat transfer whilst boiling can be represented by the same description as prior to boiling. This is again a simplified representation of boiling for which the heat transfer varies throughout different stages of the initiation of boiling [20]. The boiling process will on one hand isolate the wall with a vapour film and on the other hand increase heat transfer due to the stimulation of convection [20]. Impact of the uncertainty in the heat transfer for liquids is assessed in Section 5.1.2.
- If boiling occurs at constant pressure and therefore at constant temperature, no assumptions are required. This is because it results in $\frac{dT_{bulk2}}{dt} = 0$ and allows rewriting the energy balance of Equation (3.2) into Equation (3.32). If boiling occurs whilst the pressure is still rising (with a closed PRV), it is appropriate to assume $\dot{H}_{evap} \gg \frac{dU_{bulk2}}{dt}$, which also results in Equation (3.32).

Resulting equations

$$\dot{H}_{evap} = Q_{int2} + Q_{12} \quad (3.32)$$

$$\dot{H}_{evap} = Q_{int2} + Q_{int3} + Q_{12} \quad (3.33)$$

$$\dot{V}_{evap-1} = \frac{\dot{H}_{evap}}{\rho_{vap}\Delta h_{evap}} \quad (3.34)$$

3.3.7. Adaptations towards a tank with PRV

PRV behaviour

1. The pressure increase that can occur with a PRV can have a significant impact on the results, therefore a representation of the behaviour of a PRV is required.
2. The PRV is modelled highly simplified as a device that is closed (meaning that the outflow is zero, see Equation (3.35)) below the setting pressure of the PRV p_{PRV} . When the PRV is closed, the pressure inside the tank is determined by Equation (3.36). When p_{PRV} is reached, the PRV maintains this pressure by outflow of the vapour phase. The situation with the PRV opened is identical to the situation where there is no PRV except for the fact that now $p = p_{PRV}$ instead of $p = p_{amb}$. Therefore, only for the situation in which the PRV is closed, new governing equations need to be set up.
3. Here it is assumed that:
 - The PRV experiences no leakage when closed.
 - The PRV has no resistance when opened.
 - There is no pressure drop after opening. This neglects typical PRV behaviour.

Heat capacity

1. As in a tank that is closed off with a PRV the pressure can build up, the heat capacity at constant pressure does no longer apply.
2. The heat capacity is modelled by a multiplication of the mass multiplied by its specific heat capacity at constant volume c_v . It is split up into an addition of the methanol vapour heat capacity $m_{vap}c_{v-vap}$ with the heat capacity of the gas inside the tank $m_{gas}c_{v-gas}$. For the liquid phase, a multiplication of its mass with c_p is taken.
3. Here it is assumed that:
 - The compressibility of the liquid phase can be neglected due to which the choice of c_p remains appropriate.
 - The specific heats of the vapour can be represented by the c_v values as the increase in volume due to the reduction rate of liquid volume is assumed to be negligible towards other volume flow rates.

Compression work

1. When the PRV is closed, pressure can build up. During a pressure build up, the evaporation rate transfers work into the vapour phase and can result in an additional temperature and pressure increase. As this can have a significant effect on the rate of the pressure increase and the subsequent outflow, modelling this phenomenon is required.
2. The work is represented by $\delta W = pdV_{bulk1}$, which here is $p(-\dot{V}_{evap-1})$. The resulting energy balance is displayed in [Equation \(3.37\)](#).
3. Here it is assumed that the work done is reversible.

Resulting equations

$$\dot{V}_{out} = 0 \quad (3.35)$$

$$p = \left(\frac{m_{gas}}{M_{gas}} + \frac{m_{vap}}{M_{cargo}} \right) \frac{RT_{bulk1}}{V_{bulk1}} \quad (3.36)$$

$$\frac{dU_{bulk1}}{dt} = (m_{vap}c_{v-vap} + m_{gas}c_{v-gas}) \frac{dT_{bulk1}}{dt} = Q_{int1} - Q_{12} + p\dot{V}_{evap-1} \quad (3.37)$$

3.4. Model synthesis

In this section, the governing equations are used to derive a model that solves the equations involved simultaneously. The model is written in differential form, meaning that at each point, the derivative can be determined on the current state of the system. Therefore, a set of seven state parameters have been identified by the author for which this holds. For most state parameters, the equations are a straightforward rewrite of the fundamentals in [Section 3.3](#) and are presented in [Section 3.4.1](#). However, for the evaporation rate with saturated conditions and the energy balance in the vapour phase when a PRV is modelled, additional steps are required. These are described in [Section 3.4.2](#) and [Section 3.4.3](#). Finally, an overview of the model is provided in [Section 3.4.4](#).

3.4.1. Definition of state equations

When modelling air as the only ambient condition, there are varying temperatures in four regions and varying liquid mass, vapour mass and gas mass inside the tank. Then, the seven state parameters in [Equation \(3.38\)](#) can fully determine the state of the model illustrated in [Figure 3.1](#) and [Figure 3.3](#).

$$\vec{y} = \begin{bmatrix} y_1 \\ y_2 \\ y_3 \\ y_4 \\ y_5 \\ y_6 \\ y_7 \end{bmatrix} = \begin{bmatrix} T_{bulk1} \\ T_{wall1} \\ m_{liq} \\ m_{vap} \\ m_{gas} \\ T_{bulk2} \\ T_{wall2} \end{bmatrix} \quad (3.38)$$

Rewriting [Equation \(3.1\)](#), [Equation \(3.2\)](#), [Equation \(3.3\)](#) and [Equation \(3.4\)](#), results in the description for dT_{bulk1}/dt , dT_{bulk2}/dt , dT_{wall1}/dt and dT_{wall2}/dt , respectively in [Equation \(3.39\)](#). Here, dT_{bulk1}/dt is only for the aerated tank and requires further derivation to adapt it to a tank with PRV. This is presented in [Section 3.4.3](#). The mass flows ([Equation \(3.24\)](#), [Equation \(3.25\)](#) and [Equation \(3.26\)](#)) can directly be substituted in [Equation \(3.39\)](#). In non-saturated conditions, the evaporation rate described in [Equation \(3.19\)](#) can be used. For saturated conditions, the evaporation rate presented in [Equation \(3.20\)](#) requires further derivation. This is presented in [Section 3.4.2](#).

$$\vec{y} = \begin{bmatrix} \dot{y}_1 \\ \dot{y}_2 \\ \dot{y}_3 \\ \dot{y}_4 \\ \dot{y}_5 \\ \dot{y}_6 \\ \dot{y}_7 \end{bmatrix} = \begin{bmatrix} dT_{bulk1}/dt \\ dT_{wall1}/dt \\ dm_{liq}/dt \\ dm_{vap}/dt \\ dm_{gas}/dt \\ dT_{bulk2}/dt \\ dT_{wall2}/dt \end{bmatrix} = \begin{bmatrix} \frac{Q_{int1}-Q_{12}}{m_{vap}c_{p-vap}+m_{gas}c_{p-gas}} \\ \frac{-Q_{int1}+Q_{in1}}{m_{wall1}c_{p-wall}} \\ -\dot{V}_{evap-1}\rho_{vap} \\ \rho_{vap}(\dot{V}_{evap-1} - y_{vapbulk1}\dot{V}_{out}) \\ -\rho_{gas}(1 - y_{vapbulk1})\dot{V}_{out} \\ \frac{Q_{int2}+Q_{12}-\dot{H}_{evap}}{m_{liq}c_{p-liq}} \\ \frac{-Q_{int2}+Q_{in2}}{m_{wall2}c_{p-wall}} \end{bmatrix} \quad (3.39)$$

When also modelling seawater against the tank floor, the eight state parameters presented in Equation (3.40) describe the system.

$$\vec{y} = \begin{bmatrix} y_1 \\ y_2 \\ y_3 \\ y_4 \\ y_5 \\ y_6 \\ y_7 \\ y_8 \end{bmatrix} = \begin{bmatrix} T_{bulk1} \\ T_{wall1} \\ m_{liq} \\ m_{vap} \\ m_{gas} \\ T_{bulk2} \\ T_{wall2} \\ T_{wall3} \end{bmatrix} \quad (3.40)$$

Compared to the not modelling seawater, the description for dT_{bulk2}/dt is altered as it now is a rewrite of Equation (3.5) and the description for dT_{wall3}/dt is added which is a rewrite of Equation (3.6).

$$\vec{y} = \begin{bmatrix} \dot{y}_1 \\ \dot{y}_2 \\ \dot{y}_3 \\ \dot{y}_4 \\ \dot{y}_5 \\ \dot{y}_6 \\ \dot{y}_7 \\ \dot{y}_8 \end{bmatrix} = \begin{bmatrix} dT_{bulk1}/dt \\ dT_{wall1}/dt \\ dm_{liq}/dt \\ dm_{vap}/dt \\ dm_{gas}/dt \\ dT_{bulk2}/dt \\ dT_{wall2}/dt \\ dT_{wall3}/dt \end{bmatrix} = \begin{bmatrix} \frac{Q_{int1}-Q_{12}}{m_{vap}c_{p-vap}+m_{gas}c_{p-gas}} \\ \frac{-Q_{int1}+Q_{in1}}{m_{wall1}c_{p-wall}} \\ -\dot{V}_{evap-1}\rho_{vap} \\ \rho_{vap}(\dot{V}_{evap-1} - y_{vapbulk1}\dot{V}_{out}) \\ -\rho_{gas}(1 - y_{vapbulk1})\dot{V}_{out} \\ \frac{Q_{int2}+Q_{int3}+Q_{12}-\dot{H}_{evap}}{m_{liq}c_{p-liq}} \\ \frac{-Q_{int2}+Q_{in2}}{m_{wall2}c_{p-wall}} \\ \frac{-Q_{int3}+Q_{in3}}{m_{wall3}c_{p-wall}} \end{bmatrix} \quad (3.41)$$

3.4.2. Evaporation rate with saturated conditions

To arrive at an expression for \dot{V}_{evap-1} , first a derivative of the vapour mass towards the temperature is derived $dm_{vap-sat}/dT_{bulk1}$ by taking the derivative of Equation (3.42) in Equation (3.43). This incorporates the assumptions presented in Section 3.3.3.

$$m_{vap-sat} = y_{vap-bulk1-sat}V_{bulk1}\rho_{vap} = \frac{10^{A-\frac{B}{C+T_{bulk1}}}V_{bulk1}M_{cargo}}{RT_{bulk1}} \quad (3.42)$$

$$\begin{aligned} \frac{dm_{vap-sat}}{dT_{bulk1}} &= \\ &= \frac{d}{dT_{bulk1}} \left(\frac{10^{A-\frac{B}{C+T_{bulk1}}}}{T_{bulk1}} \right) \frac{V_{bulk1}M_{cargo}}{R} \\ &= \left(\frac{\ln(10)10^{A-\frac{B}{C+T_{bulk1}}}}{T_{bulk1}} \frac{B}{(C+T_{bulk1})^2} - \frac{10^{A-\frac{B}{C+T_{bulk1}}}}{T_{bulk1}^2} \right) \frac{M_{cargo}V_{bulk1}}{R} \end{aligned} \quad (3.43)$$

With this result, the evaporation flow in saturated conditions merely is a multiplication of known terms and is presented in Equation (3.44).

$$\dot{V}_{evap-sat} = \frac{1}{\rho_{vap}} \frac{dm_{vap-sat}}{dT_{bulk1}} \frac{dT_{bulk1}}{dt} \quad (3.44)$$

3.4.3. Adaptations towards a tank with PRV: Energy balance in the vapour phase

In the combined scenario where the PRV is closed and saturation occurs, rewriting equation Equation (3.37) into a description for dT_{bulk1}/dt (see Equation (3.45)) results in an algebraic loop. This is because in that case, \dot{V}_{evap-1} (see Equation (3.44)) is a function of dT_{bulk1}/dt .

$$\frac{dT_{bulk1}}{dt} = \frac{Q_{int1} - Q_{12} + p\dot{V}_{evap-1}}{m_{vap}c_{v-vap} + m_{gas}c_{v-gas}} \quad (3.45)$$

Writing this explicitly in terms of dT_{bulk1}/dt , Equation (3.46) is obtained.

$$\left(\frac{dT_{bulk1}}{dt}\right)_{sat} = \frac{Q_{int1} - Q_{12}}{m_{vap}c_{v-vap} + m_{gas}c_{v-gas} - p \frac{dm_{vap-sat}}{dT_{bulk1}} \frac{1}{\rho_{vap}}} \quad (3.46)$$

3.4.4. Model overview

When coupling the input equations in Equation (3.48) into the system described in Equation (3.47), a system of Ordinary Differential Equations (ODEs) is obtained. The system described here is for when modelling seawater as this is the more complex model, for the non-saturated condition for either the open tank or the PRV tank in the situation where the PRV is opened and for when liquids are present in the tank. After the description of this system, the adaptations to other conditions are provided. To show the interactions between the presented equations, the descriptions provided here are in terms of the state vector \vec{y} .

$$\vec{y} = \begin{bmatrix} y_1 \\ y_2 \\ y_3 \\ y_4 \\ y_5 \\ y_6 \\ y_7 \\ y_8 \end{bmatrix} = \begin{bmatrix} dT_{bulk1}/dt \\ dT_{wall1}/dt \\ dm_{liq}/dt \\ dm_{vap}/dt \\ dm_{gas}/dt \\ dT_{bulk2}/dt \\ dT_{wall2}/dt \\ dT_{wall3}/dt \end{bmatrix} = \begin{bmatrix} \frac{Q_{int1} - Q_{12}}{y_4 c_{p-vap} + y_5 c_{p-gas}} \\ \frac{-Q_{int1} + Q_{in1}}{m_{wall1} c_{p-wall}} \\ -\dot{V}_{evap-1} \rho_{vap} \\ \rho_{vap} (\dot{V}_{evap-1} - y_{vapbulk1} \dot{V}_{out}) \\ -\rho_{gas} (1 - y_{vapbulk1}) \dot{V}_{out} \\ \frac{Q_{int2} + Q_{int3} + Q_{12} - \dot{H}_{evap}}{y_3 c_{p-liq}} \\ \frac{-Q_{int2} + Q_{in2}}{m_{wall2} c_{p-wall}} \\ \frac{-Q_{int3} + Q_{in3}}{m_{wall3} c_{p-wall}} \end{bmatrix} \quad (3.47)$$

$$\begin{aligned}
V_{liq} &= \frac{y_3}{\rho_{liq}} \\
\epsilon &= \frac{V_{liq}}{A_{floor}H_{tank}} \\
H_{liq} &= H_{tank}\epsilon \\
A_{tank1} &= A_{floor} + (H_{tank} - H_{liq})L_{circ} \\
A_{tank2} &= H_{liq}L_{circ} \\
A_{tank3} &= A_{floor} \\
m_{wall1} &= A_{tank1}t_p\rho_{wall} \\
m_{wall2} &= A_{tank2}t_p\rho_{wall} \\
m_{wall3} &= A_{tank3}t_p\rho_{wall} \\
Q_{int1} &= k_{vap}A_{tank1}(y_2 - y_1) \\
Q_{in1} &= k_{in}A_{tank1}(T_{amb} - y_2) \\
Q_{int2} &= k_{liq}A_{tank2}(y_7 - y_6) \\
Q_{in2} &= k_{in}A_{tank2}(T_{amb} - y_7) \\
Q_{int3} &= k_{liq}A_{tank3}(y_8 - y_6) \\
Q_{in3} &= k_{liq}A_{tank3}(T_{sea} - y_8) \\
Q_{12} &= k_{vap}A_{floor}(y_1 - y_6) \\
\rho_{vap} &= \frac{pM_{cargo}}{Ry_1} \\
\rho_{gas} &= \frac{pM_{gas}}{Ry_1} \\
y_{vapsurf-sat} &= \frac{10^{A - \frac{B}{C+y_6}}}{p10^{-5}} \\
y_{vapbulk1} &= \frac{y_4 Ry_1}{V_{bulk1} p M_{cargo}} \\
V_{bulk1} &= \frac{y_4}{\rho_{vap}} + \frac{y_5}{\rho_{gas}} \\
dT_{bulk1}/dt &= \frac{Q_{int1} - Q_{12}}{y_4 c_{p-vap} + y_5 c_{p-gas}} \\
\dot{V}_{evap-1} &= \beta_{bulk1}(y_{vapsurf-sat} - y_{vapbulk1})A_{floor} \\
\dot{V}_{out} &= \frac{V_{bulk1}}{y_1} \frac{dT_{bulk1}}{dt} + \dot{V}_{evap-1} \\
\dot{H}_{evap} &= \rho_{vap} \dot{V}_{evap-1} h_{vcond}
\end{aligned} \tag{3.48}$$

When the vapour phase is saturated, the derivative of the saturation pressure curve depicted in Equation (3.49) is required for the evaporation flow that is shown in Equation (3.50).

$$\frac{dm_{vap}}{dT_{bulk1}} = \left(\frac{\ln(10)10^{A - \frac{B}{C+y_1}} \frac{B}{(C+y_1)^2}}{y_1} - \frac{10^{A - \frac{B}{C+y_1}}}{y_1^2} \right) \frac{M_{cargo} V_{bulk1}}{R} \tag{3.49}$$

$$\dot{V}_{evap-1} = \frac{1}{\rho_{vap}} \frac{dm_{vap-sat}}{dT_{bulk1}} \frac{dT_{bulk1}}{dt} \tag{3.50}$$

In the combined event in which the PRV is closed and the vapour phase is saturated, the derivative of the temperature of the vapour phase is described by Equation (3.51).

$$\frac{dT_{bulk1}}{dt} = \frac{Q_{int1} - Q_{12}}{y_4 c_{v-vap} + y_5 c_{v-gas} - p \frac{dm_{vap-sat}}{dT_{bulk1}} \frac{1}{\rho_{vap}}} \tag{3.51}$$

If the vapour phase is non-saturated and the PRV is closed, the derivative of the temperature of the vapour phase is described by [Equation \(3.52\)](#).

$$\frac{dT_{bulk1}}{dt} = \frac{Q_{int1} - Q_{12} + p\dot{V}_{evap-1}}{y_4c_{v-vap} + y_5c_{v-gas}} \quad (3.52)$$

Independent of the other conditions, when the tank is empty, [Equation \(3.53\)](#) through to [Equation \(3.55\)](#) apply.

$$Q_{int3} = k_{vap}A_{tank3}(y_8 - y_1) \quad (3.53)$$

$$Q_{12} = -Q_{int3} \quad (3.54)$$

$$\dot{V}_{evap-1} = 0 \quad (3.55)$$

Again independent of other conditions, when the liquid is boiling, [Equation \(3.56\)](#) and [Equation \(3.57\)](#) apply. Applying these equations results in $\frac{dT_{bulk2}}{dt} = 0$.

$$\dot{H}_{evap} = Q_{int2} + Q_{int3} + Q_{12} \quad (3.56)$$

$$\dot{V}_{evap-1} = \frac{\dot{H}_{evap}}{\rho_{vap}\Delta h_{evap}} \quad (3.57)$$

3.5. Solving the model

Despite being an analytical model, it requires a numerical solver. To do so, the model is written in Matlab and the set of differential equations is solved with the ODE15S numerical solver. This ODE solver is selected as it is fast, accurate and allows for the definition of a tolerance level to ensure stability while capturing all phenomena.

Within the model, a few other measures are taken to ensure stability. These measures relate to the empty tank situation, the opening and closing of the PRV and the limiting factor in evaporation being mass transfer or the saturation limit.

For the empty tank situation, a cut-off value needs to be defined to avoid having a zero in the numerator of the equation for dT_{bulk2}/dt . It is taken such that is at least two orders of magnitude smaller than 1% of the initial liquid mass but large enough that a stable calculation is obtained.

For maintaining stability when opening and closing the PRV, a pressure margin dp_{switch} is used which is at least two orders of magnitude smaller than p_{PRV} . When the PRV is closed and the pressure inside the tank exceeds the setting pressure of the PRV plus the pressure margin $p > p_{PRV} + dp_{switch}$, the PRV opens. As presented in [Section 3.3.7](#), when the PRV is opened the outflow is set to such a rate that $p = p_{PRV}$. Still at each step, the pressure is calculated according to the ideal gas law, see [Equation \(3.36\)](#). When that value is below $p_{PRV} - dp_{switch}$, the PRV closes again.

At last, for the limiting factor in the evaporation flow, a factor $\eta_{\dot{V}-switch}$ is defined that switches between $\dot{V}_{evap-mt}$ and $\dot{V}_{evap-sat}$, when $\dot{V}_{evap-mt} > \eta_{\dot{V}-switch}\dot{V}_{evap-sat}$. Switching back is the other way around. To capture effects with a minimum accuracy of 1%, this factor should be between 1 and 1.01.

3.6. Modelling parameters

The modelling parameters used as inputs for the model are displayed in [Table 3.2](#). Here the sources from the parameters are provided. However, some parameters require additional elaboration.

The heat transfer coefficients for the vapour phase k_{vap} and liquid phase k_{liq} determine the rates of the heat ingress and therefore have a very direct impact on the results. Both are assumed constant, however they depend strongly on the dynamics of the fluid under consideration [11].

The value of the pressure sets the ambient and initial tank pressure. The value is set assumed at $p = 100$ kPa or 1 bar.

Most of the thermophysical properties are extracted from the Refprop database [22]. This is a database by the National Institute of Standards and Technology (NIST) from the U.S. government. It enables retrieval of thermophysical properties at various temperatures, pressures and vapour fractions in a mixture. Despite that Refprop enables the calling of the database by a script at varying temperatures and pressures, the parameters are extracted at fixed temperature and pressure values. This is

to retain a reproducible and independent model. Most parameters are retrieved at a temperature of $T_{par} = 15$ °C and $p_{par} = 100$ kPa. Only the heat capacities of methanol vapour are assessed at a lower pressure. This approach is described later in this section. For the characteristics of air, Refprop uses air as the mixture defined by the GERG-2008 mixture model [23]. Here, an air mixture is defined which consists of nitrogen, argon and oxygen at 75.57, 1.2691, 23.16% volume, respectively.

Table 3.2: Modelling parameters used

Symbol	Value	Unit	Source
k_{vap}	5	W/(m ² K)	[10] [9]
k_{liq}	5000	W/(m ² K)	[11]
k_{in}	5	W/(m ² K)	Described in text
p	101.3	kPa	Described in text
T_{par}	15	°C	Described in text
p_{par}	101.3	kPa	Described in text
R	8.314463	J/(K mole)	[19]
c_{p-wall}	475	J/(kg K)	[24]
c_{p-vap}	$3.3768 \cdot 10^3$	J/(kg K)	[22]
c_{p-air}	$1.0063 \cdot 10^3$	J/(kg K)	[22]
c_{p-N2}	$1.0413 \cdot 10^3$	J/(kg K)	[22]
c_{v-vap}	$2.7730 \cdot 10^3$	J/(kg K)	[22]
c_{v-air}	717.636	J/(kg K)	[22]
c_{v-N2}	743.013	J/(kg K)	[22]
c_{p-liq}	$2.4763 \cdot 10^3$	J/(kg K)	[22]
ρ_{wall}	7800	kg/m ³	[24]
ρ_{liq}	795.691	kg/m ³	[22]
Δh_{vevap}	$1.184 \cdot 10^6$	J/kg	[22]
λ_{air}	0.0251	W/(m K)	[22]
λ_{N2}	0.0251	W/(m K)	[22]
M_{air}	0.0290	kg/mole	[22]
M_{N2}	0.0280	kg/mole	[22]
M_{cargo}	0.0320	kg/mole	[22]
Pr_{air}	0.7212	-	[22]
Pr_{N2}	0.7191	-	[22]
Sc	1.14	-	[25]
Le_{air}	$\frac{Sc}{Pr_{air}} = 1.5807$	-	[19]
Le_{N2}	$\frac{Sc}{Pr_{N2}} = 1.5852$	-	[19]
A	5.2041	-	[21]
B	$1.5813 \cdot 10^3$	-	[21]
C	-33.50	-	[21]

Antoine parameters

The Antoine parameters A, B and C, presented in Table 3.2, for methanol are described for the temperature range between 288.1 and 356.83 K by [21] and are stated to provide a satisfactory fit within these ranges. As the temperature range of interest exceeds these values, the data from Refprop [22] is used to assess between which limits the Antoine parameters from [21] have an acceptable accuracy, here defined as having an absolute error below 1% of the vapour pressure value. From Figure 3.6 it can be read that the range of acceptable accuracy lies between 263.2 and 510.9 K.

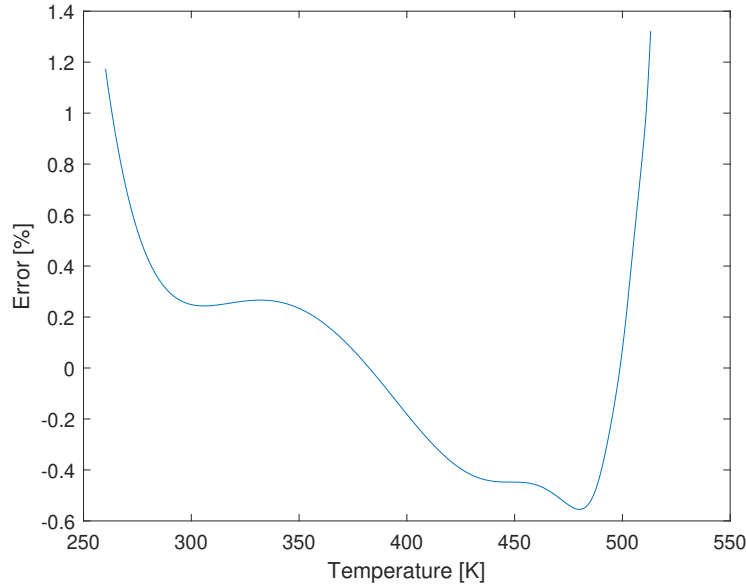


Figure 3.6: Error between the vapour pressure curve of methanol described by Refprop [22] and by the Antoine parameters presented in [21]

Specific heat capacities of vapour

As methanol as a pure substance is liquid at the combination of T_{par} with p_{par} , the heat capacities of methanol vapour are determined at T_{par} and at a vapour fraction of 1, which is attained at a reduced pressure. As Refprop enables the assessment of mixture characteristics [22], the accuracy of this approach can be determined. However, the availability of mixture characteristics is limited and data for methanol mixtures are unavailable. Therefore, the accuracy is assessed for ethanol.

There are two methods illustrated by which a pure methanol gas can be obtained: maintaining constant pressure while increasing the temperature or maintaining constant temperature and reducing the pressure. The specific heat for pure methanol attained by the first method is referred to as c_{p-T} and the second as c_{p-p} , referring to the varied parameter. As a baseline, from Refprop the specific heat at constant pressure is directly retrieved for a saturated ethanol nitrogen mixture $c_{p-mix-RP} = 1056.4$ J/(kg K). Mixture values for the c_p 's are also described with the c_{p-T} and c_{p-p} .

$$\begin{aligned}
 c_{p-mix-T} &= y_{vap}c_{p-T} + (1 - y_{vap})c_{pN2} \\
 &= 0.0427 * 1718.5 + (1 - 0.0427) * 1041.3 = 1070.3 \text{ J/(kg K)} \\
 c_{p-mix-p} &= y_{vap}c_{p-p} + (1 - y_{vap})c_{pN2} \\
 &= 0.0427 * 1395.7 + (1 - 0.0427) * 1041.3 = 1056.5 \text{ J/(kg K)}
 \end{aligned} \tag{3.58}$$

From this, an error can be evaluated.

$$\begin{aligned}
 error_{mix-T} &= \frac{c_{p-mix-T} - c_{p-mix-RP}}{c_{p-mix-RP}} = 1.32\% \\
 error_{mix-p} &= \frac{c_{p-mix-p} - c_{p-mix-RP}}{c_{p-mix-RP}} = 0.0096\%
 \end{aligned} \tag{3.59}$$

As the accuracy of the vapour phase in this mixture is of interest, the error is attributed to the vapour phase.

$$\begin{aligned}
 error_{mix-T,attributed} &= \frac{error_{mix-T}}{y_{vap}} = 30.8\% \\
 error_{mix-p,attributed} &= \frac{error_{mix-p}}{y_{vap}} = 0.226\%
 \end{aligned} \tag{3.60}$$

Defining an attributed error level of 1% as acceptable, the attributed error of the method for which temperature is reduced $error_{mix-T,attributed}$ is unacceptable, but the attributed error of the method for

which pressure is reduced $error_{mix-T,attributed}$ is. Despite that this analysis is executed for ethanol instead of methanol, the margin that the error has towards the acceptability level gives confidence for the reliable use of this method for another alcohol.

Inputs for the mass transfer coefficient

The mass transfer coefficient β_{bulk} is evaluated in Equation (3.18) and has k_{vap} , ρ_{bulk1} , c_{p-vap} and the Lewis number Le as inputs. The Lewis number is the ratio of thermal diffusivity to mass diffusivity and can be evaluated by the ratio of the Schmidt number over the Prandtl number [19]. The Prandtl number is the ratio of momentum diffusivity to thermal diffusivity of a gas [19] and can directly be retrieved from Refprop [22]. The Schmidt number however, describes the ratio of kinematic viscosity to mass diffusivity [19]. Mass diffusivity is a characteristic that describes the behaviour of one fluid in other fluids. For a combination of two fluids, this is described by the binary diffusion coefficient and is obtained experimentally [19]. Therefore, also the Schmidt number requires experimental data or Computational Fluid Dynamics (CFD) simulations for its assessment. For methanol in air at, the Schmidt number is described $Sc = Sc_{air} = 1.14$ by [25] at 25°C. Application towards the Lewis number is in that case obvious (see Equation (3.61)). As for a lack of experimental data, for methanol in nitrogen, the Schmidt number for methanol in air is used (see Equation (3.62)). As air contains mostly nitrogen (75.57% by volume is assumed in this assessment), assuming a general Schmidt number is not expected to have severe implications. This line of thought is illustrated by the close resemblance of Pr_{air} with Pr_{N_2} .

$$Le_{air} = \frac{Sc}{Pr_{air}} = \frac{1.14}{0.7212} = 1.5807 \quad (3.61)$$

$$Le_{N_2} = \frac{Sc}{Pr_{N_2}} = \frac{1.14}{0.7191} = 1.5852 \quad (3.62)$$

The largest uncertainty is expected in the evaluation of the Schmidt number with respect to flow characteristics. In a review of literature on Schmidt numbers [25], differences of more than an order of magnitude are encountered between different cases studied in experiments.

To verify agreement on the correct order of magnitude, a comparison of a comparable case as a ship tank is made. In [9] a description of mass transfer of ethanol in air inside an aerated tank that is cooling down due to a rain shower is presented. Here, a Lewis number is assumed of 1.15. No justification for this choice is provided, but its results are validated by [11] and show airflow values of a correct order of magnitude. Using the Schmidt number for ethanol in air described by [25] ($Sc=1.50$), a Lewis number of 2.08 is obtained. This is of the same order of magnitude, but does not provide full validation.

Heat transfer coefficients

In this research, two heat transfer coefficients are involved: The heat transfer coefficient of the vapour phase k_{vap} and the heat transfer coefficient of the liquid phase k_{liq} .

The models described by [9] and [10], only describe a vapour phase and assume a heat transfer coefficient of $k = 5 \text{ W}/(\text{m}^2 \text{ K})$ for an aerated tank that is cooling down due to a rain shower. By [11] a comparison is made of these models with experimental data. For a tank of $V = 603 \text{ m}^3$ containing dry air, highly accurate resemblance is obtained and the heat transfer coefficient is expected to be suitable. For tanks containing water, methanol or acetone vapours, deviations from the measurements are found. This however, is attributed to formation of a condensation film as a result of the cooling of the tanks. This does not pose a problem for the model in this research, as the focus is on heating and evaporation. Therefore, the assumed value of $k_{vap} = 5 \text{ W}/(\text{m}^2 \text{ K})$ is expected to be representative.

For the value of the heat transfer from the ambient into the wall, the same value as from the wall into the vapour phase $k_{in} = k_{vap} = 5 \text{ W}/(\text{m}^2 \text{ K})$ is assumed. Onboard a ship, the tank is either surrounded by seawater or cofferdams. Here representing cofferdams, the flow characteristics of an enclosed tank are expected to match well with the cofferdam also being an enclosed space. Therefore, assuming $k_{in} = k_{vap} = 5 \text{ W}/(\text{m}^2 \text{ K})$ is expected to be appropriate. Further implications on the assumptions regarding the surroundings of the tank are discussed Chapter 4 for each different scenario.

In [11] a liquid heat transfer coefficient of $k = 5000 \text{ W}/(\text{m}^2 \text{ K})$ is used. The heat transfer into the liquid phase is strongly limited by the heat transfer rate from the ambient air into the wall, which is described by a much smaller heat transfer coefficient k_{in} . Therefore, the exact value of the liquid heat transfer coefficient does not significantly influence the model outcomes. As a result, the value can be safely assumed at $k_{liq} = 5000 \text{ W}/(\text{m}^2 \text{ K})$.

3.7. Conclusions

In this chapter, a model is developed of a ship's fuel tank filled with methanol under influence of heat ingress. The tank is either aerated or closed off with a PRV. The model couples the most significant thermodynamic balances and vapour balance. The system is described analytically and the resulting set of ODEs is solved numerically. Due to the nature of the model, every parameter throughout every step of the model can be extracted, plotted and analysed. As a result of this, insight is gained into these separate elements and how they find a balance. These insights are extracted from the model in the next chapter.

4

Case study

In this chapter, simulation results are illustrated by a set of case studies. Simulations are executed for:

- three different scenarios [Section 4.1.1](#);
- three different tank sizes as described in ?? and briefly mentioned below;
- both for an open tank and a tank closed off with a Pressure Relief Valve (PRV);
- both an empty tank with $\epsilon_0 = 10\%$ and a filled tank with $\epsilon_0 = 90\%$;
- both for a tank with all walls subjected to the changing environment and a tank for which the tank floor is adjacent to seawater.

Descriptions of the three scenarios are provided:

- In scenario 1, the transient from night to day is modelled.
- In scenario 2, a fire surrounding the tank is modelled.
- In scenario 3, the critical post-bunker situation is modelled in which a tank with initially no vapours is filled with methanol up to two different filling levels.

Furthermore, a PRV setting pressure p_{PRV} of 170 kPa is assumed, the seawater is assumed to be equal to the initial temperature of the tank. For general observations, the intermediate tank size, tank 2, is used for illustration. However, for all simulations the results are tabulated in [Table 4.2](#) and discussed in [Section 4.6](#).

4.1. Choice of executed simulations

In this section, the choices on which simulations are executed are elaborated on. These choices result in the simulations as presented in the first four columns of [Table 4.2](#). These are all simulations that are executed in this case study.

4.1.1. Definition of scenarios

The inputs that require to be determined to define scenarios are the ambient temperature T_{amb} , the initial temperature of the tank wall and tank contents T_0 and the initial level of saturation ϕ_0 . Three different scenarios are defined and discussed in this section. These are night to day, fire and the most critical post bunker situation of which an overview is provided in [Table 4.1](#).

Table 4.1: Definition of scenarios

Scenario	Description	T_{amb} [C]	T_0 [C]	ϕ_0 [%]
1	Night to day	60	15	100
2	Fire	950	15	100
3	Most critical post bunker situation	60	60	0

Scenario 1: Night to day

As the nominal dynamic scenario, the transition from night to day is modelled. Safety of Life at Sea (SOLAS) [8] prescribes that use of fuels with a flashpoint lower than 60°C comes with certain restrictions. When extending the reasoning of these regulations, 60°C can be expected to be a reasonable upper boundary for the temperature of the tank contents. This temperature can be a result of multiple heat sources such as the ambient air or surrounding engines and other machinery producing heat. This context is provided to the model as an ambient air temperature of $T_{amb} = 60^\circ \text{C}$.

In Moncalvo [10] and Iannaccone [13] the lower boundary value for the outside temperature is selected to be 15 and 16°C, respectively. Therefore, an initial temperature of $T_0 = 15^\circ \text{C}$ is chosen.

As the starting point is the night, the previous transition was from day to night. In such a cooling scenario, condensation occurs through saturation of the vapours. As a result, the initial condition for the transition from night to day is at saturation level, resulting in $\phi_0 = 100\%$.

Scenario 2: Fire

This scenario intends to capture the most critical situation, a fire. Therefore the largest temperature increase is modelled and the initial temperature is assumed at $T_0 = 15^\circ \text{C}$, equal to the assumed night temperature. The fire is assumed to be at 950°C. As the fire is the ambient, the ambient temperature is assumed at $T_{amb} = 950^\circ \text{C}$. As the night is chosen as initial condition, also saturated initial conditions are selected for this scenario and therefore $\phi_0 = 100\%$.

Scenario 3: Most critical post bunker situation

This scenario intends to illustrate the effect of non-saturated conditions. The most critical situation regarding this aspect is expected to be the initial filling of the fuel tank of a newbuilt. Before bunkering, the tank will be filled with only air or nitrogen and no methanol vapours will be present yet. After filling the tank, part of the liquid methanol will evaporate until saturation is occurring. As saturation levels are higher at higher temperatures, this scenario is especially critical at high temperatures.

To isolate the effects of the non-saturated conditions from other influences, no temperature difference is modelled and the ambient temperature and the initial temperature of the tank and its contents are equal. These temperatures are set at the highest value that can be reasonably expected. In the description of scenario 1, this is presented to be 60 °C, so therefore $T_0 = T_{amb} = 60^\circ \text{C}$.

As a tank is modelled that initially contains no vapours, $\phi_0 = 0\%$.

4.1.2. Selection of tank dimensions

The three ship tanks are selected through a range of three different orders of magnitude and are a rectangular representation of actual ship tanks. Here, the tanks are presented from small to large:

Tank 1

The smallest tank is labelled tank 1. It is of the order of magnitude of the tanks onboard the DAMEN Stantug 1205 and the GreenPilot vessel. The fuel tanks of the first are 2m³ in volume. The latter are 1.6m³, here a maximum filling volume of 1.46m³ is stated, equal to a filling level of 91%. The dimensions of the tanks are unknown, but derived from other DAMEN vessels of a similar size, the ratios are determined. Altogether, this results in the dimensions to be assumed at $LxBxH = 2x2x0.5 = 2 \text{ m}^3$.

Tank 2

The medium sized tank is labelled tank 2 and is selected to be one order of magnitude larger than tank 1 and represents a fuel tank designed onboard the DAMEN RSD2513-Methanol. It represents either the port side or starboard side tank, which share the wall in between. As there is only one wall dividing the two tanks, one could choose to model the two tanks as one. However, in that case, the steel wall separating the tank will provide an unknown amount of heat flow through the sheet of steel into the contents of the tank. That heat flow is not described in the model. To be conservative, the tank is therefore modelled per side.

The outer dimensions of the tank are $LxBxH = 5.9x3x2.5 \text{ m}$, which spans a volume of 44.3 m³. It is however not a fully rectangular tank and contains only a volume of 26 m³. As the evaporation rate is a function of the free surface area, the length and breadth are adapted from the original dimensions and an average height is determined that results in a volume of 26 m³. This results in the dimensions being $LxBxH = 5.9x3.0x1.47 = 26 \text{ m}^3$.

Tank 3

The largest tank is labelled tank 3 and is yet again one order of magnitude larger. It does not directly represent a ship, however its length and width dimensions are the upper boundaries that are found within DAMEN for mid-sized vessels and are $LxB = 10x12$ m. To arrive at a volume of the right order of magnitude, the following dimensions are assumed $LxBxH = 10x12x2 = 240$ m³.

4.1.3. Mitigation measures for methanol outflow

The tank without mitigation measures is an airbreathing tank which is fully surrounded by the ambient air. Two measures are modelled that mitigate the outflow of methanol, both individually and combined. These are a PRV and locating the ship's tank in a ship such that its tank floor is adjacent to the sea. For the PRV a setting pressure at which it opens is selected at $170kPa$. For the sea, a temperature needs to be assumed. As of the high heat transfer ability between liquids, it is unlikely that the temperature of the liquid bulk T_{bulk2} and the temperature of the sea T_{sea} are far apart. To retain the ability to compare the simulations, for all simulations T_{sea} is assumed to be equal to T_0 .

4.1.4. Initial filling grade

It is expected that the extremities are found at extremities of the filling grade, both the empty tank and the fully filled tank is modelled. As ship tanks are usually not fully drained, the empty tank is assumed to have a filling grade of $\epsilon_0 = 10\%$. Ship tanks are usually not fully filled either to allow for expansion of the liquid. Therefore, the filling grade of the filled tank is assumed to be $\epsilon_0 = 90\%$.

4.1.5. Duration of simulation

As in scenario 1, the transition from night to day is modelled, for this scenario a simulation of 12 hours is assumed to be appropriate. As in scenario 2 and 3, the major transients are expected to be captured, for ease of comparison the same simulation period is assumed.

4.1.6. Resulting set of simulations

All variations combined result in a set of 72 simulations. However, for ease of comparison the open tanks and PRV tanks are plotted in the same simulations. Finally, this results in a total of 36 simulations. In [Table 4.2](#), a selection of parameters of all simulations is tabulated which are referred to throughout the remainder of this chapter.

Table 4.2: Outflow values, outflow timing, tank pressures and hazardous area radii ^a for all executed simulations. Gray cells represent outcomes without mitigation measures, yellow cells with PRV, blue cells with the tank floor adjacent to seawater and green cells with both.

Scen.	ϵ_0	Sea	Tank	(\dot{m}_{MeOH}) max open [kg/s]	t_{max} open [min]	r_{HA} open [m]	p_{max} PRV [kPa]	t_{PRV} [min]	(\dot{m}_{MeOH}) max PRV [kg/s]	t_{max} PRV [min]	r_{HA} PRV [m]
1	10	No	1	3.09e-05	530	0.0861	170	623	1.10e-05	665	0.0512
			2	0.000134	720	0.180	144	NA	0	NA	0
			3	0.000646	720	0.397	133	NA	0	NA	0
		Yes	1	4.40e-06	3.55	0.0323	108	NA	0	NA	0
			2	5.69e-05	6.47	0.117	109	NA	0	NA	0
			3	0.000437	10.9	0.326	108	NA	0	NA	0
	90	No	1	4.84e-07	2.85	0.0106	125	NA	0	NA	0
			2	5.64e-06	2.07	0.0366	114	NA	0	NA	0
			3	4.84e-05	2.67	0.108	110	NA	0	NA	0
		Yes	1	4.36e-07	1.01	0.0101	106	NA	0	NA	0
			2	5.48e-06	2.13	0.0361	107	NA	0	NA	0
			3	4.75e-05	2.18	0.107	106	NA	0	NA	0
2	10	No	1	0.0237	138	2.43	170	17.6	0.0233	146	2.41
			2	0.116	201	5.40	170	28.2	0.111	294	5.31
			3	0.737	256	13.7	170	35.7	0.726	267	13.6
		Yes	1	8.48e-05	2.66	0.143	170	41.4	1.76e-05	41.4	0.0648
			2	0.00103	4.93	0.503	170	37.5	0.000329	37.5	0.283
			3	0.00777	7.26	1.39	170	46.04	0.00237	46.0	0.764
	90	No	1	0.0357	104	2.99	170	35.0	0.0355	107	2.98
			2	0.195	189	7.02	170	46.3	0.193	244	6.98
			3	0.992	338	15.9	170	54.6	0.976	443	15.8
		Yes	1	8.86e-06	0.821	0.0459	170	59.5	1.12e-06	60.4	0.0162
			2	0.000109	1.57	0.163	170	56.7	1.63e-05	56.7	0.0623
			3	0.000942	1.81	0.480	170	62.0	0.000122	62.0	0.172
3	10	No	1	0.000711	5.33	0.417	170	24.5	7.17e-05	24.5	0.131
			2	0.00307	15.4	0.871	170	78.9	0.000249	78.9	0.246
			3	0.0207	19.4	2.27	170	111	0.00152	111	0.611
		Yes	1	0.000827	6.70	0.450	170	17.2	0.000185	17.2	0.212
			2	0.00366	20.2	0.951	170	50.5	0.000817	50.5	0.447
			3	0.0248	26.9	2.49	170	68.7	0.00554	68.7	1.17
	90	No	1	0.000840	0.740	0.453	170	1.81	0.000190	1.81	0.215
			2	0.00371	2.26	0.958	170	5.56	0.000817	5.56	0.447
			3	0.0252	2.92	2.51	170	7.57	0.00554	7.57	1.17
		Yes	1	0.000840	0.740	0.453	170	1.89	0.000185	1.89	0.212
			2	0.00372	2.26	0.958	170	5.56	0.000819	5.56	0.448
			3	0.0252	2.92	2.51	170	7.57	0.00555	7.57	1.17

^aDue to limited applicability of the hazardous area description in [7], its values that are smaller than 1m should only be used to provide interpretation to outflow values and be treated as effectively resulting in a radius of 1m.

4.2. Interpreting outflow values with IEC norm

To give interpretation to outflow values, the IEC norm on hazardous area sizing [7] is followed. In general, it states that the flammability risks should be assessed with a method that is validated as suitable or careful interpretation of the results is required [7].

The procedure in sizing the hazardous area starts with the description of the volumetric release characteristic. This describes the increase in volume that is explosive if the mixture were homogeneous [7]. This is a function of the lower explosivity limit (LEL) on volume basis LEL_V , the maximum mass

flow of expelled methanol $(\dot{m}_{MeOH})_{max}$ and the density of the vapours when around the vent mast ρ_{vap-vm} and is displayed in Equation (4.1). The equations here are rewritten in terms of the symbols used in this research. To determine the density, a temperature of 20° C is assumed, which is in line with what is assumed in the IEC norm [7].

$$\dot{V}_{explosive} = \frac{(\dot{m}_{MeOH})_{max}}{\rho_{vap-vm}LELV} \quad (4.1)$$

Secondly, it is determined whether the outflow is characterized as a heavy gas, diffusive or a jet [7]. In this assessment a diffusive gas is assumed as a subsonic release is expected and methanol vapours can be assumed to be neutrally buoyant. For the diffusive gas, the hazardous area scaling is defined as a straight line on a double logarithmic scale as displayed in Figure 4.1. As it describes a straight line, it can straightforwardly be described by an equation. This is presented in Equation (4.2). This equation can extend the description of hazardous areas outside of the range of Figure 4.1, however it is stated in [7] that this should not be done. Therefore, all hazardous area radius values in Table 4.2 that are smaller than 1m should only provide an interpretation for outflow values as in these cases the IEC norm prescribes a 1m radius [7].

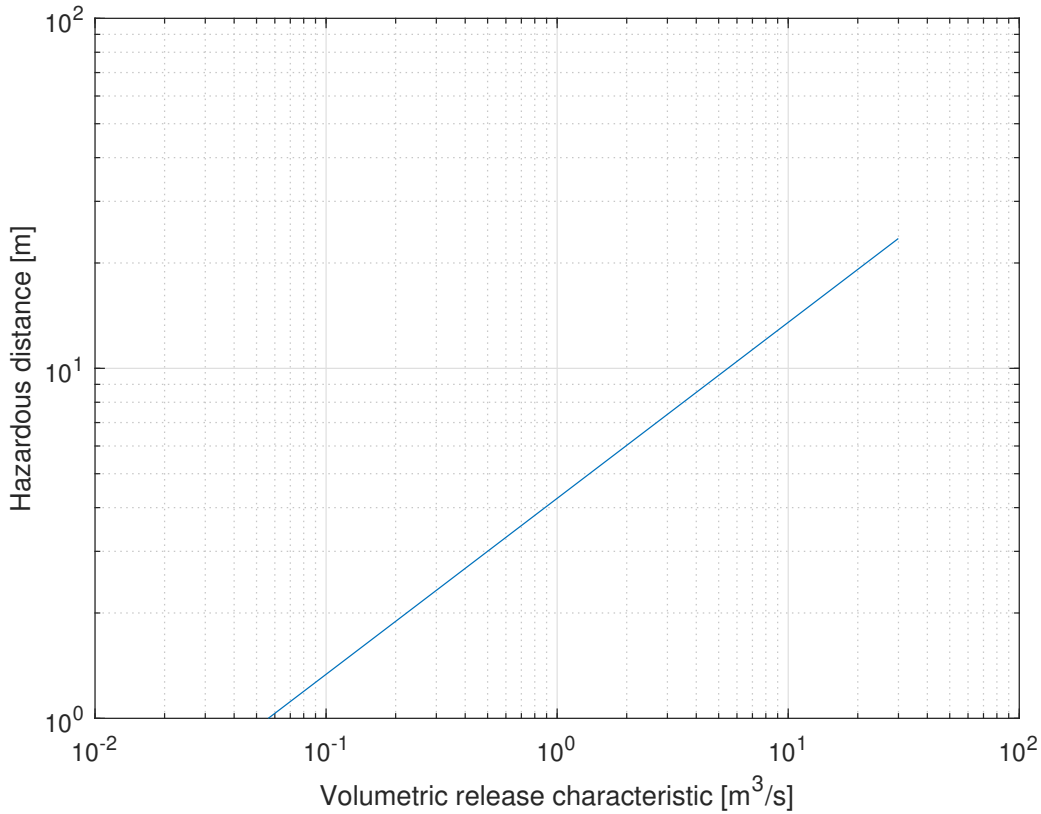


Figure 4.1: Hazardous area sizing based on the volumetric release characteristic [7]

$$r_{HA} = 4.29\dot{V}_{explosive}^{0.503} = 4.29\left(\frac{(\dot{m}_{MeOH})_{max}}{\rho_{vap-vm}LELV}\right)^{0.503} \quad (4.2)$$

4.3. Scenario 1: Night to day

From Table 4.2 it can be seen that in scenario 1, the subscenarios in which the tanks are almost empty ($\epsilon_0 = 10\%$), result in the highest outflows. Therefore, a selection of the plots related to this is analysed in this section.

4.3.1. No mitigation measures

To read data on the tank without mitigation measures, the lines and plots related to the open tank in Figure 4.2, Figure 4.3 and Figure 4.4 need to be observed. It can be read in Figure 4.2 that the temperature in wall 1 rises most rapidly, followed by bulk 1 and slowest are bulk 2 and wall 2 with an almost identical temperature profile. After 12 hours, bulk 1 reaches more than 50°C. In Figure 4.3, it can be observed that the first peak in outflow of methanol mass is mainly caused by expansion, whilst the highest outflow is mainly a result of the evaporation flow. In the second half of the simulation, the total outbreathing rate is stagnating whilst the outflow of methanol mass is increasing. This is a result of increasing vapour fraction as shown in Figure 4.4.

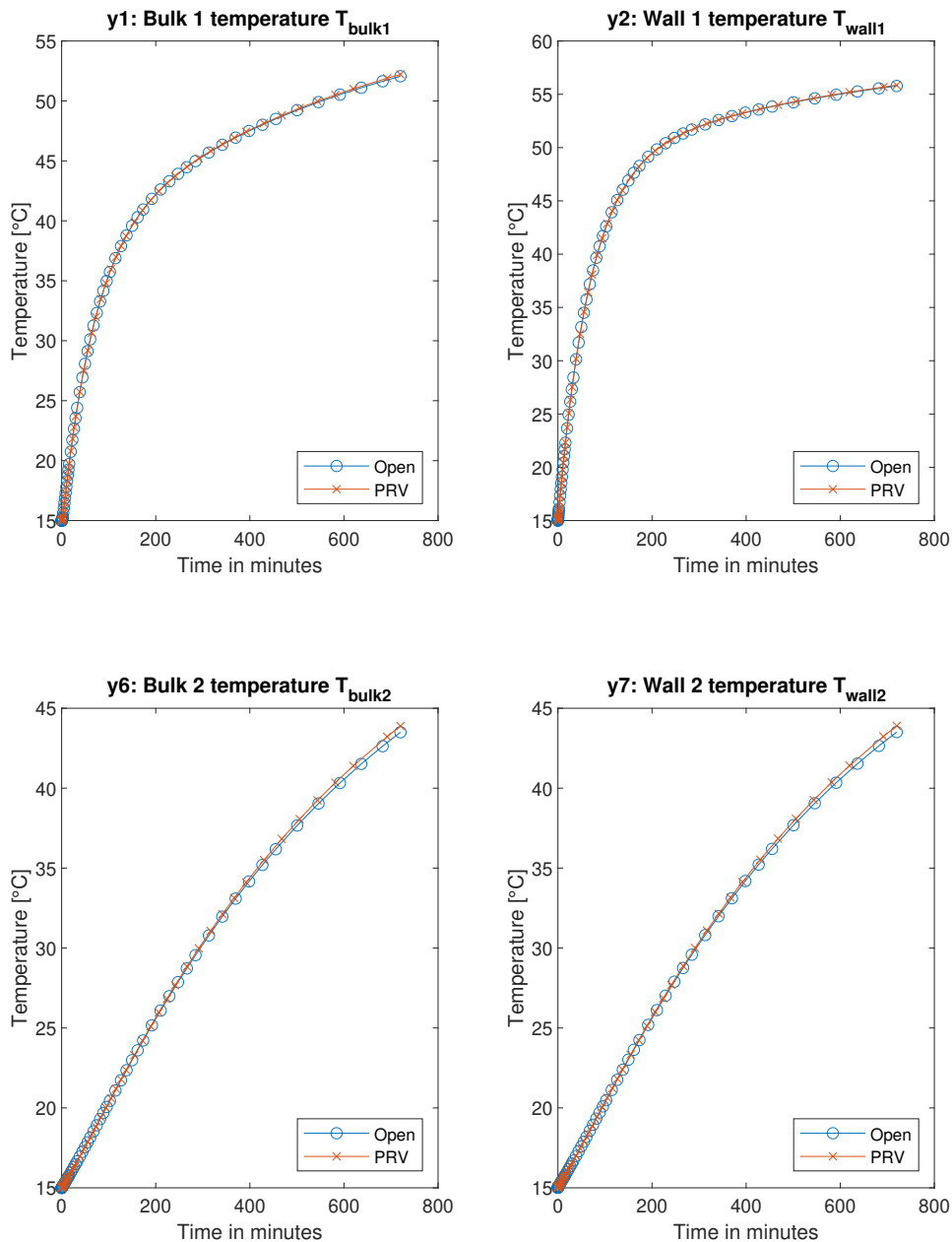


Figure 4.2: Temperatures for scenario 1, $\epsilon_0=10\%$ and Tank 2 with all walls surrounding ambient air

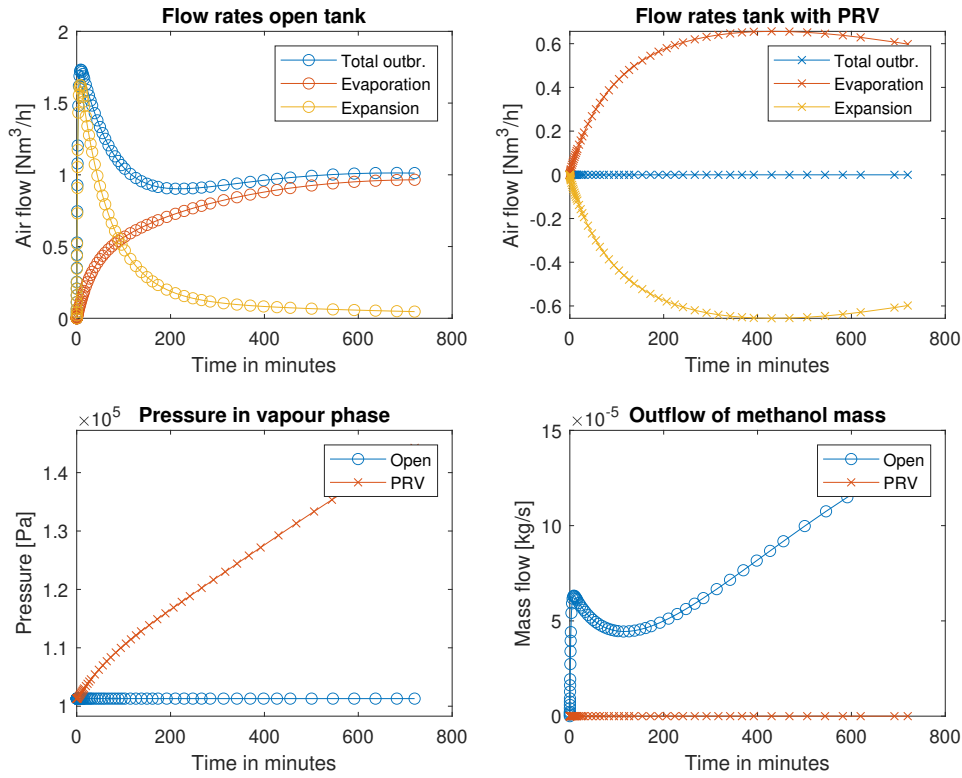


Figure 4.3: Volume and mass flows and pressure build up for scenario 1, $\epsilon_0=10\%$ and Tank 2 with all walls surrounding ambient air

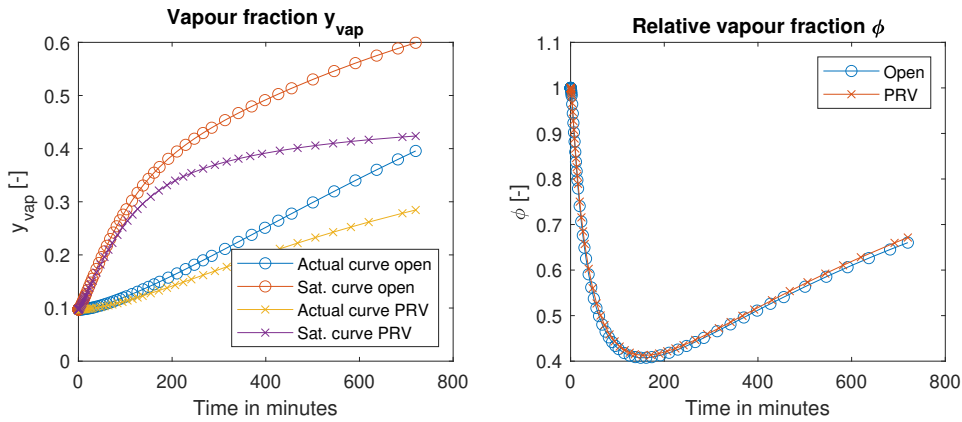


Figure 4.4: Relative and absolute vapour fractions for scenario 1, $\epsilon_0=10\%$ and Tank 2 with all walls surrounding ambient air

4.3.2. Influence of PRV

For all but one subscenario of scenario 1, the PRV is able to prevent outflow of methanol vapours. In Figure 4.2 it can be seen that this has only minor influence on the development of the temperatures over time. In Figure 4.2 it can be seen that when the PRV is closed, the volume that is occupied by newly evaporated methanol is compensated by compression (negative expansion) of the vapour phase. Together with the effect of the rising temperature in the vapour phase, this results in a pressure build-up.

The only subscenario of scenario 1 for which the PRV opens, is Tank 1 with $\epsilon_0 = 10\%$, for which the volume and mass flows and pressure build up are displayed in Figure 4.5. Compared to the same scenario for Tank 2 (see Figure 4.3) a relatively fast pressure build up can be observed, which ultimately results in opening of the vent mast.

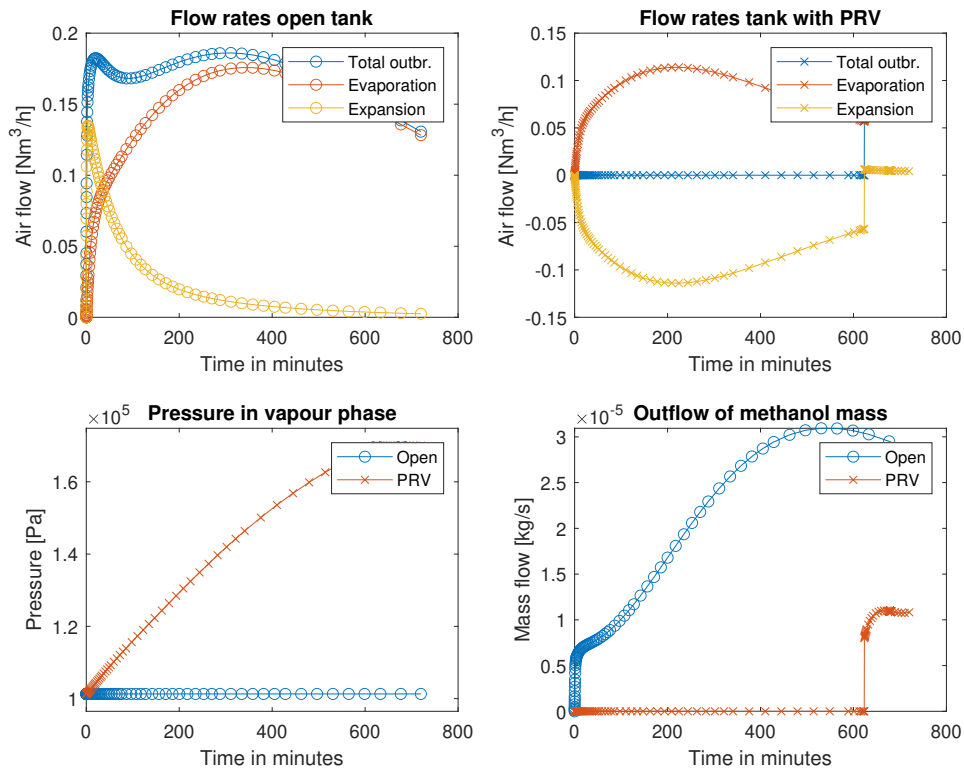


Figure 4.5: Volume and mass flows and pressure build up for scenario 1, $\epsilon_0 = 10\%$ and Tank 1 with all walls surrounding ambient air

4.3.3. Influence of tank floor against seawater

Comparing Figure 4.6 with Figure 4.3, it can be observed that for the open tank the initial peak in expansion rate experiences only minor influence by the presence of seawater against the tank floor. The evaporation rate however, becomes much smaller. Therefore, in this case the outflow is largely driven by the expansion of the vapour phase.

This is reflected by the temperature profiles over time (see Figure 4.7), which experience a similarly steep incline near the start as in Figure 4.2 for the temperature in bulk 1. However, the temperature increase in bulk 2 is less than 0.1°C instead of almost 30°C . Altogether, for the $\epsilon_0 = 10\%$ cases it can be derived from Table 4.2 that the maximum methanol outflow value is reduced by the presence of seawater with a factor of 7.0, 2.3 and 1.5 for tank 1, 2 and 3, respectively.

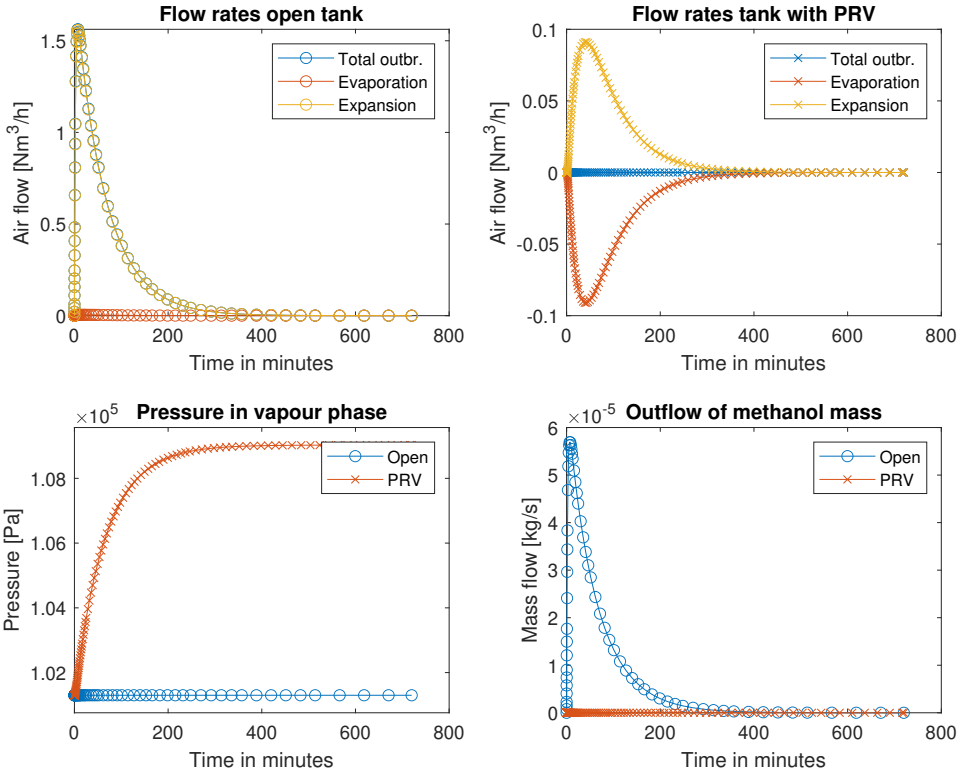


Figure 4.6: Volume and mass flows and pressure build up for scenario 1, $\epsilon_0=10\%$ and Tank 2 with one wall adjacent to seawater

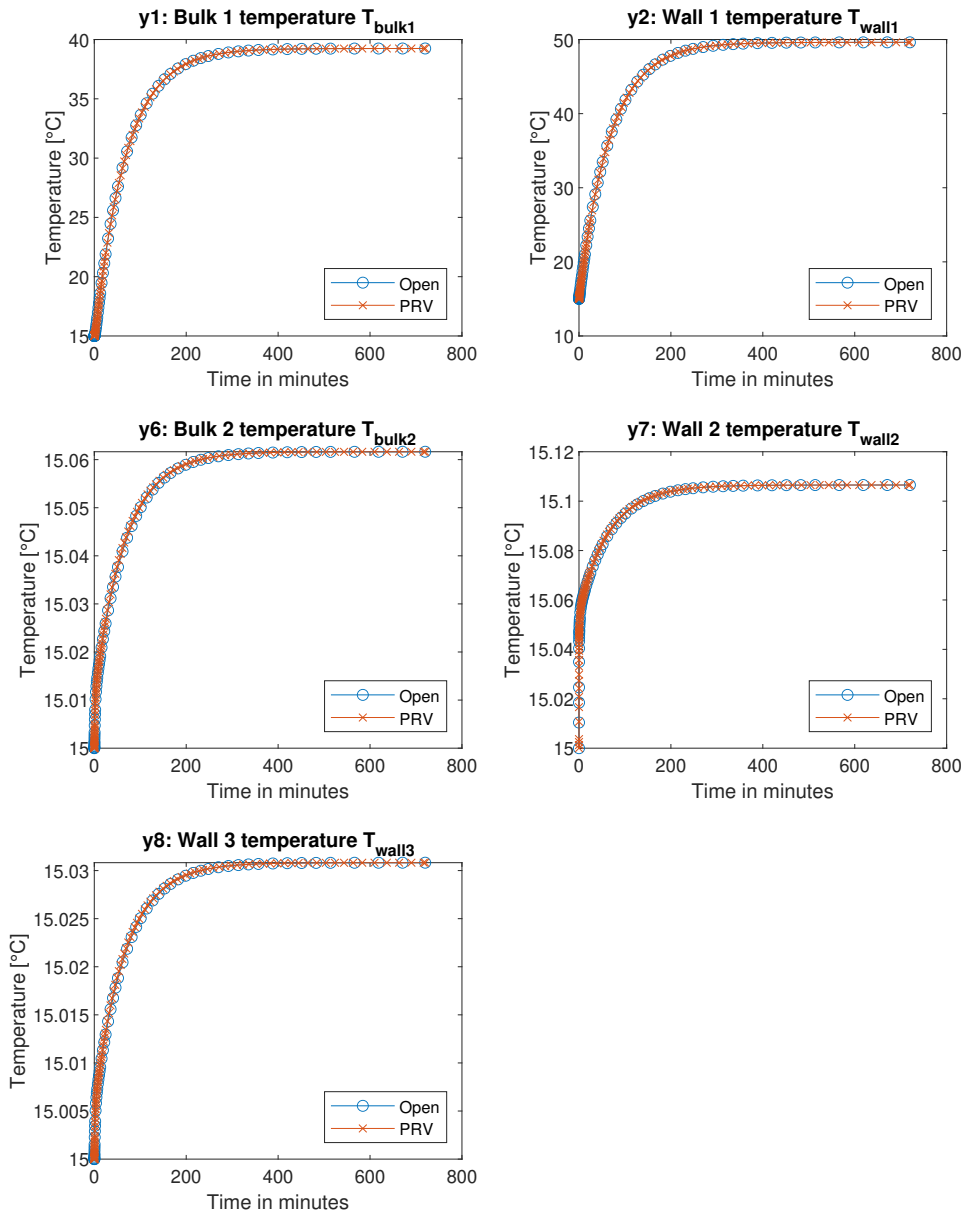


Figure 4.7: Temperatures for scenario 1, $\epsilon_0=10\%$ and Tank 2 with one wall adjacent to seawater

4.3.4. Combined influence

With the combination of the usage of a PRV and having the tank floor against the sea, neither of the executed simulations experience venting. As can be seen in Figure 4.6, the evaporation volume flow is fully compensated by compression. Also, in Table 4.2 a pressure build-up is observed of no more than 10 kPa for all tank sizes, having still 60 kPa margin until the PRV opens.

4.4. Scenario 2: Fire

4.4.1. No mitigation measures

It is observed that all subscenarios of scenario 2 that do not have the tank floor adjacent to the sea, experience boiling. Of these, the tanks with $\epsilon_0 = 10\%$ arrive at the point until there is no liquid remaining and neither of the tanks with $\epsilon_0 = 90\%$ arrive at this point. An example of this is illustrated in Figure 4.8 and Figure 4.9. In Figure 4.8 the boiling point is observed at the location where the temperature increase in bulk 2 stagnates. In the same graph, the point where the tank runs dry is observed at the sudden increase in the temperature of wall 2.

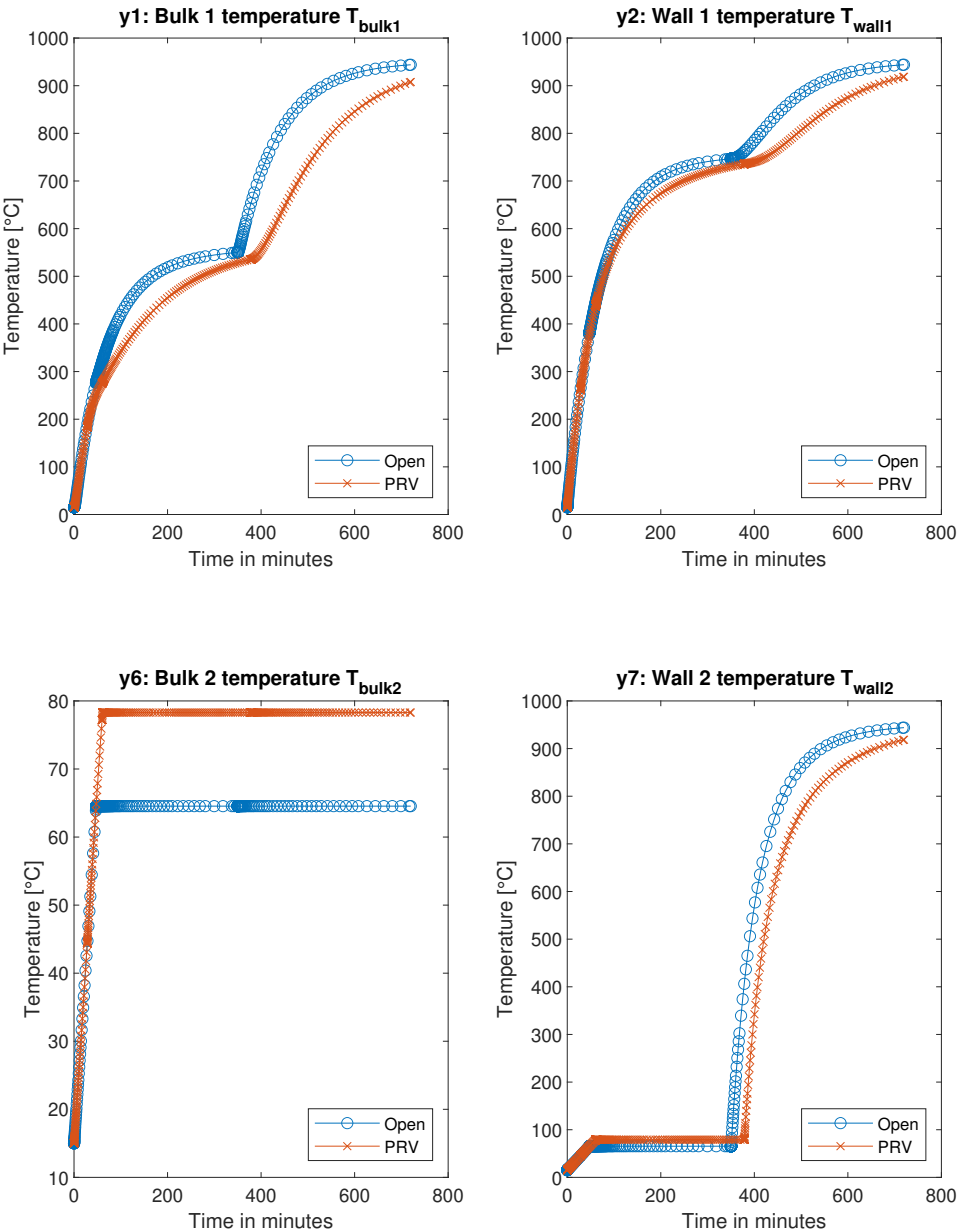


Figure 4.8: Temperatures for scenario 2, $\epsilon_0=10\%$ and Tank 2 with all walls surrounding ambient air

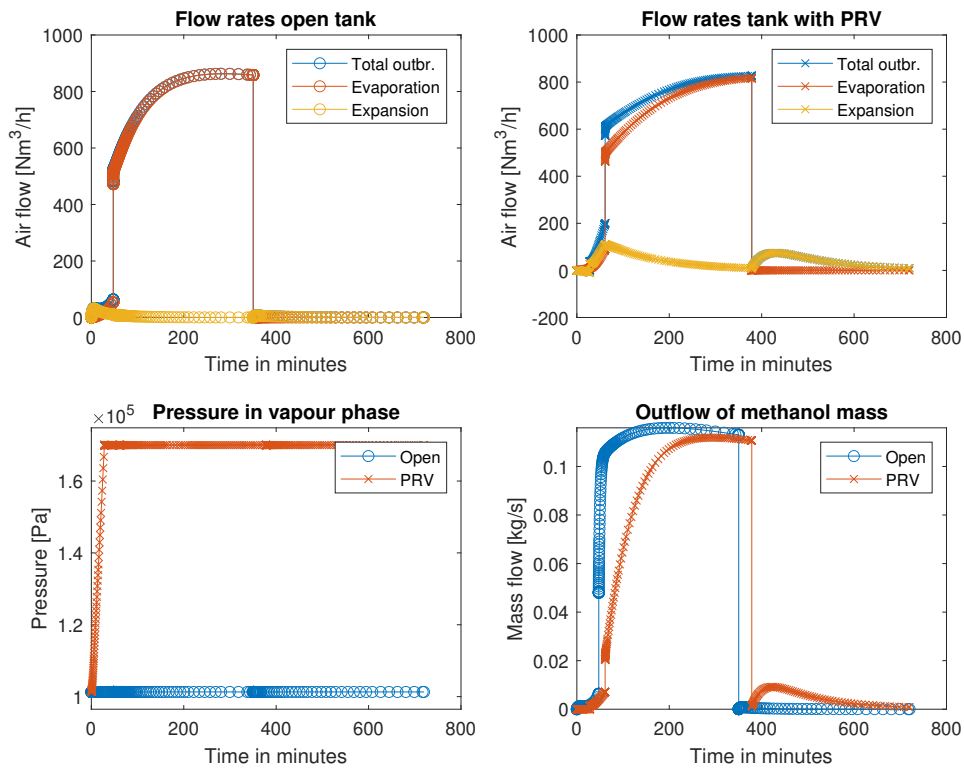


Figure 4.9: Volume and mass flows and pressure build up for scenario 2, $\epsilon_0=10\%$ and Tank 2 with all walls surrounding ambient air

However, the largest outflows in Table 4.2 are observed at the tanks that are filled initially at $\epsilon_0 = 90\%$, being 16 to 30% larger than the same sub scenario but initially filled at $\epsilon_0 = 10\%$. This is displayed in Figure 4.10. Here, the largest outflow is observed after 201 minutes when the liquid is boiling for a while.

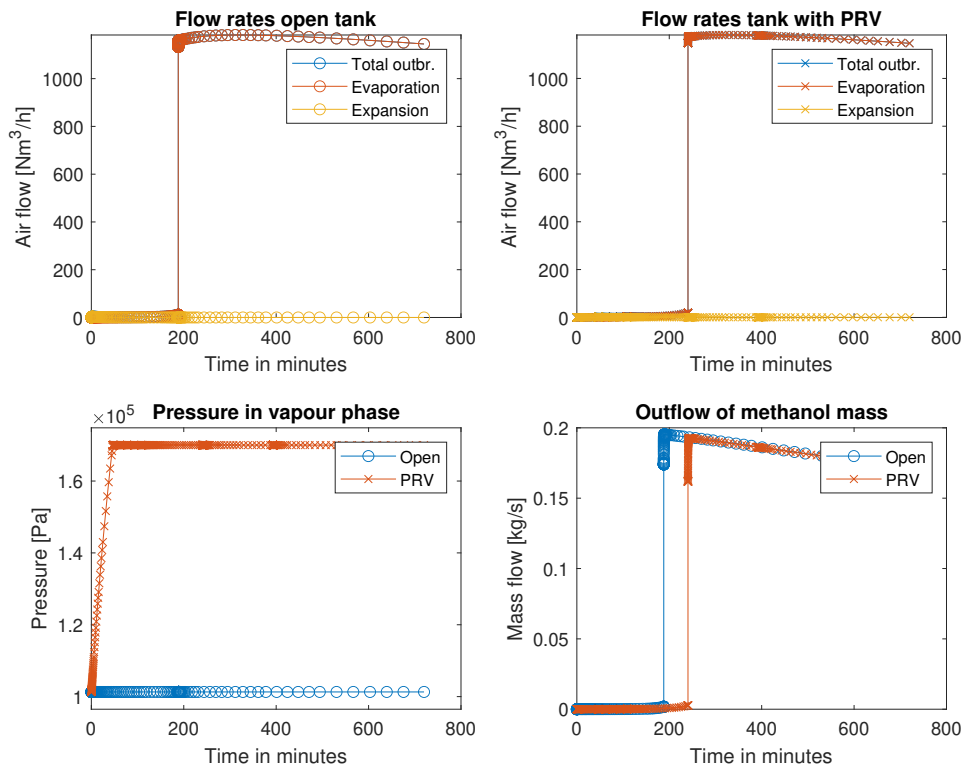


Figure 4.10: Volume and mass flows and pressure build up for scenario 2, $\epsilon_0=90\%$ and Tank 2 with all walls surrounding ambient air

4.4.2. Influence of PRV

From Table 4.2 it can be seen that both for $\epsilon_0 = 10\%$ as for $\epsilon_0 = 90\%$, adding a PRV to the system has a marginal impact on the maximum outflow value, being less than 4% for all tank sizes. However, the PRV prevents venting of vapours for 17.6 to 54.6 minutes depending on tank size and initial filling level. Furthermore, the peak in outflow is delayed. However, the amount of delay varies between 2.63 and 105 minutes. For example, in Figure 4.10 it can be seen that the PRV opens already after 46.3 minutes. However, the peak in outflow occurs when boiling starts after 244 minutes, which is 54.4 minutes later than if no PRV was present.

Noteworthy is that in the temperature plot of bulk 2 in Figure 4.8 it can be seen that the boiling point of the liquid methanol is higher for the PRV tank compared to the open tank.

4.4.3. Influence of tank floor against seawater

Opposed to the subscenarios in which the tanks do not have their tank floor against the sea, in neither of the simulations the boiling point of methanol is reached. In Table 4.2 it can be seen that these subscenarios correspond to two to three orders of magnitude lower methanol outflow values. Here, the tanks related to $\epsilon_0 = 10\%$ provide the largest outflow values, of one order of magnitude larger than when $\epsilon_0 = 90\%$. Therefore, temperatures and the flow and pressure plots for $\epsilon_0 = 10\%$ are presented in Figure 4.11 and Figure 4.12, respectively. In comparing Figure 4.8 with Figure 4.11 it can be observed that the temperature increases in bulk and wall 2 are strongly dampened by the presence of seawater. Furthermore, in Figure 4.12, it can be observed that the volume flow rate of the expansion effect is more significant than the evaporation effect and provides an early peak in outflow.

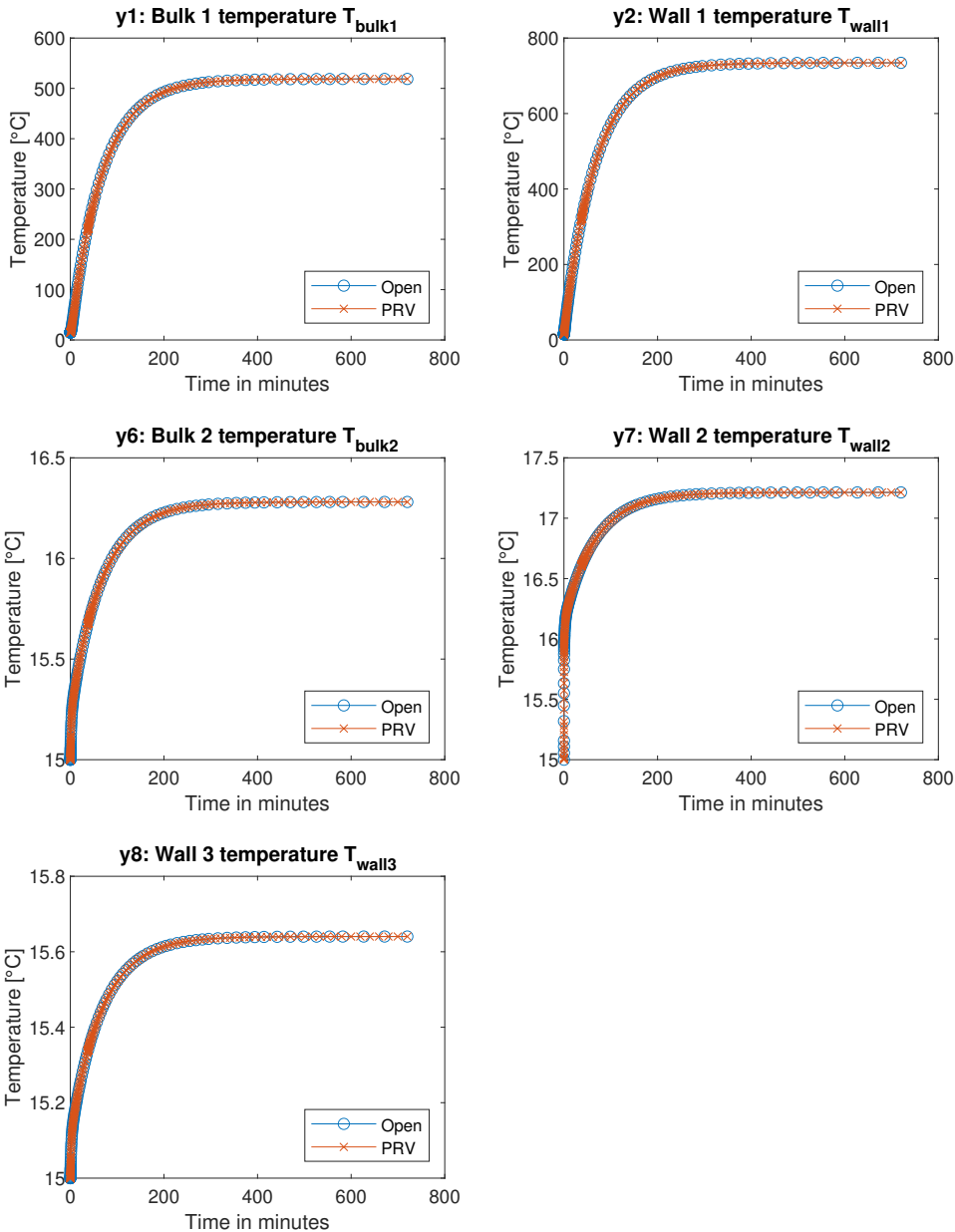


Figure 4.11: Temperatures for scenario 2, $\epsilon_0=10\%$ and Tank 2 with one wall adjacent to seawater

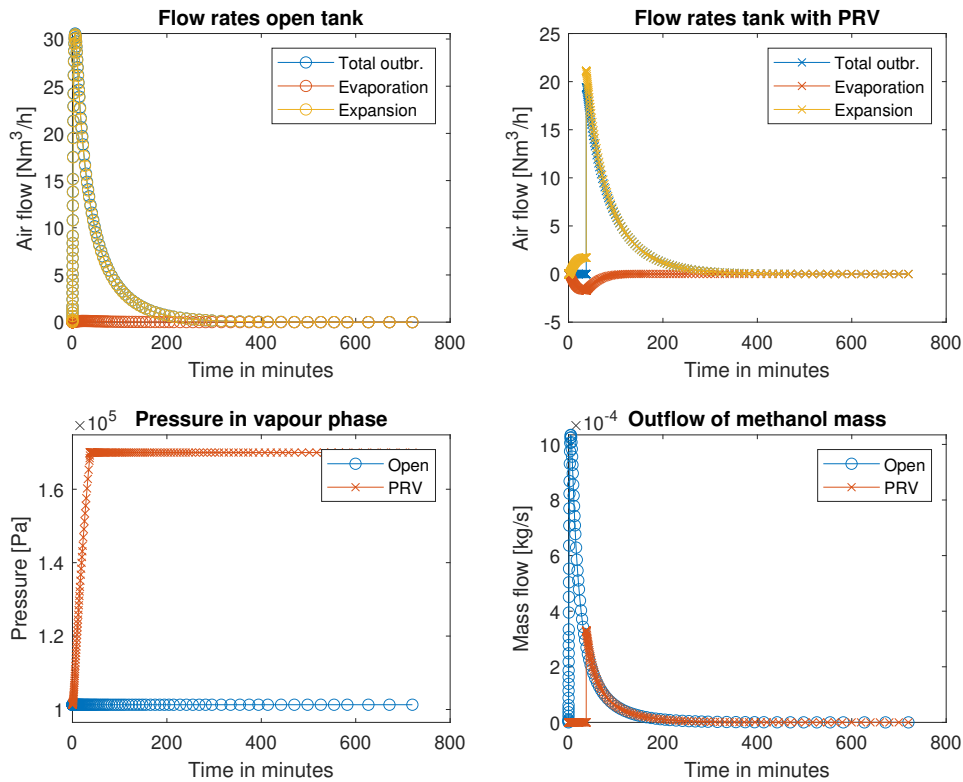


Figure 4.12: Volume and mass flows and pressure build up for scenario 2, $\epsilon_0=10\%$ and Tank 2 with one wall adjacent to seawater

4.4.4. Combined influence

Adding a PRV to the tank that is adjacent to seawater, provides an additional reduction in outflow values of a factor 3 to 5 for the $\epsilon_0 = 10\%$ cases and 6 to 8 for the $\epsilon_0 = 90\%$ cases as can be derived from Table 4.2. In Figure 4.12 it can be seen that the outflow peak caused by the expansion flow is partially contained by the PRV. Furthermore, from Table 4.2 it can be read that for both initial filling grades, the PRV stays closed for at least 37.5 minutes. Also, for the $\epsilon_0 = 10\%$ cases the peak is no longer attained within the first 8 minutes but this is delayed for more than half an hour. For the $\epsilon_0 = 90\%$ cases, the difference is larger where the peak is no longer attained within the first 2 minutes but after approximately one hour.

4.5. Scenario 3: Most critical post bunker situation

It can be read from Table 4.2 that for all sub-scenarios of scenario 3, the $\epsilon_0 = 90\%$ cases results in the highest outflow values. Therefore, only these are discussed here.

4.5.1. No mitigation measures

It is observed in Figure 4.13 that the energy consumed by evaporation results in a temperature decrease in bulk and wall 2 of approximately 0.12°C. Bulk 1 experiences a temperature drop of 0.073°C and wall 1 only 0.035°C. Also, the smaller the drop, the larger the delay at which the drop occurs. Furthermore, in Figure 4.14 it can be observed that the outflow is dominated by the evaporation rate, which peaks at the start of the simulation. It can be read from Table 4.2 that for all $\epsilon_0 = 90\%$ cases within this subscenario, this peak occurs within the first three minutes of the simulation.

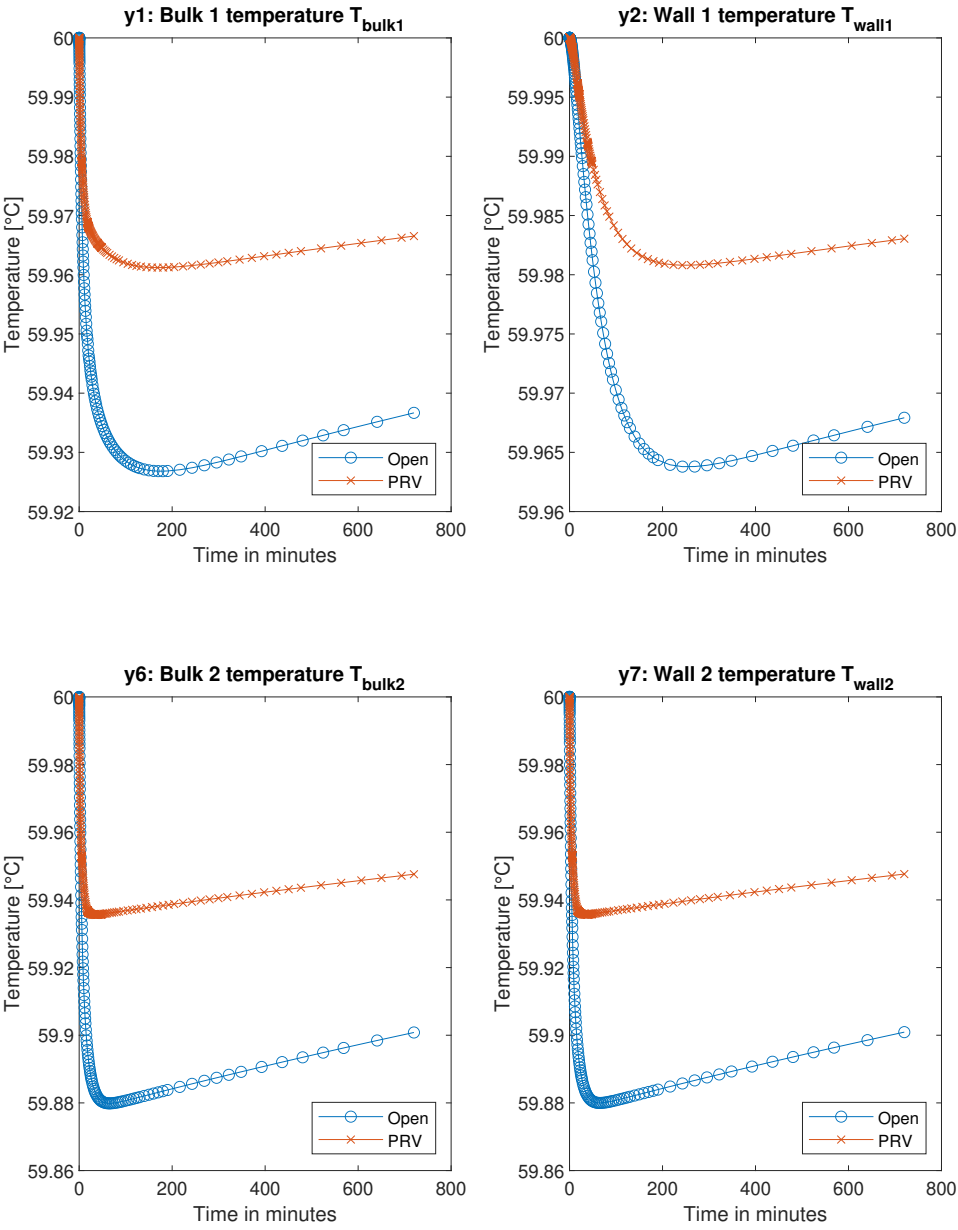


Figure 4.13: Temperatures for scenario 3, $\epsilon_0=90\%$ and Tank 2 with all walls surrounding ambient air

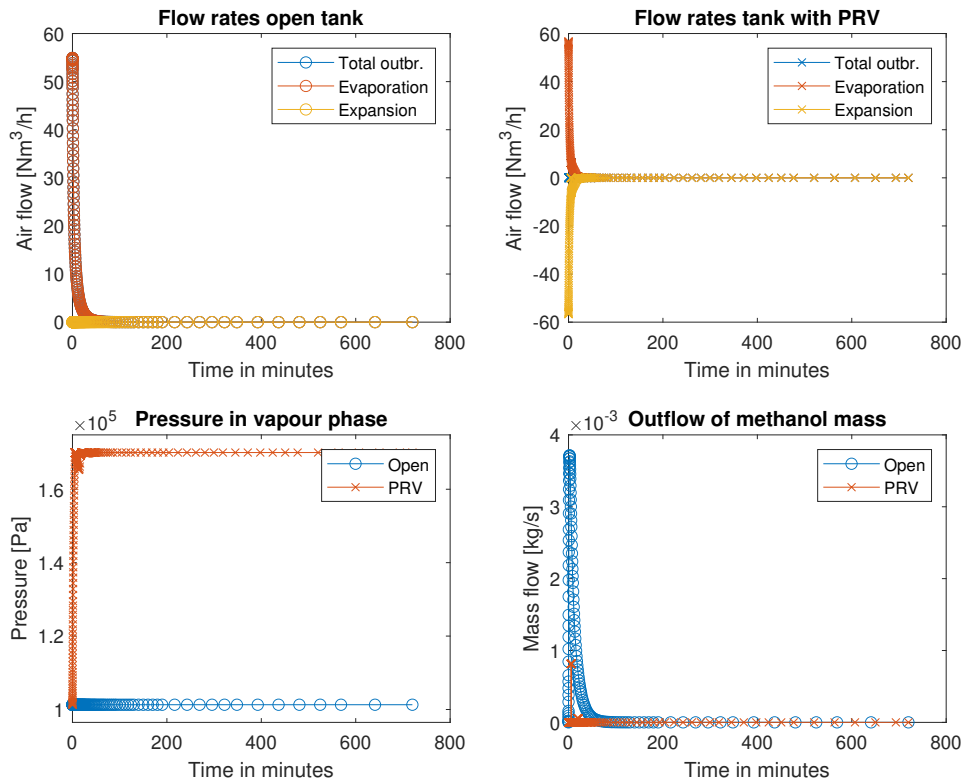


Figure 4.14: Volume and mass flows and pressure build up for scenario 3, $\epsilon_0=90\%$ and Tank 2 with all walls surrounding ambient air

4.5.2. Influence of PRV

As can be seen in Figure 4.14, that compared to the open tank, a large part of the peak in evaporation flow is contained by the PRV. From Table 4.2, it can be observed that for all $\epsilon_0 = 90\%$ cases within this subscenario this results in a reduction of the outflow of a factor of 4 to 5.

4.5.3. Influence of tank floor against seawater

When seawater is present at the tank floor, it can be observed in Table 4.2 that a slightly large methanol mass is expelled. Derived from this table for the $\epsilon_0 = 90\%$ cases this increase is very minimal, being less than 0.02%. For the $\epsilon_0 = 10\%$ cases, this influence is larger and an increase in methanol mass outflow between 16 and 20% is observed. As of this minimal difference, no further results on this subscenario are provided.

4.5.4. Combined influence

In the combined case of having both a PRV and having the tank floor adjacent to seawater, the same observations of the effect of these individual measures are made as when observing them individually in the previous paragraphs. Again for the $\epsilon_0 = 90\%$ cases (the most critical regarding outflow) it is observed from Table 4.2 that the difference in maximum outflow between the open tank and the PRV tank is a factor of 4 to 5. And again from the same table, it is observed that for the $\epsilon_0 = 90\%$ cases there are only minor differences between having seawater or air adjacent to the tank floor.

4.6. Cross comparison

4.6.1. Observations on tank size

In general, in the executed simulations within a subscenario, the larger a tank the larger outflow of methanol mass. There is however one exception as a result of the faster pressure build up in small tanks with a PRV. As observed in scenario 1 with all walls surrounding ambient air, of the tanks with a PRV, it is only the smallest tank from which an outflow occurs. However, when venting is inevitable, the larger tanks experience larger outflows.

4.6.2. Influence of mitigation measures

Outflows without mitigation measures

Without mitigation measures, the maximum methanol outflow values can be ordered from large to small per scenario:

1. Scenario 2 (fire) for the tank with $\epsilon_0 = 90\%$ with outflow values varying from 0.0357 to 0.992 kg/s, depending on tank size. This corresponds to a hazardous area radius of 2.99 to 15.9m, respectively.
2. Scenario 3 (most critical post bunker situation) for the tank with $\epsilon_0 = 90\%$ with outflow values varying from 0.000840 to 0.0252 kg/s, depending on tank size. This corresponds to a hazardous area radius of less than 1m to 2.51m, respectively.
3. Scenario 1 (night to day) for the tank with $\epsilon_0 = 10\%$ with outflow values varying from $3.09e-5$ to 0.000646 kg/s, depending on tank size. This corresponds to a hazardous area radius of less than 1m for both values.

Influence of PRV

In all executed simulations, the presence of a PRV delays the peak in outflow of methanol mass. The significance of this delay differs however from 1 minute up to 105 minutes. Next to that, there always is an amount of time during which the PRV remains closed. This also differs greatly from 1.8 minutes up to 624 minutes.

Also in all executed simulations, the presence of a PRV reduces the maximum value for the outflow of methanol mass. For most subscenarios, only a fraction of the outflow remains, with reduction factors ranging between 3 and 14. The exceptions are the fire scenarios, in which all tank walls are surrounded by air. Here, only reductions ranging between 0.5 and 3.6 % are obtained.

Influence of tank floor against seawater

The significance of the presence of seawater against the tank floor on methanol mass outflow can be ordered per scenario from large to small:

1. In scenario 2 the influence is largest. The largest outflows are observed whilst the liquid phase is boiling, which can be prevented by the presence of seawater against the tank floor. This results in a reduction in outflow values of three to four orders of magnitude.
2. In scenario 1 the presence of seawater strongly reduces the evaporation rate however the peak in expansion rate is only slightly reduced. The effect of this presence strongly depends on tank size and varies between a reduction factor of 1.5 to 7.0.
3. In scenario 3 the presence of seawater results in a minor increase in outflow. For the most critical case regarding outflow ($\epsilon_0 = 90\%$), this increase is however less than 0.02% for all tank sizes.

Outflows with combined mitigation measures

As the effectiveness of the mitigation measures varies per scenario, the ordering of scenarios on maximum methanol mass outflow values changes:

1. Scenario 3 is found to have the largest outflow values. Within this scenario, there is only a minor difference between the $\epsilon_0 = 10\%$ cases and the $\epsilon_0 = 90\%$ cases. The latter being slightly larger with outflow values ranging between 0.000840 and 0.0252 kg/s. This corresponds to a hazardous area radius of less than 1m and 1.17m, respectively. For this scenario with $\epsilon_0 = 90\%$, the reduction factor ranges between 3.7 and 3.9.
2. Scenario 2 experiences a large reduction factor. Now the $\epsilon_0 = 10\%$ cases correspond to the largest outflow with values ranging between $1.76e-5$ to 0.00237 kg/s. This corresponds to a hazardous area radius of less than 1m for both values. For this scenario with $\epsilon_0 = 10\%$ reduction factors of 311 up to 1345 are obtained and with $\epsilon_0 = 90\%$ reduction factors of $8.13e3$ up to $3.19e4$ are obtained.
3. Scenario 1 experiences no outflow when both mitigation measures are applied. In this case, the pressure build up is less than 10 kPa, leaving more than 60 kPa margin towards opening the PRV.

5

Discussion

The results obtained in this study are twofold: a thermodynamical model is described of a ship's methanol fuel tank; and with this model, a case study is executed on three ship tanks in three different scenarios. As a result, the reliability of the model directly influences the case study. Therefore, these are presented subsequently.

5.1. Uncertainties in model outcomes

In deriving the model, a set of assumptions is made for many of which it is clear that the impact is negligible. However, for the assumptions presented in this section, this requires further assessment. Note that whenever the impact of an assumption is stated to be conservative, this means that it stimulates the overestimation of eventual outflows of methanol mass. Throughout the derivation of the model, assumptions are made on the situation in which the vapour phase becomes saturated. However, in none of the scenario outcomes this point is reached. Therefore, these assumptions do not affect the outcomes in this analysis and are not discussed here.

5.1.1. Impact of uncertainty in Schmidt number

To assess the impact of the uncertainty in the Schmidt number, for all scenarios, two additional simulations are executed. The Schmidt number is an uncertain input in determining the mass transfer rate and therefore the evaporation rate. As the uncertainty in the Schmidt number is of an order of magnitude, one simulation is executed with the number multiplied by 10 and one divided by 10. The simulations are executed for the most critical value for ϵ_0 for a particular scenario, which are those that result in the highest outflow of methanol mass. For each simulation the deviation from the nominal value (1x Schmidt) is presented for the outflow parameters in [Table 5.1](#). As the large deviations in impact are expected between different scenarios and not to drown in data, the assessment is limited to the intermediate tank size, tank 2.

It is notable in [Table 5.1](#) that although the Schmidt number is either multiplied or divided by a factor of ten, the deviations in maximum output range within -78.1% and 357% (both for the tanks with and without PRV). The latter is especially significant, because if the Schmidt number were to be ten times larger than estimated, this would result in 357% more outflow. It is more important that a ship is safe than that its spaces are used optimally. Therefore, the other way around is less interesting as overestimating the outflow by 78.1% would result in a conservative estimate.

The impact of this uncertainty is here discussed per subscenario, where the scenario is split up between having or not having seawater adjacent to the tank floor. With the same line of thought as for the extremes, the subscenarios are ordered from large to small positive effect. The values for the open tank are taken which are more complete as the PRV tank does not always provide an outflow.

- Significant impact
 - Scenario 3 with and without seawater experience an increase in methanol outflow of 357% when the Schmidt number is multiplied by 10. In this scenario, the outflow peak is solely caused by evaporation (and even damped by compression due to cooling of the vapour

phase) which is driven by the initially dry vapour phase. Therefore, the height of the initial peak in evaporation is linearly dependent with the mass transfer coefficient β (see Equation (3.19)) which scales with $Sc^{2/3}$ (see Equation (3.18) and Table 3.2). However, as at the start, no vapours are present in the vapour phase yet, no methanol mass is expelled. Only when the methanol concentration level in the vapour phase starts to rise, methanol is expelled. However, this increase in concentration dampens the evaporation rate by reducing the concentration difference that is the driving force in Equation (3.19). This is expected to be the main effect of why a multiplication by 10 of the Schmidt number results in a 357% increase in outflow in this scenario.

- Small impact

- For scenario 1 without seawater, the increased value is 4.45%. The damping effect discussed for scenario 3 is stronger here as the evaporation process also experiences a limit by the relatively slow increase of the temperature of the liquid phase compared to the fast evaporation rate in scenario 3. Next to that, there is also a significant expansion term that contributes to a direct outflow of methanol vapours as opposed to scenario 3 the vapour phase initially contains methanol.
- Scenario 2 with and without seawater experience an increase of 2.54% and 0.000%, respectively. Without seawater, the maximum outflow is hardly or not influenced as this occurs when methanol is boiling. In that case, the evaporation rate is no longer influenced by the mass transfer equation but by the energy supplied to the boiling liquid. With seawater, the maximum outflow is largely governed by the expansion of the vapour phase that expels a large volume of this phase. Relatively to the expansion volume, there is hardly any evaporation volume contributing to the outflow as the liquid phase hardly warms up. Therefore, any increase in the evaporation rate has a negligible impact on the total outflow of methanol mass.
- For scenario 1 with seawater an increase in methanol mass outflow of 0.452% is observed. Here, the same reasoning as for scenario 2 with seawater applies.

From these observations, it can be concluded that the effect of the Schmidt number only has a significant impact on scenario 3. Therefore, for the initial bunkering of a vessel, there is an uncertainty in outflow values caused by the uncertainty in the Schmidt number. For a tenfold division of the Schmidt number, this is however limited to an increase of 357%, still significantly less than a tenfold multiplication (which would be equal to a 900% increase). Furthermore, during normal operations and in the instance of fire, the impact of this uncertainty is very limited.

Table 5.1: Error percentages induced by variations in Schmidt number Sc , values for tank 2

Sc.	Sea	ϵ_0 crit	x Sc	Effect on $(\dot{m}_{MeOH})_{max}$ open [%]	Effect on r_{HA} open [%]	Effect on $(\dot{m}_{MeOH})_{max}$ PRV [%]	Effect on r_{HA} PRV [%]
1	No	10	0.1	4.45%	2.21%	-	-
			10	-17.9%	-9.47%	-	-
	Yes	10	0.1	0.452%	0.231%	-	-
			10	-0.197%	-0.103%	-	-
2	No	90	0.1	-0.00512%	0.000%	0.094%	0.047%
			10	0.000%	0.000%	0.177%	0.090%
	Yes	10	0.1	2.54%	1.27%	2.26%	1.13%
			10	-1.27%	-0.64%	5.59%	2.78%
3	No	90	0.1	357%	115%	357%	115%
			10	-78.1%	-53.4%	-78.1%	-53.4%
	Yes	90	0.1	357%	115%	356%	115%
			10	-78.1%	-53.4%	-78.0%	-53.3%

5.1.2. Impact of uncertainty in liquid heat transfer coefficient

Heat transfer is an essential element in the derived model. Its coefficients can vary largely in order of magnitude [11] and are very sensitive to its contexts [19]. In [11] a validation is executed on the modelling of cooling of land based storage tanks. Accurate modelling is achieved for dry tanks (containing only air and no vapours) with a heat transfer coefficient of $5 \text{ W}/(\text{m}^2 \text{ K})$. Therefore, it is expected that within the context of storage tanks, the chosen value provides an accurate representation of the complex, real life phenomena. For the liquid heat transfer coefficient, [11] suggest a value of $5000 \text{ W}/(\text{m}^2\text{K})$. Here, any form of validation is lacking and therefore it is required to assess the impact it has on model outcomes.

The impact of uncertainty in the assumed value for the liquid heat transfer coefficient is assessed with the same approach as the uncertainty of the Schmidt number. However, now the heat transfer coefficient k_{liq} is multiplied and divided by 10. The impact of this is displayed in Table 5.2 and is discussed here. Notable from this table is that the largest impact on a $(\dot{m}_{MeOH})_{max}$ value for the open tank is only 1.11%. Two questions are elaborated on:

How can the impact on almost all parameters be so low?

- The impact on all calculations where no sea is modelled is small as in these cases the path the heat travels is limited by the heat transfer rate of the ambient air as $0.1k_{liq} = 500 \gg k_{vap} = 5 \text{ W}/(\text{m}^2\text{K})$. This holds for all scenarios.
- For when there is seawater it is found in Section 4.3.3 and Section 4.4.3 that the outflow peak is mainly driven by the expansion of the vapour phase. This is only indirectly influenced by k_{liq} via Q_{12} . Also Q_{12} is limited by k_{vap} and therefore also here limited influence is observed by changing k_{liq} .
- In scenario 3, with or without the presence of seawater there is hardly any temperature development in the liquid bulk phase (see Section 4.5.1 and Section 4.5.3) which therefore does not significantly affect the evaporation rate. Changing k_{liq} will therefore also not cause dramatic changes in the evaporation rate.

How come that of the PRV values only scenario 2 with modelling seawater shows large deviations?

- For scenario 2 with modelling seawater and the PRV, the small increase in evaporation rate induced by less cooling of the liquid phase by the seawater has some time to build up before opening the PRV. Whereas for the open case, the peak is really caused by the initial expansion. Therefore, the difference observed in the PRV case is much larger than in the open case. This effect is clearly visible in Figure 5.1 compared to Figure 4.12.

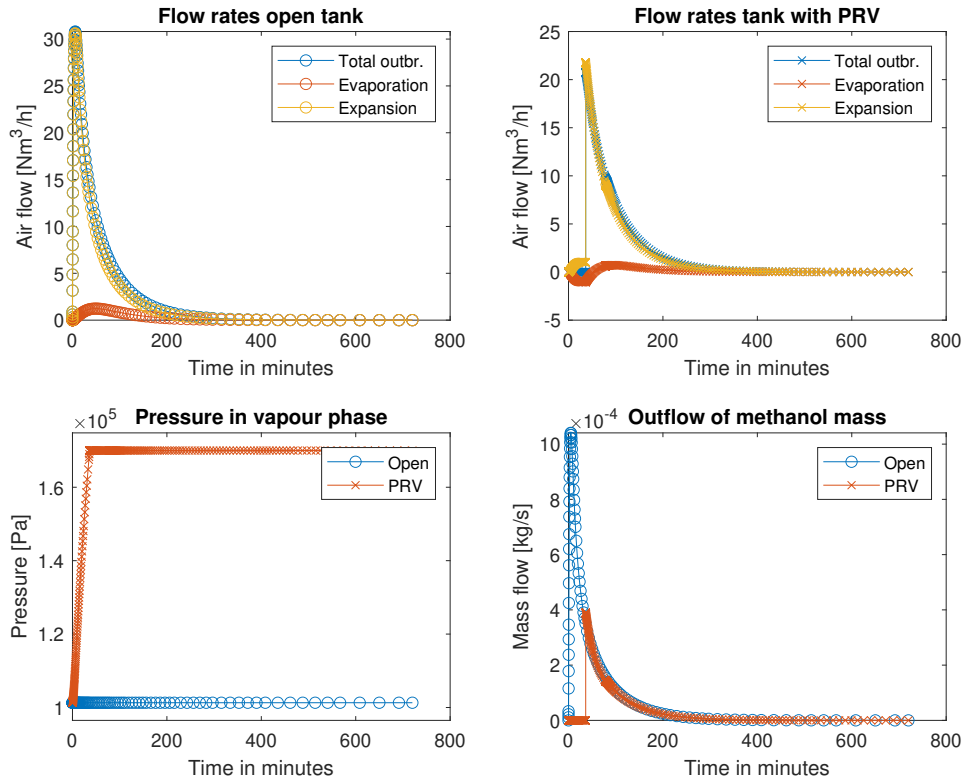


Figure 5.1: Volume and mass flows and pressure build up for scenario 2, $\epsilon_0=10\%$ and Tank 2 with one wall adjacent to seawater for $0.1k_{liq}$

Table 5.2: Error percentages induced by variations in heat transfer coefficient for liquids k_{liq} , values for tank 2

Scen.	Sea	ϵ_0 crit	$\times k_{liq}$	Effect on $(\dot{m}_{MeOH})_{max}$ open [%]	Effect on r_{HA} open [%]	Effect on $(\dot{m}_{MeOH})_{max}$ PRV [%]	Effect on r_{HA} PRV [%]
1	No	10	0.1	-0.816%	-0.412%	-	-
			10	0.0824%	0.0445%	-	-
	Yes	10	0.1	1.11%	0.555%	-	-
			10	-0.371%	-0.188%	-	-
2	No	90	0.1	-0.820%	-0.410%	-0.973%	-0.488%
			10	0.0717%	0.0384%	0.0936%	0.0473%
	Yes	10	0.1	0.619%	0.312%	18.1%	8.7%
			10	-0.483%	-0.242%	-2.89%	-1.47%
3	No	90	0.1	-0.00269%	-0.00104%	-0.0330%	-0.0157%
			10	0.00000%	0.0000%	-0.0318%	-0.0157%
	Yes	90	0.1	-0.0215%	-0.0104%	-0.191%	-0.0961%
			10	0.137%	0.0689%	0.700%	0.351%

5.1.3. Impact of neglecting heat flow between wall sections

The impact of neglecting the heat flow between wall 1 and 2 is assessed here. This assumption is expected to have a much more significant impact than neglecting the heat flow between wall 2 and 3. This is because around the boundary between wall 2 and 3 the liquid bulk is present which has a much higher heat conductivity than the vapour phase which is adjacent to wall 1. Therefore, the relative impact of the heat flow between wall 1 and 2 is expected to be larger.

A fairly crude process is followed which only aims to provide an indication of how appropriate this assumption is. As the heat conductivity of the liquid phase is much larger than that of the vapour phase, the temperature gradient in wall 1 is much lower than in wall 2 and therefore it can be safely assumed that the temperature gradient in wall 1 is limiting the heat transfer between the two wall regions. As in

the model, constant temperatures are assumed throughout the walls and the heat transfer coefficient is the heat conductivity of the material multiplied by the distance over which the gradient occurs, to assess this heat flow, it is required to assume this distance. It is assumed that the ratio of this distance with the tank wall thickness should be equal to the ratio of the heat transfer coefficient of the steel with the heat transfer coefficient of the vapour phase. With the heat conductivity of steel being $\lambda_{steel} = 15$ [W/(m K)] (for stainless steel) [26], this distance is assumed to be 20 times the thickness of the tank wall as then the heat transfer coefficient of steel is approximately 20 times the heat transfer coefficient of the vapour phase, $k_{steel} = \lambda_{steel}/(20t_p) = 15/(20 * 0.007) = 107$ [W/(m² K)] $\approx 20k_{vap} = 20 * 5 = 100$ [W/(m² K)]. With this, the heat transfer rate can be calculated as follows.

$$Q_{wall} = k_{steel}L_{circ}t_p(T_{wall1} - T_{wall2}) \quad (5.1)$$

Due to lower heat conductance of the vapour phase, the relative impact on the temperature in wall 1 will be most significant. Therefore, assessing its significance should be executed in comparison with the energy flows inside this wall.

The ratio's Q_{wall}/Q_{int1} and Q_{wall}/Q_{in1} show very similar behaviour over time. For scenarios 1 and 2, the values start at zero and asymptotes towards a value. Therefore, the end value can be used for assessment. For scenario 3, this ratio starts at a large value and rapidly diminishes until it also asymptotes towards a value. The impact of this initial period is however very small as in this initial period the heat flows have not yet gained their strength. Combining this with its fast asymptotic behaviour, also here the end value can be used for assessment. As it is of interest how the significance of the heat flow in the wall is towards the total flows in the wall, the lowest value of Q_{wall}/Q_{int1} or Q_{wall}/Q_{in1} interest is of interest. For the different tank sizes and scenarios, these values are displayed in Table 5.3.

One main observation is that the relative extent of Q_{wall} with the other heat flows inside wall 1 increases with decreasing tank size. This is a result of the tank wall thickness being constant with varying tank size. Therefore, for smaller tanks the wall thickness is relatively large compared to its other dimensions. For the different tank sizes, the ranges are as follows:

- For tank 1, the heat flow in the wall is between 0.264 and 0.621 of other heat flows and is 0.435 on average.
- For tank 2, the heat flow in the wall is between 0.131 and 0.288 of other heat flows and is 0.215 on average.
- For tank 3, the heat flow in the wall is between 0.0537 and 0.114 of other heat flows and is 0.0836 on average.

It differs per scenario (not per tank size) whether neglecting the heat flow in the wall is conservative. Therefore, this is discussed per subscenario for the open cases as most of the PRV cases experience no outflow.

- Scenario 1 with modelling only air as ambient condition and $\epsilon_0 = 10\%$: Here both the liquid and the vapour phase are warming up, but the vapour phase heats up faster. Therefore, the heat flow in the wall has a positive value and if it were not neglected it would cool the vapour phase and warm the liquid phase. As the peak in outflow is caused by evaporation (see Figure 4.3), this will cause a slight increase in evaporation rate. It is expected that this impact is small, as the heat capacity of the vapour phase is much smaller than that of the liquid phase and thus the effect on the heat transfer will be small. Therefore, the impact of this assumption is not conservative although the impact is small.
- Scenario 1 with also modelling seawater at the tank floor and $\epsilon_0 = 10\%$: Here the outflow peak is almost solely caused by expansion of the vapour phase (see Figure 4.6). Due to the presence of seawater against the tank floor the liquid bulk temperature remains relatively low, neglecting the heat flow in the wall means neglecting a cooling effect of the vapour phase. Therefore, the impact of this assumption is conservative and can be significant.
- Scenario 2 with modelling only air as ambient condition and $\epsilon_0 = 90\%$: In this case, the peak in outflow is determined by the evaporation rate of the boiling liquid (see Figure 4.10). Therefore, the additional heating that is neglected by not modelling heat flow in the wall would increase the

boiling rate. With the same reasoning as for the first subscenario, this impact is expected to be small. Additionally, the volume of the liquid phase is 9 times as large as in that subscenario, making the relative impact even less. So the impact of neglecting the heat flow in the wall is expected not to be conservative but is expected to be small in magnitude.

- Scenario 2 with also modelling seawater at the tank floor and $\epsilon_0 = 10\%$: As in the subscenario of scenario 1 with seawater, the outflow peak is determined by the expansion of the vapour phase (see [Figure 4.12](#)). Therefore, the same reasoning as in that subscenario applies and the impact of neglecting the heat flow in the wall is conservative and possibly significant in magnitude.
- Scenario 3 with modelling only air as ambient condition and $\epsilon_0 = 90\%$ or with also modelling seawater at the tank floor and $\epsilon_0 = 90\%$: In scenario 3, independent of whether or not seawater is modelled, the liquid bulk experiences a minor temperature drop (see [Figure 4.13](#)). The heat flow in the wall would stabilize this temperature drop and therefore increase the evaporation rate. The impact of the assumption therefore strictly is not conservative but the extent is negligible even if the ratios in [Table 5.3](#) are high.

Table 5.3: Ratios of wall heat flows to heat flows in wall 1

Scen.	Sea	ϵ_0 crit	Tank	Q_{wall}/Q_{in1} final open [-]	Q_{wall}/Q_{int1} final open [-]	Q_{wall}/Q_{in1} final PRV [-]	Q_{wall}/Q_{int1} final PRV [-]
1	No	10	1	0.345	0.453	0.330	0.451
			2	0.188	0.213	0.187	0.213
			3	0.0799	0.0872	0.0795	0.0870
	Yes	10	1	0.457	0.457	0.457	0.457
			2	0.215	0.215	0.215	0.215
			3	0.0880	0.0880	0.0880	0.0880
2	No	90	1	0.450	0.461	0.452	0.463
			2	0.242	0.247	0.245	0.249
			3	0.102	0.102	0.102	0.103
	Yes	10	1	0.572	0.572	0.572	0.572
			2	0.282	0.282	0.282	0.282
			3	0.106	0.106	0.106	0.106
3	No	90	1	0.537	0.572	0.536	0.571
			2	0.274	0.282	0.274	0.282
			3	0.105	0.106	0.114	0.109
	Yes	90	1	-0.227	0.577	-0.264	0.621
			2	-0.150	0.277	-0.131	0.288
			3	-0.111	0.109	-0.0537	0.109

5.1.4. Impact of assuming constant enthalpy of evaporation with varying temperature

In the model, the enthalpy of evaporation is assumed to be constant. As depicted in [Figure 5.2](#), it varies with temperature. As described in [Section 3.6](#), the value at 78.3°C is selected. The relevant temperature range is between 0 and 78.3°C being the lowest temperature in all scenarios and the boiling point of methanol at 1.7 bar [22], respectively.

It can be observed from [Figure 5.2](#), that for temperatures lower than 78.3°C, the enthalpy of evaporation is underestimated. In this region, the cooling effect of evaporating methanol is overestimated. The maximum error (occurring at 0°C), is 9.4%. The impact on eventual outflow in the modelled scenarios is however very limited and is conservative. In scenario 1, the heat flows drive the volume flows and are at least an order of magnitude larger than the enthalpy flow for evaporating methanol. Also, the underestimation of the cooling effect results in a conservative assessment as it stimulates evaporation. In scenario 3, the outflow is governed by the concentration difference between the vapour phase and the free surface of the liquid phase. As the temperature impact of the evaporation on the liquid bulk phase is marginal, also here the impact of the error in the enthalpy of evaporation is minimal and conservative. In scenario 2, prior to boiling the impact of the constant enthalpy is evaporation is driven

by the same effects as in scenario 1. Additionally, the temperature differences and therefore the heat flows are much larger, reducing the relative impact of the error in the enthalpy of evaporation. When boiling starts to occur, evaporation consumes all incoming heat and is fully determined by the enthalpy of evaporation, however at this temperature the error in the value for the enthalpy of evaporation is zero.

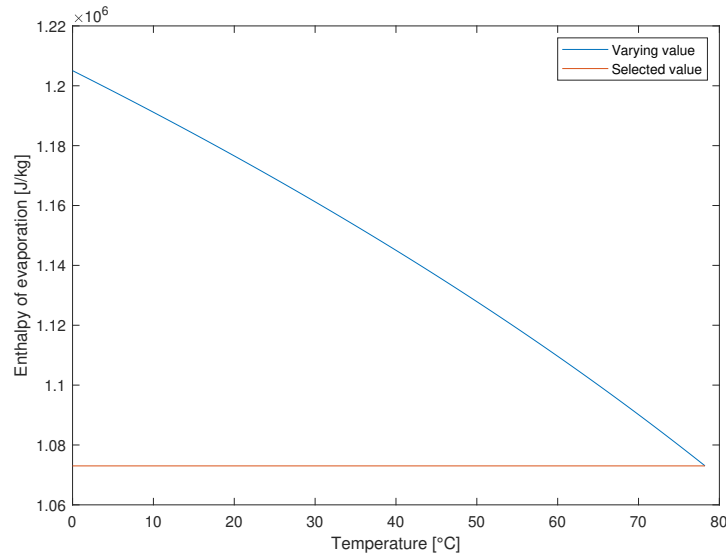


Figure 5.2: Selected value for the enthalpy of evaporation versus the values presented in [22]

5.1.5. Unquantified aspects of uncertainty

Various aspects of uncertainty are not quantified in this research, but are worth mentioning:

- In the heating scenarios (scenario 1 and 2), the tank is fully surrounded or almost fully surrounded with the tank floor as only exception by the warmed environment. For the night to day scenario, this is not very unlikely. However, for the fire scenario it is very unlikely that a ship's tank is fully surrounded by fire. Therefore, for scenario 2 this assumption is highly conservative.
- Also for the heating scenarios, neglecting the thermal insulance of the wall and a possible coating is conservative.
- For scenario 3, neglecting this thermal insulance is not conservative as in practice the damping of the evaporation induced reduction in the temperature of the liquid bulk will be lower than modelled. The impact of this assumption is however negligible as it can be observed in Section 4.5 that for the critical value of the initial filling grade $\epsilon_0 = 90\%$ even the presence of the seawater has no impact on outflow values.
- In scenario 3 when modelling seawater, for comparability with the no seawater case, the temperature of the seawater is assumed at 60°C . This is because the ambient temperature of the no seawater case is assumed at 60°C . As a result of this high seawater temperature, for the $\epsilon_0 = 10\%$ cases, the simulations with seawater result in higher outflows. It is namely observed that the seawater dampens the temperature reduction in the liquid bulk caused by evaporation. However, a seawater temperature of 60°C is unlikely high and in practice the presence of seawater will prevent such high temperatures to be reached. Finally, it can be concluded that this element of modelling scenario 3 with the presence of seawater is highly conservative.
- A highly simplified representation of a PRV is used. This neglects the behaviour of the PRV that after opening it remains open until a lower pressure than the PRV setting pressure is reached. In this research however, it is modelled that when the PRV setting pressure is reached, any excess that might increase the tank pressure above this setting pressure is expelled. However, it is not expected that the "productivity" of the tank to generate outflow mass will significantly change due

to this behaviour and in [Section 6.2.2](#) it is described how the model in this research can be used to determine the maximum outflow whilst modelling the typical PRV behaviour.

5.1.6. Conservative assessment of total impact

As the resulting outflow values in this research prove to result in very practicable hazardous area radii, it can be afforded to be on the conservative side. Being on the safe side increases the likelihood of adoption of the findings in this research by for example classification societies whilst the presented values stay away from unworkable hazardous area proportions. Therefore, of the findings in this assessment of uncertainties only the possible underestimation of outflow values are incorporated in the overview presented here and the uncertainties presented in this chapter that can result in an overestimation of outflow values are excluded.

To arrive at a conservative assessment of how to treat the outcome of each scenario, a comparison of the different uncertainties is made and presented in [Table 5.4](#). Here, per subscenario for the uncertainty in the Schmidt number and the liquid heat transfer coefficient the highest values from [Table 5.1](#) and [Table 5.2](#), respectively are repeated; for the impact of neglecting the heat flow in the wall, the outcomes of the assessments from [Section 5.1.3](#) are repeated and for the enthalpy of evaporation also the outcome is repeated.

Scenarios for which the outcomes require careful interpretation due to possibly significant underestimation of the mass outflow are:

- Scenario 2 when modelling seawater against the tank floor: Here, the uncertainty in the liquid heat transfer coefficient provides the largest uncertainty and together with the uncertainty in the Schmidt number it sums up to 23.7%. This is however only for when a PRV is used.
- Scenario 3 either when modelling only air as ambient condition as when also modelling seawater against the tank floor: In both cases, the uncertainty in the Schmidt number can result in a 357% larger methanol mass flow from the vent mast than what is modelled. Together with the uncertainty in the liquid heat transfer coefficient, this results in a possible underestimation of 358%.

The possible underestimation of the mass outflows is suggested to serve as a safety factor when treating the values in further risk assessments. Rewriting the total uncertainty percentages results in a safety factor for scenario 2 without modelling seawater of 1.237 and for scenario 3 of 4.58. The other scenarios, (scenario 1 with or without modelling seawater and scenario 2 without modelling seawater) are expected to provide accurate results where a possible underestimation is very small or small.

Table 5.4: Possible underestimations caused by uncertainties discussed and total impact on scenarios

Scen.	Sea	ϵ_0 crit	Uncertainty	Possible underestimation	
1	No	10	Schmidt	4.45%	
			k_{liq}	0.0824%	
			Q_{wall}	Small	
			Δh_{evap}	Not	
				Total	Small
	Yes	10	Schmidt	0.452%	
			k_{liq}	1.11%	
			Q_{wall}	Not	
Δh_{evap}			Not		
			Total	Very small	
2	No	90	Schmidt	0.177%	
			k_{liq}	0.0936%	
			Q_{wall}	Small	
			Δh_{evap}	Not	
				Total	Very small
	Yes	10	Schmidt	5.59%	
			k_{liq}	18.1%	
			Q_{wall}	Not	
Δh_{evap}			Not		
			Total	Intermediate	
3	No	90	Schmidt	357%	
			k_{liq}	0.000%	
			Q_{wall}	Negligible	
			Δh_{evap}	Not	
				Total	Significant
	Yes	90	Schmidt	357%	
			k_{liq}	0.700%	
			Q_{wall}	Negligible	
Δh_{evap}			Not		
			Total	Significant	

5.2. Applicability

5.2.1. Limitations on input parameters

The assessment of the impact of assumptions is only executed for the scenarios modelled in this research. There is more room for variations however, the following limitations towards the application of the model apply:

- The initial filling grade of the tank should not be less than $\epsilon_0 = 10\%$ for heating scenarios in which no sea is modelled. In that case, when reducing ϵ_0 any further a point will arise in which the temperature of the liquid phase will rise faster than that of the vapour phase. As a result, saturation of the vapour phase can occur. This is modelled, however no assessment on the impact of the assumptions made modelling this is executed.
- The initial filling grade of the tank should not be more than $\epsilon_0 = 90\%$ for any scenario. When in heating scenarios, increasing ϵ_0 any further a point will arise in which the expansion of the liquid phase becomes significant towards that of the vapour phase and possibly even liquid might be expelled which is not modelled.
- The tank size should not be smaller than 2 m^3 or larger than 240 m^3 and results obtained for very different tank shapes should be interpreted carefully.
- The temperature of the liquid bulk should remain within the ranges in which the Antoine parameters provide an acceptable result. As boiling prevents this temperature from exceeding the

boiling temperature, this only concerns a minimal temperature. Therefore T_0 should not be less than 263.2K (see [Section 3.6](#)).

- It should always be the case that $T_{amb} \geq T_0$ as otherwise cooling will occur, which contains behaviour that is not modelled.
- The setting pressure of the PRV should not exceed 170 kPa but can be reduced towards the ambient pressure. This is because a reduction will move the modelled behaviour towards the behaviour of the open tank (which equals the situation of the PRV tank in which $p_{PRV} = p_{amb}$) for which also an assessment of the impact of the made assumptions is executed.

5.2.2. Suggested applications

Model applications

When using the model with an appropriate level of caution for the uncertainties, it can be used in a set of suggested applications.

The model can be used to determine the amounts of nitrogen consumed by a tank to size the nitrogen blanketing system. The model is only suitable for modelling outflows. Therefore, a designer should first use the model to identify during which transient outflows are expected and secondly use the model to assess how much nitrogen flows out per transient.

Together with a classification society, a ship designer can define scenarios that require assessment. Using these scenarios as an input, several uses can be identified. First of all, for tank designs that involve a PRV, it can be assessed whether an opening of the PRV and therefore an outflow can be expected.

If the hazardous area size that is described by the IEC-norm [7] is accepted, two additional possibilities arise in assessing scenarios. Firstly, a ship's tank and superstructure can be designed to ensure that the combination of hazardous area size with superstructure layout that results in compliance with the restrictions that are posed on hazardous areas. Secondly, an existing ship design can be assessed for compliance.

Case study applications

Insight is gained into what outflow values can be expected and the effectiveness and working of mitigation measures. These outflow values can either be used as a starting point in developing a model of a plume for the range of outflow values or if the method for describing a plume as described in the IEC-norm [7] is accepted, values for the hazardous area radius obtained by the simulation can be compared with the nominal radius in the IEC-norm of 10m [7].

Possibly of even more relevance is the understanding that the modelled scenarios provide in the effect of changing conditions and the development and interaction of the tank parameters over time. Prior to this research, this understanding was lacking and ship's methanol fuel tanks were treated as a black box. With these observations, the black box is opened and a first look is taken.

Conclusions and recommendations

6.1. Conclusions

In this research, a model is developed that describes the thermodynamic behaviour of a ship's methanol fuel tank and its contents through an analytical description. As such a description is lacking in any form in literature, this analytical description provides understanding of the underlying mechanisms. Also, insights can be obtained into the appropriateness of regulations and the effectiveness of mitigation measures that can prevent outflow of large quantities of methanol. It is the model description that answers the first sub research question presented in the introduction, the analysis on mitigation measures that answers the second sub question and together, the main question is answered.

The model that is developed in this research is based on a selection of the thermodynamic phenomena found in a literature based inventory. A tank is modelled that is either fully surrounded by air or has as only exception the tank floor modelled to be touching the seawater. It can be an open tank or closed-off with a PRV. It describes heat balances for:

- bulk 1: the vapour phase that contains methanol vapours and either air or nitrogen;
- wall 1: the walls adjacent to the vapour phase;
- bulk 2: the liquid phase, containing the liquid methanol;
- wall 2: the walls adjacent to the liquid phase;
- wall 3: if seawater is modelled, the tank floor is no longer part of wall 2 and is modelled to have its own heat balance.

The description of the model results in a set of Ordinary Differential Equations (ODEs) which is then solved numerically. This method of deriving a model enables examining every contribution towards possible outflows individually.

As a nominal risk mitigation measure against toxicity and flammability hazards, regulations prescribe the use of hazardous areas. Inside these areas, there are limitations on the usage of electrical equipment and presence of occupants. The area under consideration is the hazardous area surrounding the vent mast connected to the ship's fuel tank. When methanol outflow data is lacking, a fixed hazardous area size of 10m radius is prescribed. It is found that for the nominal casus (of night to day) without the usage of mitigation measures, this is highly conservative. For a fire surrounding the tank and for the initial bunkering of the ship, it provides the correct order of magnitude as large amounts of methanol are vented when no mitigation measures are taken.

Two mitigation measures are found that can prevent the venting of large amounts of methanol from the vent mast of a ship's fuel tank. The effects on the two modelled heating scenarios (which are night to day and fire) are discussed here.

- Closing off the vent mast with a Pressure Relief Valve (PRV) prevents venting during the night to day scenario for the larger tank sizes. It however has very limited effect on the fire scenario.

- Locating the tank floor against the seawater provides a very strong stabilizing effect regarding temperatures and for an open tank, it results in very small outflows even in the fire scenario, that corresponds to a hazardous area radius of no more than 1.39m.
- Combining both mitigation measures prevents venting for the night to day scenario and reduces the hazardous area radius for the fire scenario to less than 1m.

Despite the effectiveness of these safety measures regarding the heating scenarios, care has to be taken with bunkering the vessel for the first time. As in that situation, the air inside the tank does not yet contain vapours, it is found that this drives evaporation to such a strong extent that it results in the largest outflows after application of the mitigation measures, resulting in a hazardous area radius of up to 1.17m.

As regulations include a description of hazardous area size for known methanol outflow values, the findings of this research can be used to define hazardous area radii without a need for changing regulations. The model described in this research enables simulating methanol outflow values for different tank dimensions (albeit only rectangular) and absence or presence of the mentioned mitigation measures. It has to be noted, that to do so, classification bureaus need to be well aware of the reliability of the model. In the discussion, this is elaborated on per scenario. Here the impacts of uncertainties on outflow values are assessed. The outcomes can serve as safety factors.

With the developed model, the simulated scenarios and interpretation of regulations, insights are obtained into the behaviour of methanol in a ship's fuel tank and effective risk mitigation measures are found. With these measures, even the largest hazardous area radius is found to be of practicable size.

6.2. Recommendations

6.2.1. Applicability

Tank shape: The tank modelled is rectangular, in practice however ship's fuel tanks can have very complicated shapes in which the area is much larger than for the same rectangular volume. As the model is an analytical model, the value describing the area of the tank can be straightforwardly changed to the correct value. However, care should be taken to where this area is added, as it can be the area touching the vapour phase or the liquid phase and it might influence the free surface area of the liquid phase.

Other fuels: The model is described for methanol. However, it are only the input parameters that are specifically describing methanol. Therefore, use of this model can be extended to the storage of other fluids while being cautious about the transferability of the assumptions made in this research. Using this model for other liquids that are stored together with a gas, such as Diesel or gasoline, is particularly straightforward. More complex is the transfer of this model to fluids stored purely such as LNG, hydrogen or ammonia.

Plume modelling: The model only describes a mass and volume outflow out of the tank and does not include a plume model. Only for interpretation of the results, the IEC-norm [27] is used. If this is not an acceptable method or if the expected overestimation by this method is undesirable, it is recommended to develop a plume model.

Fire protection: Only a tank that is in direct contact with the ambient air is modelled. However, the impact that a fire protection layer can have can be modelled. This fire protection will decrease the heat transfer into the tank and therefore the rate of a pressure build-up and/or outflow.

6.2.2. Accuracy

Mass transfer: A fixed Schmidt number is assumed to describe mass transfer for all tank sizes under all circumstances. Next to the uncertainty contained in this number, it might require a different description for different tank sizes and different temperatures. The uncertainty in the Schmidt number affects the mass transfer description and therefore the evaporation rate. It is however expected that it is of the correct order of magnitude. More research on describing the mass transfer relation is recommended. Various approaches can be valuable: Additional literature research can be executed; A Computational Fluid Dynamics (CFD) study can be executed; Or an experiment can be executed.

PRV behaviour: The model entails a large simplification of the behaviour of a PRV. The PRV is modelled to have no resistance when opened, no leakage when closed and experiences no pressure drop after opening. As the "productivity" of the tank to generate outflow is expected not to be influenced

by this behaviour, the model can be used to select the number of PRVs. By using data from PRV manufacturers, two options arise in incorporating this:

- The PRV behaviour can be included in the model. This will provide the most complete results, but will require executing a new assessment of the uncertainties.
- For the chosen PRV setting pressure, one can execute the desired simulations with the model presented in this research. If it is found that the PRV opens, within the period of opening one can search for the highest concentration level of methanol vapours and select this value. With this concentration value, the number of PRVs selected for the ship design and the volume flow determined by the resistance characteristics of the PRV, one can directly obtain the maximum methanol mass outflow rate. When also incorporating the setting chosen for the pressure drop in the PRV and the ideal gas law, also the outflow duration can be obtained. This does not require further assessment of uncertainties.

Validation: For the model in this research, no integral validation has been executed. The model that forms the basis of this research, is validated. Despite that, performing an experiment is recommended. Here, a tank containing methanol can be placed in a cold location until a stable situation is obtained, to subsequently be moved towards a warmer location. Measurements performed on the tank can then be compared to a simulation of the tank used.

Sloshing: The model leaves sloshing out of the scope. The impact of sloshing is unknown. It is however expected not to be severe as its main impact is expected to be the short period increase in free surface area over which evaporation takes place. This is not expected to be very significant. However, this estimation can not be substantiated and therefore more research is recommended.

Bibliography

- [1] Jasper Faber et al. *Fourth IMO GHG Study*. 2020.
- [2] Karin Andersson et al. "Shipping and the Environment". en. In: *Shipping and the Environment : Improving Environmental Performance in Marine Transportation*. Ed. by Karin Andersson et al. Berlin, Heidelberg: Springer, 2016, pp. 3–27. ISBN: 978-3-662-49045-7. DOI: [10.1007/978-3-662-49045-7_1](https://doi.org/10.1007/978-3-662-49045-7_1).
- [3] Chempros and Toxic. *Toxic Chemiekaarten*. 37th ed. SDU Uitgevers, Oct. 2021.
- [4] S. Verhelst et al. "Methanol as a fuel for internal combustion engines". English. In: *Progress in Energy and Combustion Science* 70 (2019), pp. 43–88. ISSN: 0360-1285. DOI: [10.1016/j.pecs.2018.10.001](https://doi.org/10.1016/j.pecs.2018.10.001).
- [5] Valérie Masson-Delmotte et al., eds. *Climate Change 2021: The Physical Science Basis. Contribution of Working Group I to the Sixth Assessment Report of the Intergovernmental Panel on Climate Change*. Cambridge University Press, 2021.
- [6] International Maritime Organization (IMO). *MSC.1/Circ.1621 INTERIM GUIDELINES FOR THE SAFETY OF SHIPS USING METHYL/ETHYL ALCOHOL AS FUEL*. London, UK, Dec. 2020.
- [7] European Committee for Electrotechnical Standardization. *IEC EN 60079-10-1 Explosive atmospheres - Part 10-1: Classification of areas - Explosive gas atmospheres*. Brussels, Dec. 2015.
- [8] International Maritime Organization (IMO). "SOLAS 1974 International convention for the safety of life at sea, 1974 (MSC.202(81)) (onbeheerd) - Netherlands Regulatory Framework (NeRF) – Maritime". In: London, UK, Jan. 2014.
- [9] D Fullarton, J Evripidis, and E. U Schlünder. "Influence of product vapour condensation on venting of storage tanks". en. In: *Chemical Engineering and Processing: Process Intensification* 22.3 (Nov. 1987), pp. 137–144. ISSN: 0255-2701. DOI: [10.1016/0255-2701\(87\)80040-5](https://doi.org/10.1016/0255-2701(87)80040-5).
- [10] D. Moncalvo et al. "Breathing losses from low-pressure storage tanks due to atmospheric weather change". English. In: *Journal of Loss Prevention in the Process Industries* 43 (2016), pp. 702–705. ISSN: 0950-4230. DOI: [10.1016/j.jlp.2016.06.006](https://doi.org/10.1016/j.jlp.2016.06.006).
- [11] N. Schmidt et al. "Modelling of breathing phenomena within large storage tanks during rapid cooling with ambient rain". English. In: *Technische Mechanik* 39.1 (2019), pp. 97–112. ISSN: 0232-3869. DOI: [10.24352/UB.OVGU-2019-010](https://doi.org/10.24352/UB.OVGU-2019-010).
- [12] M. Al-Breiki and Y. Bicer. "Technical assessment of liquefied natural gas, ammonia and methanol for overseas energy transport based on energy and exergy analyses". English. In: *International Journal of Hydrogen Energy* 45.60 (2020), pp. 34927–34937. ISSN: 0360-3199. DOI: [10.1016/j.ijhydene.2020.04.181](https://doi.org/10.1016/j.ijhydene.2020.04.181).
- [13] T. Iannaccone et al. "Numerical simulation of LNG tanks exposed to fire". English. In: *Process Safety and Environmental Protection* 149 (2021), pp. 735–749. ISSN: 0957-5820. DOI: [10.1016/j.psep.2021.03.027](https://doi.org/10.1016/j.psep.2021.03.027).
- [14] M.S. Zakaria, K. Osman, and M.N.M. Musa. "Boil-off gas formation inside large scale liquefied natural gas (LNG) tank based on specific parameters". English. In: *Applied Mechanics and Materials* 229-231 (2012). ISBN: 9783037855102, pp. 690–694. ISSN: 1662-7482. DOI: [10.4028/www.scientific.net/AMM.229-231.690](https://doi.org/10.4028/www.scientific.net/AMM.229-231.690).
- [15] Y. Cao et al. "Safety design analysis of a vent mast on a LNG powered ship during a low-temperature combustible gas leakage accident". English. In: *Journal of Ocean Engineering and Science* 7.1 (2022), pp. 75–83. ISSN: 2468-0133. DOI: [10.1016/j.joes.2021.06.001](https://doi.org/10.1016/j.joes.2021.06.001).
- [16] D.-H. Doh et al. "A swirl static mixer with diluent for reducing the flammable extent of venting gases in a low-flashpoint fueled vessel". English. In: *Journal of Mechanical Science and Technology* 33.7 (2019), pp. 3311–3321. ISSN: 1738-494X. DOI: [10.1007/s12206-019-0626-1](https://doi.org/10.1007/s12206-019-0626-1).

- [17] David H. Slade. *METEOROLOGY AND ATOMIC ENERGY*. Tech. rep. U.S. Atomic Energy Commission, Division of Technical Information, Jan. 1968.
- [18] Phani P. K. Raj and Ashok S. Kalelkar. *ASSESSMENT MODELS IN SUPPORT OF THE HAZARD ASSESSMENT HANDBOOK*. Cambridge Massachusetts: Arthur D. Little, Inc., Jan. 1974.
- [19] T. L. Bergman et al., eds. *Fundamentals of heat and mass transfer*. 7th ed. Hoboken, NJ: Wiley, 2011. ISBN: 978-0-470-50197-9.
- [20] Anthony F. Mills. *Basic heat and mass transfer*. eng. 2nd ed. Upper Saddle River, NJ: Prentice Hall, 1999. ISBN: 978-0-13-096247-8.
- [21] D. Ambrose and C. H. S. Sprake. "Thermodynamic properties of organic oxygen compounds XXV. Vapour pressures and normal boiling temperatures of aliphatic alcohols". en. In: *The Journal of Chemical Thermodynamics* 2.5 (Sept. 1970), pp. 631–645. ISSN: 0021-9614. DOI: [10.1016/0021-9614\(70\)90038-8](https://doi.org/10.1016/0021-9614(70)90038-8).
- [22] Eric Lemmon, Marcia Huber, and Mark McLinden. *NIST Standard Reference Database 23: Reference Fluid Thermodynamic and Transport Properties-REFPROP, Version 9.1*. en. May 2013.
- [23] O. Kunz and W. Wagner. "The GERG-2008 Wide-Range Equation of State for Natural Gases and Other Mixtures: An Expansion of GERG-2004". In: *Journal of Chemical & Engineering Data* 57.11 (Nov. 2012). Publisher: American Chemical Society, pp. 3032–3091. ISSN: 0021-9568. DOI: [10.1021/jc300655b](https://doi.org/10.1021/jc300655b).
- [24] Thomas W. Eagar and Aaron D. Mazzeo. "Welding Process Fundamentals". en. In: (Oct. 2011). DOI: [10.31399/asm.hb.v06a.a0005577](https://doi.org/10.31399/asm.hb.v06a.a0005577).
- [25] Carlo Gualtieri et al. "On the Values for the Turbulent Schmidt Number in Environmental Flows". en. In: *Fluids* 2.2 (June 2017). Number: 2 Publisher: Multidisciplinary Digital Publishing Institute, p. 17. ISSN: 2311-5521. DOI: [10.3390/fluids2020017](https://doi.org/10.3390/fluids2020017).
- [26] R. S. Graves et al. "The thermal conductivity of AISI 304L stainless steel". en. In: *International Journal of Thermophysics* 12.2 (Mar. 1991), pp. 409–415. ISSN: 1572-9567. DOI: [10.1007/BF00500761](https://doi.org/10.1007/BF00500761).
- [27] European Committee for Electrotechnical Standardization. *IEC EN 60079-10 Electrical apparatus for explosive gas atmospheres Part 10: Classification of hazardous areas*. 4th ed. Brussels, Apr. 2003.